# DEVELOPMENT OF A NOVEL ORGAN CULTURE SYSTEM ALLOWING INDEPENDENT CONTROL OF LOCAL MECHANICAL VARIABLES AND ITS IMPLEMENTATION IN STUDYING THE EFFECTS OF AXIAL STRESS ON ARTERIAL REMODELING

A Thesis
Presented to
The Academic Faculty

By

Zachary Dominguez

In Partial Fulfillment
Of the Requirements for the Degree
Master of Science in Mechanical Engineering

Georgia Institute of Technology

December, 2008

**DEVELOPMENT OF A NOVEL ORGAN CULTURE SYSTEM ALLOWING INDEPENDENT CONTROL OF LOCAL MECHANICAL VARIABLES AND ITS IMPLEMENTATION IN STUDYING THE EFFECTS OF AXIAL STRESS ON ARTERIAL REMODELING**

Approved by:

Dr. Raymond Vito, Advisor
School of Mechanical Engineering
*Georgia Institute of Technology*

Dr. Alexander Rachev
School of Mechanical Engineering
*Georgia Institute of Technology*

Dr. Rudolph Gleason
School of Mechanical Engineering
*Georgia Institute of Technology*

Date Approved: August 13th, 2008

# ACKNOWLEDGEMENTS

There are a number of people who have made this project possible and deserve special mention. First, I would have not even have had this wonderful opportunity if it were not for Dr. Raymond Vito. He afforded me this opportunity to take part in a level of research that has forever impacted the way I will view the world. His dedication to the process of discovery was contagious as I became more and more enamored by the possibilities of this research. Also, despite many difficulties throughout this research, his continued support and positive attitude always motivated me to persevere.

I would also like to thank Dr. Alexander Rachev who is the originator of many of the novel ideas presented here in this research. Dr. Rachev was an incredible resource whose ability to theorize is unmatched. Dr. Rachev helped reinforce the idea that a wrong answer is better than no answer, and that one should always defend a well thought out argument. This rationale proved useful not only for this project, but as a general way of handling any situations, both personally and professionally.

I would like to thank Dr. Rudolph Gleason for reading and reviewing my thesis. Additionally, I would like to thank Dr. Gleason for his input into the early stages of developing this system. Much of my knowledge of arterial remodeling and solid biomechanics is a direct result of Dr. Gleason and his teaching methods. His ability to articulate even complex concepts relating to biomechanics and remodeling in a classroom setting made this research area both interesting and accessible. I feel very lucky to have had the opportunity to work with these three distinguished academics, each of whom is highly regarded in the field of biomechanics.

I would like to thank my fellow researchers in both the Vito and Gleason lab, especially Dr. Brian Wayman, whose research set the stage for my work. I owe much to those who have helped guide me as I attempted to carve my niche in the lab. It was a great relief to always know that sound advice is just around the corner.

I would like to extend a broad thank you to all of the support staff at Georgia Tech. Specifically, the staff at the Parker H. Petit Institute for Bioengineering and Bioscience, the staff in the George W. Woodruff School of Mechanical Engineering Facilities Shop, and the staff in the Woodruff School Office of Student Services. These ladies and gentlemen offered tremendous counseling throughout my time at Georgia Tech, and always with a smile on their faces. I would like to thank Holifield Farms and all its employees for generously donating tissue as well as creating a positive atmosphere.

Lastly, I would like to thank my family and friends, mostly for the emotional support they offered throughout this process. Thank you to my friends, both at Georgia Tech and elsewhere, who helped take my mind off work whenever I needed a break. Thank you to my family for encouraging me to always put forth one hundred percent. Thank you to my parents for the unconditional love they have given me all my life. I am more proud to call them my parents than they can ever realize.

Finally, thank you to May Win Oo, who had the unenviable task of being by my side throughout this process. Her love, selflessness, compassion, and sense of humor drove me every day, especially when times were at their toughest. Her motto ("Aja Aja") helped motivate me when all else seemed hopeless. I only hope that one day I can be a fraction of the rock that she was for me.

# TABLE OF CONTENTS

# LIST OF TABLES

# LIST OF FIGURES

# SUMMARY

Arterial remodeling is a process by which arteries respond to sustained changes in their mechanical environment. In general, this process occurs in a way such that the local mechanical environment (circumferential stress, shear stress, and axial stress) that an artery is exposed to is maintained at a homeostatic level. However, most studies, both in vivo and ex vivo, utilize a methodology that controls only the global parameters (transluminal pressure, flow rate, and axial stretch ratio). This approach often confounds the results since the actual drivers of remodeling cannot be independently isolated. Past research in this lab has attempted to solve this problem by developing a methodology and system capable of independently controlling each of the local parameters. The present study focused on the continued development of this approach, in an effort to improve the precision of the system and fully automate its operation. It also examined the effect of an independent increase of axial stress using the newly developed system.

First, a novel methodology was developed building on previous work in this lab. An organ culture system capable of monitoring and controlling the three global parameters was developed. An ultrasound system was incorporated into the design to allow for nondestructive measurement of an artery's cross sectional geometry at any point during the culture period. This combination of hardware was then incorporated into an iterative LabVIEW scheme which afforded the user the ability to define specific values for the local mechanical parameters. Also, user interaction was minimized using this combination of hardware and software, adding yet another level of sophistication over existing systems.

Porcine common carotid arteries were cultured for seven days in this newly developed system under physiologically normal circumferential and shear stresses and a constant axial stress of either 150 kPa or 300 kPa. The material response (axial stress-strain and circumferential stress-strain) of the arteries were tested both prior to and following the culture period. Additionally, general arterial morphology, tissue viability, and collagen synthesis were examined in order to gauge the effectiveness of the organ culture system and assess any arterial remodeling.

The organ culture system developed for this study was capable of achieving target values of stress within a period of approximately 3-5 hours, after which the prescribed levels of stress were maintained. Average stress through the duration of the experiment differed by at most 6.7% from the target value. At the end of the culture period, unloaded arterial walls tended to thicken and diameters decrease. The various stains used in this study demonstrated cell viability through the culture and the preservation of general arterial morphology. All arteries exhibited similar levels of collagen synthesis, suggesting a regular turnover of collagen.

The elevated axial stress appeared to cause a softening of the artery in both the axial and circumferential direction. It was hypothesized that this softening was the result of changing collagen structure, specifically the crimping pattern or density, which in turn manifested itself as an altered mechanical response. However, there was also softening in control arteries that could not be explained using a remodeling mechanism. It is possible that the gross circumferential softening seen in the control arteries was the result of organ culture effects, and not any active remodeling processes.

# I. BACKGROUND

## *1.1 General Arterial Structure and Function*

The main purpose of arteries is to transport blood from the heart through the body to the capillaries. This blood carries the oxygen and nutrients needed for survival to the capillaries which facilitate oxygen and nutrient transfer into surrounding tissues. The diameters of arteries decrease with increasing distance from the heart. This phenomenon limits pressure losses and encourages flow as arteries branch into arterioles and capillaries.

Arteries are heterogeneous structures comprised of three distinct, concentric layers: the innermost layer or intima, the middle layer or media, and the outermost layer or adventitia. Between each of these layers are sheets of elastin referred to as the elastic laminae which further differentiate the layers of the blood vessel. The internal elastic lamina separates the intima and the media while the external elastic lamina separates the media and adventitia.

The intima is composed of a basal lamina membrane and endothelial cells. Endothelial cells are embedded in a basal lamina membrane which consists of collagen, cell adhesion molecules, and proteoglycans. Healthy endothelial cells are flat and elongated in the direction of flow. Endothelial cells are unique in that they are nonthrombogenic in order to allow for normal, unimpeded blood flow through the lumen. Endothelial cells can sense changes in the flow induced shear stress at the lumen wall and

respond by initiating the release of vasoconstrictors or vasodilators which are transduced by smooth muscle cells in an effort to maintain homeostasis.

The media generally accounts for a majority of the wall thickness and is composed of smooth muscle cells, elastin, collagen, and proteoglycans. The spindle-shaped smooth muscle cells are oriented either circumferentially or helically throughout the media. Smooth muscle cells provide active tension control (i.e. vascular tone) that allows arteries to respond rapidly to changes in the environment. The elastin and collagen network is primarily responsible for the mechanical properties of the media. Elastin is very compliant and allows energy return over a wide range of deformations. Due to their crimped nature, collagen fibers do not generally affect the mechanical properties under small deformations, but add a tremendous amount of stiffness at large deformations once they straighten.

The adventitia is made up of mostly collagen, some elastin, fibroblasts, proteoglycans, and, in some vessels, nerves and vasa vasorum. The adventitia, with its relatively high collagen content, stiffens and reinforces the arterial wall at high pressures. However, due its lack of an organized microstructure, its contribution to the mechanical properties of the artery wall is not completely understood. The adventitia also acts as a means of tethering the artery to surrounding tissue.

Arterial tissue exhibits complex mechanical properties which arise from its structure as described above. Arteries exhibit a nonlinear stress-strain response due to the combination of elastin and collagen present which represent the main load bearing structures within the arterial wall. As described above, collagen molecules are crimped when unloaded but gradually straighten and carry proportionally greater loads as

deformation increases. Arteries are viscoelastic since they exhibit creep, stress relaxation, hysteresis, and rate dependencies. Arteries are generally modeled as incompressible, orthotropic materials due to their high water content and orientation of structural fibers.

## *1.2 Arterial Remodeling*

The mechanical environment to which an artery is exposed can be described in terms of both global and local parameters. The global parameters are defined as blood pressure, flow rate, and axial force while the local parameters are defined as circumferential stress, flow induced shear stress, and axial stress. The global and local parameters are related via force equilibrium equations and the flow equation, along with geometric parameters and the fluid viscosity.

Arterial remodeling is a process by which arteries respond to sustained changes in their mechanical environment. The result of remodeling is a change in the dimensions and/or the mechanical properties of the artery. Remodeling is part of normal physiological processes and, when self-limited, is referred to as adaptation. In general, this adaptation occurs in a way such that the local mechanical environment to which an artery is exposed is maintained at a homeostatic level. However, it is also possible for arterial remodeling to be maladaptive and result in the development and progression of a number of pathologies such as atherosclerosis or aneurysms.

Various in vivo and organ culture studies, described below in more detail, have demonstrated that arteries respond to sustained changes in any global parameter by altering their synthetic, proliferative, or degradative activity in a manner tending to restore baseline levels of the local parameters . This conclusion makes intuitive sense as individual cells within an artery cannot “sense” the global mechanical conditions, but

rather only the local stress parameters which are more accurate descriptors of a mechanical environment for a single cell.

## *1.3 In Vivo Investigations*

Numerous in vivo studies have examined how arteries remodel due to changes in the mechanical environment. In hypertension studies, it was found that arteries experience wall thickening in order to restore circumferential stress to baseline levels. This wall thickening was accomplished through smooth muscle cell hypertrophy and matrix synthesis. In addition, lumen diameter was maintained so as to maintain baseline levels of shear stress. These remodeling changes have been realized in as little as two weeks (Liu and Fung, 1989; Vaishnav et al., 1990; Matsumoto and Hayashi, 1994).

In studies where flow rate has been altered, arteries adjust luminal diameter such that shear stress is maintained. For example, when exposed to increased flow, endothelial cells sense increases in shear stress and upregulate vasodilators which cause smooth muscle cells to relax and the lumen to dilate. This is accompanied by an increase in wall thickness characterized by migration and proliferation of smooth muscle cells. This combination of changes causes shear stress and circumferential stress to return to baseline levels. Because lumen diameter is increased, endothelial cell proliferation ensures a constant endothelial density. Similar studies examining low flow rate conditions have shown that changes in the artery have restored shear stress and circumferential stress to baseline levels. However, this process of remodeling occurs on a much longer time scale than the hypertensive process, with changes taking place over several months (Kamiya and Togawa, 1980; Zarins et al., 1987; Masuda et al., 1989).

Still other researchers have examined the role of axial stretch on arterial remodeling, though these studies are fewer in number than the preceding studies on hypertension and flow changes. Typically, artery lengthening in vivo is achieved using either tissue expanders or fixators. Tissue expanders consist of a silicone reservoir that is placed beneath the experimental site (Collins and Swanson, 1993). The reservoir is then filled with a saline solution, which in turn pushes against surrounding tissue. This technique has been used to expand blood vessels directly by placing the expander in direct contact with the vessel, or indirectly by placing the expander in contact with tissue, such as bone, that contains the vessel. Fixators are typically attached to bone and consist of a rigid frame that applies a stress to tissue in order to promote remodeling. Soft tissues surrounding the bone are simultaneously remodeled during these procedures (Gugenheim, 1998).

Studies employing these techniques have found significant vessel lengthening. Many studies have achieved routine elongation of 25-33% (Fink et al., 1999; Huang et al., 1998; Ippolito et al., 1994; Lavini et al.). Two studies with rats have shown elongation up to 100% within only 10 days and up to 140% within 21 days with reliable patency using tissue expanders (Hong et al., 1987; Stark et al., 1987). In theory, the tissue elongation will continue indefinitely as long as the growth rate matches the extension rate. Therefore, the limiting factor in vessel lengthening is most likely the duration of the experiment.

Immediately following vessel lengthening, experimental vessels have been shown to exhibit significantly different mechanical properties when compared to control vessels. Despite this initial difference, the mechanical properties of lengthened vessels returned to

those of controls given sufficient recovery time (Fu et al., 1997; Huang et al., 1998). In addition, following lengthening, Ruiz-Razura et al. (1994) found experimental vessels were still able to exhibit vasoactivity, albeit at lower active tension levels than the controls.

More recent research has examined artery lengthening in a more direct way. Jackson et al. (2002) have shown that in vivo lengthening of a rabbit carotid artery results in tissue growth such that axial strain in the artery was restored to baseline levels. Instead of using expanders or fixators to study arterial remodeling, this group excised a section of an artery, and then apposed the cut ends to lengthen the remainder of the artery. The growth witnessed was a result of increased cell proliferation, increased collagen content, and increased elastin content. In addition, arteries were able to restore axial strain independent of endothelium, which suggests smooth muscle cell regulation of this process.

## *1.4 Organ Culture Investigations*

While in vivo studies provide invaluable information regarding arterial remodeling, it also poses many unique challenges. In-vivo studies limit precise control over a variety of factors, often confounding results (Koo and Gotlieb, 1991). For example, during vessel lengthening procedures involving tissue expanders or fixators, a vessel is often under a very complicated loading scheme - it is not under pure axial tension. In addition, in-vivo studies do not afford precise control over a variety of parameters such as flow rate, pressure, and axial force. Therefore, researchers have developed an alternative method in examining arterial remolding - namely, the use of organ culture. Organ culture offers the ability to precisely control the mechanical and

biochemical environment that an artery experiences. Because this environment may or may not be an accurate analogue of a physiologic environment, the relevance of any results to physiologic conditions may be limited. However, what organ culture studies facilitate is a more basic understanding of arterial remodeling through the precise control of the variety of factors that influence remodeling.

To perform an organ culture study, a vessel segment is explanted from a donor into an experimental system that simulates a physiologic biochemical environment. Once in place, the vessel is subject to various mechanical loads and remodeling can be observed. Originally, many studies focused on static organ culture. In these studies, tissue is bathed in a static media used to nourish the tissue (Gotlieb and Boden 1984; De Mey et al. 1989; Koo and Gotlieb 1991; Voisard et al. 1999 ). However, the physiologic relevance of a perfusion organ culture makes it a more accurate representation of physiologic conditions. In perfusion organ culture studies, there is a controllable transluminal pressure and flow which allows for a more accurate representation of in-vivo conditions (Matsumoto et al. 1999; Han and Ku 2001; Clerin et al. 2002; Gleason et al. 2004; Davis et al. 2005, Brant et al. 1987; Labadie et al. 1996; Schwartz et al. 1996; Vorp et al. 1996; Bakker et al. 2000; Surowiec et al. 2000). Perfusion organ culture studies have typically maintained artery functionality for seven to nine days (Han and Ku 2001; Clerin et al. 2002; Davis et al. 2005). In one study (Clerin et al. 2002), porcine carotid arteries were kept viable for 27 days, however, studies of this duration are rare.

Numerous organ culture studies have examined the effect of hypertension on arterial remodeling. In general, baseline levels of circumferential stress were not achieved; however, the general tendencies in these experiments are consistent with the

results observed in-vivo. Matsumoto et al (1999) observed a significant increase in wall thickness in rabbit carotid arteries cultured under hypertensive conditions for six days. Also, there was no observed change in lumen diameter during this time. Han and Ku (2001) observed increases in the lumen diameter and wall thickness along with increases in the contractile response of porcine carotid arteries exposed to hypertension. Zulliger et al (2002) observed changes in the elastic modulus and changes in contractility of arteries exposed to both hypo- and hypertensive conditions in a period of only three days. These studies demonstrate the effectiveness of using organ culture to study the effects of hypertension on arterial remodeling caused by sustained changes in circumferential stress.

Organ culture studies that have examined flow induced remodeling have been quite limited due to the time scale necessary for such remodeling to occur. Chesler et al. (1999), for example, found significant differences in matrix metalloproteinase (MMP) activity for normotensive and hypertensive vessels. However, no significant differences were seen between vessels exposed to varying levels of flow. Wayman et al. (2008) developed a method to independently control shear and circumferential stress during a three day organ culture of porcine carotid arteries. He found that while significant remodeling activity was witnessed due to sustained changes in circumferential stress, no significant remodeling was observed due to flow induced shear stress.

Despite the long time scale needed to realize arterial remodeling due to flow induced shear stress, it is still important to take shear stress into account. This is because any change in flow rate that causes a change in shear stress from its baseline level may cause some active response of the artery (e.g. dilatation or constriction of the artery). This change in geometry may then affect other stresses that the artery may be subject to

(i.e. circumferential or axial stress). To some extent, researchers have attempted to control shear stress in organ culture. However, in most studies, the shear stress is calculated using an artery's initial dimensions, then held constant throughout the experiment (Chesler et al. 1999; Han and Ku 2001; Clerin et al. 2003; Davis et al. 2005). Because shear stress is inversely proportional to the cube of the inner diameter, even small changes in arterial geometry may have a dramatic affect on the actual shear stress experienced by the artery.

Only recently have researchers started to report on the effect of axial strain or stress on arterial remodeling. Han et al. (2003) found that porcine carotid arteries held at a stretch ratio of 1.8 experienced significant increases in cell proliferation compared to control vessels kept at a stretch ratio of 1.5, while maintaining viability. Clerin et al. (2003) observed 20% increases in unloaded length when juvenile porcine carotid arteries were stretched beyond a stretch of 2 over a period of nine days. These vessels were cultured under subphsyiologic pressure and flow conditions. A subsequent study by the same group (Nichol et al., 2005) found that under normal physiologic pressure and flow rates, these increases in length were less dramatic. Davis et al. (2005) cultured porcine carotid arteries under a constant axial stress of 250 kPa or 350 kPa under physiologic pressure and flows for seven days in an effort to lengthen the arteries. They found that when stretched beyond a stretch ratio of 2.14, the unloaded length of arteries increased by approximately 13%. This increase in length was associated with a decrease in axial stiffness. Gleason et al. (2007) studied the mechanical response of mouse carotid arteries subjected to varying levels of axial strain and physiologic levels of pressure and flow for two days in culture. Interestingly, while they found significant changes in structural

responses (i.e. pressure - axial force response and axial force – length response), they did not see significant differences in the material response (i.e. circumferential stress – strain response or axial stress - strain response).

In general, organ culture studies seem to verify past research in-vivo, if not quantitatively, then qualitatively. The failure of organ culture to reproduce results from in-vivo studies may be attributable to the shorter duration that organ culture affords. Additionally, the biochemical environment may not be as nourishing to living cells as a healthy in-vivo environment which contains circulating cells. Despite this, organ culture enables the unique ability to very precisely control many of the factors that affect remodeling. Up to this point, it is debatable as to whether or not this advantage has been fully exploited.

Both in-vivo and organ culture investigations offered evidence that arteries respond to changes in their global parameters in order to restore baseline levels of their *local* parameters. This poses a unique problem since the global parameters are easily measured, but the local parameters can only be calculated given various additional parameters regarding the artery. Wayman et al. (2008) attempted to address this by independently controlling circumferential and shear stress through the continuous monitoring of arterial geometry, calculation of local parameters (circumferential and shear stress), and adjustment of global parameters (pressure and flow rate). In past studies, the effect of circumferential stress on arterial remodeling may have been confounded by the fact that an increase in pressure not only increases circumferential stress, but decreases shear stress significantly due to a change in the lumen diameter. The method described by Wayman et al. (2008) “decoupled” the variables and allowed for a

more accurate representation of how each local parameter affected various markers of remodeling. However, this method was hampered by its short duration of three days since no measurable changes in geometry or mechanical properties were observed. Instead, biological markers which precede remodeling were identified and quantified.

# II. OBJECTIVES

With the exception of Wayman et al. (2008), no studies have been able to quantify the remodeling changes due a change in a single local parameter, while keeping the other local parameters constant. This is because in general, a change in a single global parameter may result in a change in more than one local parameter. Therefore, any remodeling witnessed must be attributed to the combined effect of all of the local parameters that were changed. For example, a change in the arterial pressure during an experiment will lead to an increase in circumferential stress. However, this increase in pressure will also cause the lumen diameter to increase, thereby changing the shear stress that an artery's endothelial cells sense. Because two variables that can potentially affect remodeling have been changed in this hypothetical scenario, any remodeling that occurs cannot be accurately attributed to either local parameter.

Wayman et al. (2008) was the first to attempt to control the local mechanical environment in organ culture. While successful, there were a few major limitations to the method employed. First, because only the outer diameter of the artery could be observed during the experiment, the wall thickness could only be approximated using the condition of incompressibility. This assumption, while valid over short durations, is not ideal, especially when we are trying to promote remodeling (which may imply a change in the overall volume of the artery). Second, there was no means of measuring or controlling the axial stress of the artery. Because arteries were held at physiologically normal stretch ratios during the experiment, this was not relevant. However, for experiments in which we want to examine how axial stress affects remodeling, this method is not sufficient.

Third, the experimental setup used by these researchers needed constant user interaction throughout the duration. A more useful system may incorporate computer control such that user interaction is minimized through hardware automation.

Once a method of independently controlling the three local parameters is realized, there is a large amount of data that can be collected which will give insight into the mechanisms of remodeling. The implications of such data is especially important for a better understanding of how each local parameter works independently, or in conjunction with other local parameters, to affect remodeling. Such a system would allow us to hypothesize about the remodeling capacity of arteries and any relationships between multiple local parameters and their remodeling effects.

Additionally, the utility of a system capable of fully controlling an artery's local mechanical environment is especially applicable to tissue engineering. By monitoring and adjusting the driving factors (local stress parameters) of remodeling, we can more accurately determine how arteries respond to these changes in stress. Ultimately, one can utilize a controlled stress environment to control how tissue engineered constructs remodel in organ culture thereby making the process more effective and efficient.

The hypothesis of this work is that i*ndependent* and *complete* control of the local mechanical environment, as opposed to control of the global parameters, will reveal novel information regarding the response of porcine carotid arteries in organ culture to sustained changes in this environment. To test this hypothesis, the following specific aims were identified:

- **Specific Aim 1:** *To develop a method of independently and automatically controlling all three local parameters in organ culture*

First, a method of independently and automatically controlling the three local parameters in organ culture over a seven day period must be developed. Given an appropriate strain energy function and various artery dimensions, it is possible to calculate what combination of global parameters can achieve a certain level of axial stress, circumferential stress, and shear stress. However, such an approach is not necessary. Even without a strain energy function, it is possible to iteratively solve the governing equations in a way that allows the target values of the local parameters to be achieved. An algorithm utilizing this concept is described in detail in Section 3.2.2 Method for Independently Controlling the Local Parameters).

- **Specific Aim 2:** *To develop a hardware system capable of implementing the method described in Specific Aim 1*

In order to employ such an iterative approach as described above, there needs to be a means of monitoring pressure, flow rate, axial position, artery wall thickness, and artery diameter, as well as a way to control transluminal pressure, flow rate, and axial force. To meet these needs, several pieces of hardware needed to be added to Wayman's organ culture system. These hardware additions (described in detail in Section 3.1 Experimental System) enable complete computer control and allow a higher degree of precision than afforded in the Wayman's previous system.

- **Specific Aim 3:** *To examine the effects of an independent change of axial stress on remodeling.*

Using the method developed for Specific Aim 1, axial stress can be independently varied while circumferential stress and shear stress are held at constant physiologic levels through the duration of the experiment. This will act not only as a verification of the

method, but as a supplement to the work Wayman et al. (2008) did in studying the independent effects of circumferential and shear stress on remodeling. Also, as mentioned in the Background section, the effect of this local parameter is less studied than that of circumferential or shear stress, both in vivo and in organ culture. Therefore, any information gained from this research will add to the relatively limited body of work concerning axial stress and remodeling.

# III. METHODS

## *3.1 Experimental System*

The experimental system developed for this research is comprised of two distinct systems. The organ culture system provides a physiologic environment for the artery and includes all necessary instrumentation to control and monitor various global parameters. The data acquisition and instrument control system utilizes computer software in order to fully automate the system through the duration of the experiment.

### 3.1.1 Organ Culture Hardware

The organ culture system used in this research is an extension of the design of Wayman (2007). A schematic of a single organ culture system, along with all external hardware, is shown in Figure 2 and the actual setup is shown in Figure 1. The flow loop is comprised of a glass media reservoir, a pulse dampener (Cole-Parmer), and a polycarbonate tissue chamber connected by polypropylene elastomer tubing (Phar-Med, Cole-Parmer). Two thin walled stainless steel cannulae whose outer diameters approximately match the pressurized artery's inner diameter were mounted on opposite sides of each of the vessel chambers. Grooves were machined onto the surface of one end of each cannula to facilitate vessel mounting. The cannula attached to the distal end (relative to flow) of the artery was held in place by a tight fitting seal. The proximal cannula could move axially through a port fitted with a custom designed, low friction Teflon seal (American Variseal Corporation). The tissue chamber and media reservoir

were fitted with 0.22 micron filters (Millipore,) to facilitate gas exchange and ensure a stable pH level (7.4). A peristaltic roller pump (Masterflex, Cole-Parmer), located between the media reservoir and the pulse dampener, drove the flow.

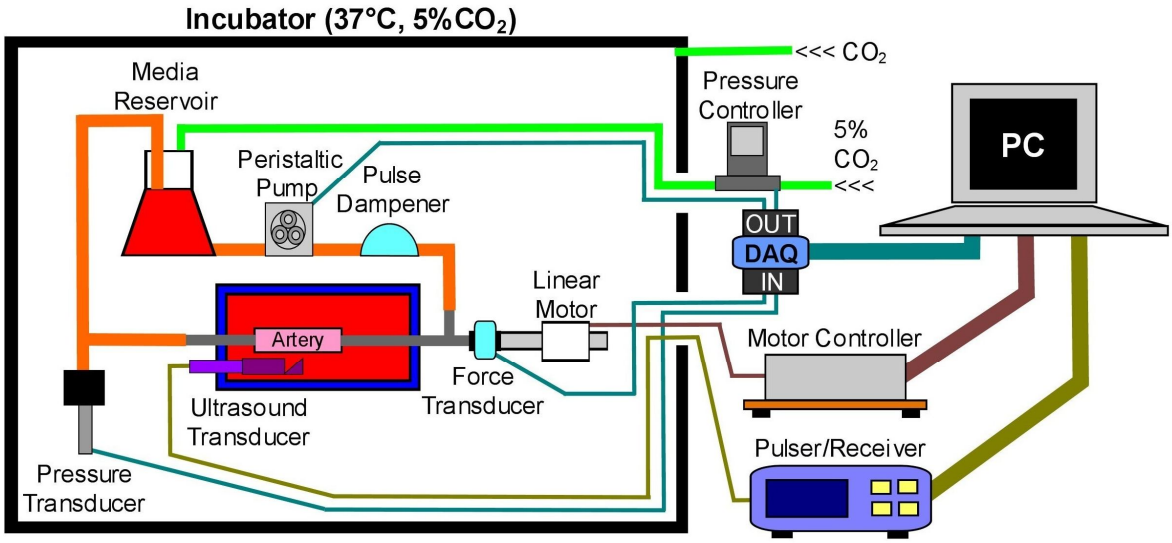


**Figure 1 - Organ Culture Schematic: A schematic showing the system hardware as well as all connections. Not shown in this schematic is the coaxial relay used to switch the pulser/receiver signal between the two ultrasound transducers. The relay is controlled through one of the DAQ board outputs.**

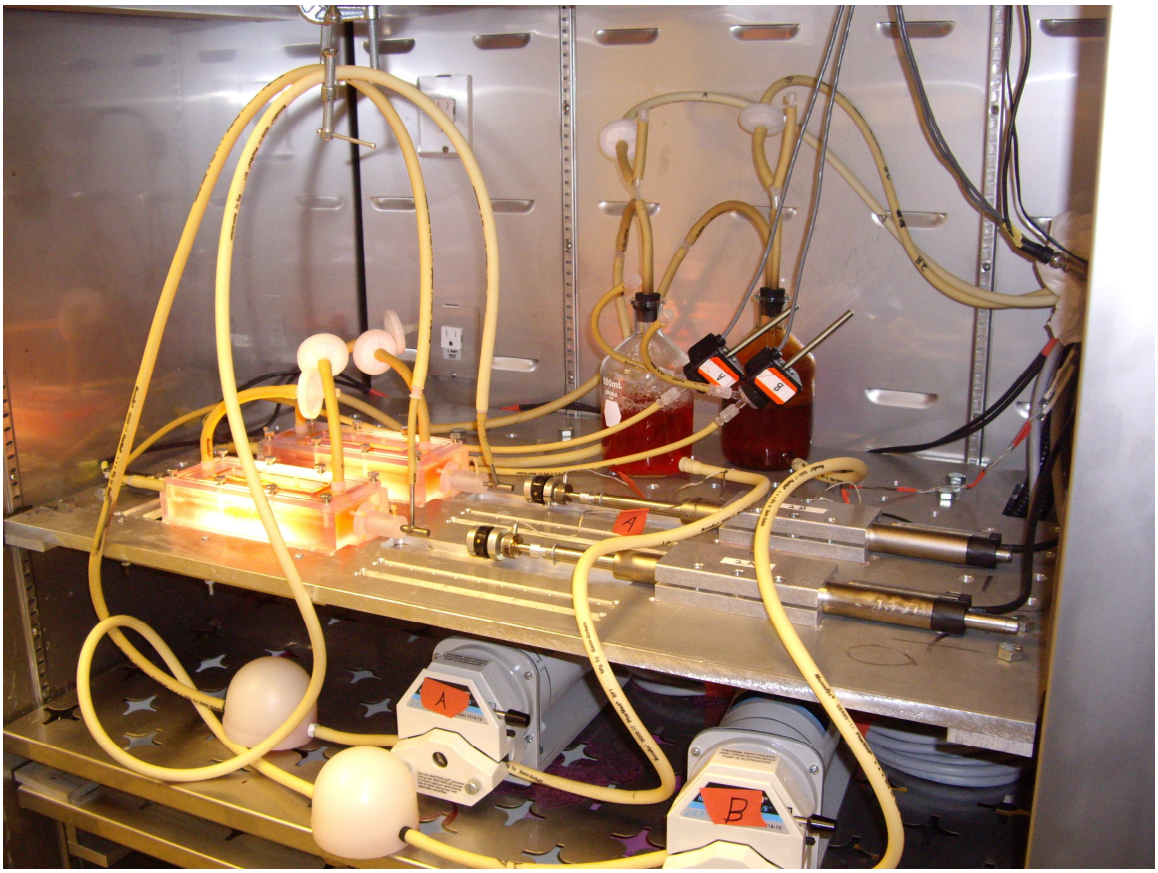


**Figure 2 - Organ Culture System: A view inside the incubator showing two organ culture systems in place. External hardware located outside the incubator is not shown in this image, but can be seen in the schematic (Figure 1).**

The media reservoir was also connected to a pressurized mixture of 5% $CO_2$, with a balance of air. This pressure was controlled by a digital pressure controller (Alicat Scientific). A pressure transducer (model 60-3002, Harvard Apparatus) located between the tissue chamber and the media reservoir measured transluminal pressure. A linear motor (motor model P01-23x160/130x270, controller model E4000, LinMot) controlled the displacement of the sliding cannula. A 0 to 10 lbf force transducer (model 31, Sensotec) was mounted between the sliding cannula and the linear motor. A 20 MHz ultrasound transducer (model V316-N-SU, NDT) and signal reflector (F198, NDT) were mounted into the distal end of the tissue chamber. A computer controlled pulser-receiver

(model 5900PR, Panametrics-NDT) was used to generate a signal (200 Hz pulse repetition frequency, 54 dB gain, 200 MHz maximum bandwidth, 50 ohms damping, and a maximum of 8 μJ available pulse energy). Data from the ultrasound signal was used to nondestructively determine the cross sectional dimensions of the artery at any instant during the experiment. A latching coaxial relay (model N1810UL-SPDT, Agilent, not shown in Figure 1) was used to switch the pulser-receiver signal between the two ultrasound transducers when running two simultaneous experiments.

Perfusion and bathing media were composed of Dulbecco's Modified Eagles Medium (DMEM, Sigma) supplemented with sodium bicarbonate (3.7 g/L, Sigma), L-glutamine (2 mM, Sigma), L-Proline (0.4 mM, Sigma), ascorbic acid (50 mg/L, Sigma), antibiotic-antimycotic solution (1%, Sigma), and calf serum (10%, Hyclone). Dextran (6.5%, Sigma) was added to the perfusion media to increase its viscosity to physiologic levels (4 cP). All solutions were vacuum filtered through 0.22 micron filters under a biological hood.

### 3.1.2 Data Acquisition and Instrument Control System

The data acquisition and instrument control system developed for this research allowed for complete computer control and monitoring of the experimental system. LabVIEW software was selected as the programming platform for all data acquisition and instrument control. LabVIEW is a powerful software program that facilitates continuous monitoring and control of various digital and analog signals. In addition, it is capable of simulating many common bench top laboratory devices (e.g. oscilloscopes), thereby eliminating the need for bulky pieces of hardware.

A data acquisition board (NI USB-6008, National Instruments) attached to the PC read analog voltage inputs from the pressure transducer and the force transducer. It wrote analog voltage outputs (0-5 V) to the peristaltic pump and the pressure controller. In addition, it used digital transistor-transistor logic to control the switching of the coaxial relay. All commands to the data acquisition board were done using the DAQ-assistant sub-VI (sub-Virtual Instrument) in LabVIEW. The linear motor controller communicated to the PC via an RS232 to USB conversion cable which simulated a serial connection. This controller unit communicated using ASCII code. LabVIEW read from and wrote to this serial port using Virtual Instrument Software Architecture (VISA) sub-VI's. The ultrasound signal was first filtered and processed in the pulser/receiver (band-pass filter 1 MHz to 20 MHz) and then sampled using a 100 MS/s digitizer (NI USB-5133) which gave us a spatial resolution of approximately 7.5 microns. Prior to each experiment, the ultrasound transducer was manually positioned so as to maximize the signal received from the artery.

Analog voltage inputs read from the pressure transducer, force transducer, and peristaltic pump needed to be converted to more useful units of millimeters of mercury (mmHg), Newtons (N), and milliliters per minute (mL/min), respectively. To accomplish this, simple conversion equations were found and programmed into the software. Because LabVIEW communicated with the linear motor in ASCII, the linear position was read and written in terms of the hardware's self defined 'units' - each defined as 0.01953 mm. Therefore, a simple conversion was done when calculating linear position.

However, some necessary parameters could not be directly determined using the data from the hardware and a simple conversion factor. Specifically, the cross sectional

dimensions and axial force. In order to determine the outside diameter, wall thickness, and axial force of the arteries, two unique algorithms were written into LabVIEW to extract these parameters from the data.

#### *3.1.2.1 Method of Calculating the Artery Geometry from Ultrasound Signal*

The digitized signal obtained from the pulser/receiver was used to determine the cross-sectional geometry of the artery. Because of the similarities in acoustic impedances between the artery and the media, a relatively high frequency (20 MHz) transducer was used. However, despite this high frequency, it was still difficult to differentiate between where the media and artery interfaces were located.

The raw ultrasound signal that was read into LabVIEW consisted of areas of low voltage, with local peaks (and valleys) of higher magnitude voltages. Each local maximum (or minimum) in voltage represented a transition between interfaces of differing acoustic impedances. However, as shown in Figure 3 below, the voltage peaks often had magnitudes that were within the range of the noise seen in the signal. While four peaks can be seen in the representative signal shown here, often one or more of the peaks was not differentiable from the level of the noise.

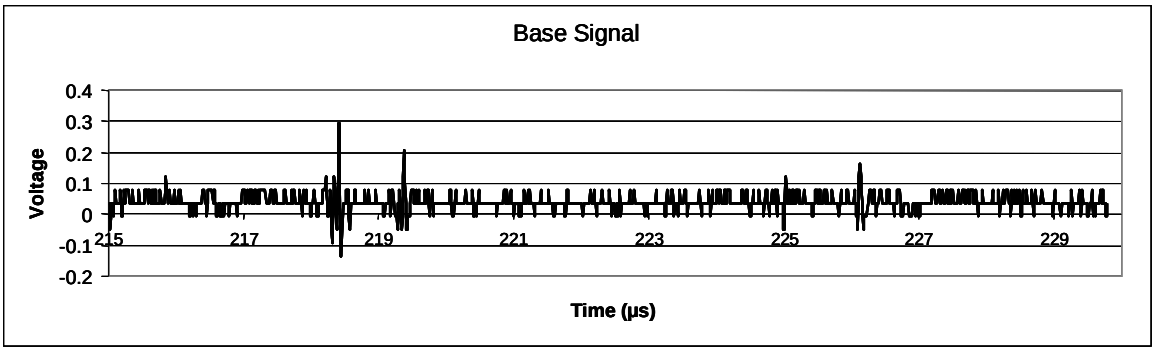


**Figure 3 – Raw Ultrasound Signal: A representative subset of an ultrasound waveform as detected displaying the locations of the four fluid-tissue interfaces. Note that some of the peaks, especially the third peak from the left, are very similar in magnitude to the noise in the system.**

To eliminate as much of the random noise as possible, an algorithm was created that would attempt to maximize the clarity of the signal. The computer sampled 800 consecutive waveform samples and summed them to generate a new, single waveform. The number of waveform samples was determined to be the minimum amount needed to consistently obtain arterial geometry. In the resulting waveform, the four peak locations were of much greater amplitude than the random noise, which was averaged to nearly zero. To further accentuate the difference in amplitude between the peaks and the noise, the summed waveform was squared. This algorithm is rather simple and acts simply to dampen the noise levels in the signal. However, for the purposes of this study, this approach proved sufficient.

Once a satisfactory waveform could be obtained, an algorithm was developed that would allow for the identification of the location of the peaks. Once the peaks were temporally located, these data could be converted into dimensions. LabVIEW includes a built in peak detection sub-VI which determines the location of the maximum value of the waveform. Once this position was located and its time value noted, that data point and data points surrounding that point on either side were assigned a value of zero. The

width of this zero subset was user-defined and selected in order to eliminate LabVIEW from selecting the same peak twice during subsequent peak detections. This process of identifying peaks was continued until four peaks were found and their time values noted.

These times were used to calculate the geometry of the artery using the following equation:

$$Length = \frac{SpeedOfSound_{medium} \cdot Time}{2} \qquad \text{Eq. 1}$$

where the speed of sound through the artery was defined as 1540 m/s (Lockwood et al., 1991; Moneta et al., 2000). Because the speed of sound through the perfusion medium is comparable to water, which is comparable to the value defined for the artery, we maintained a constant 1540 m/s through all media. The minimum and maximum time values were used to calculate the outer diameter of the artery. The two minimum values and two maximum values were used respectively to calculate the first and second wall thickness. These values were then averages to obtain an average wall thickness.

However, the four peaks identified with the LabVIEW algorithm did not always correspond to the actual locations of interest. This was the case in situations where less than four peaks appeared in the signal; the remaining peaks were simply picked out of the random noise at low levels. This also happened if the width of the user-defined zero subset was either too wide, in which case we would have eliminated a valid peak by replacing it with zeroes, or too narrow, in which case the program may have identified a second unique peak that is actually just an echo of a taller peak in the same location.

To combat this effect, the process of peak detection was iterated 8 times, giving us arrays of outside diameters and wall thicknesses comprised of 8 elements. Each of these 8 elements was individually considered. Based on a user defined range of values

corresponding to minimum and maximum values, we could eliminate dimensions that LabVIEW calculated that did not make sense. For our program, wall thickness was allowed a range of 0.1 mm to 1 mm, and outside diameter was allowed a range from 3 mm to 12 mm. Any values outside of these ranges were disregarded. From this new array of "acceptable" values, we could obtain a histogram of the dimensions calculated by LabVIEW. Ideally, these data would be displayed as a very narrow, normal distribution. This would imply consistency among our measurements. All of the values were then averaged in order to determine the actual dimension of the artery.

#### *3.1.2.2 Method of Calculating the Axial Force*

It should be noted that though a low friction seal was used at the interface between the sliding cannula and tissue chamber, some friction still existed. We therefore developed a unique protocol for measuring the axial force of each artery. At each location the artery was extended and shortened by 0.3906 mm. Because friction always acts against the direction of motion, two different force measurements were obtained depending on the direction of motion of the sliding cannula. These two force measurements were taken five times each (five measurements during artery lengthening, five measurements during artery shortening), and then averaged to obtain a high force estimate and a low force estimate. The high and low force estimates were then averaged to find a force measurement that eliminated the effect of friction. The representative schematic in Figure 4 shows how the resultant force read at the transducer ($F_R$) accounts for friction depending on the direction the cannula (the block in the schematic) is moved. Note how when the two $F_R$ values are averaged, we obtain only the force of the artery, or $F_A$.

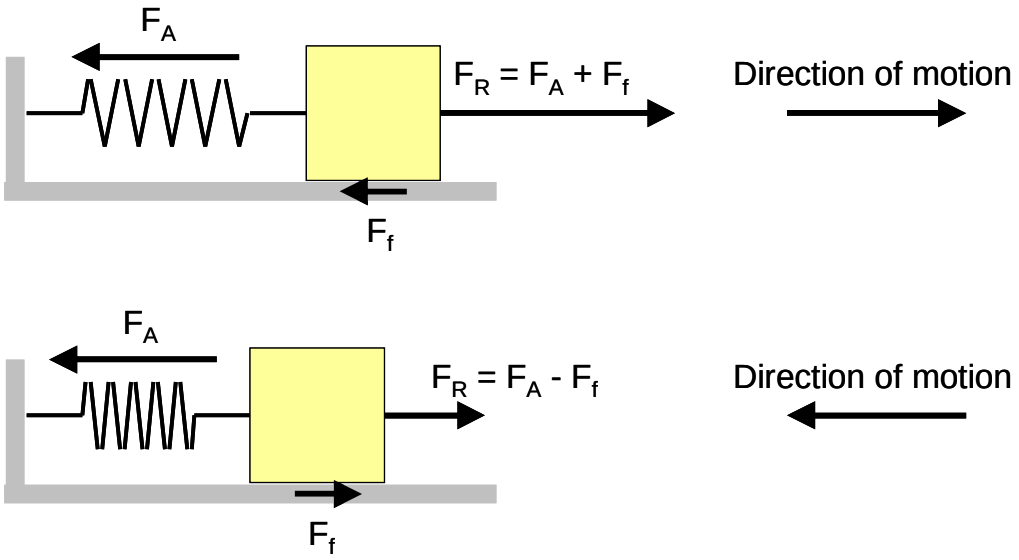


**Figure 4 - Axial Force Schematic: A simple schematic representing the mechanical forces at play between the artery, the Teflon seal, and the force transducer. This analogy applies when we model the spring (artery) with a linear response (at least over short distances) and we assume the friction between the box (cannula) and floor (seal) is the same regardless of direction.**

However, this method of calculating the axial force only holds under some assumptions. First, we assume that the force-length relationship is approximately linear over the small distance that the artery is moved back and forth. This assumption allows us to average the two resultant forces in order to determine the force in the artery. It also allows us to neglect any non-linear changes in the force of the artery due to changes in length by assuming the behavior is linear in the region between the two points. Second, we assume the coefficient of friction is consistent between cycles such that the force of friction does not depend on the direction of motion.

## *3.2 Experimental Protocol*

The following section describes how arteries were obtained prior to, maintained during, and tested before and after the experiment. The preparation of the arteries for the organ culture was done using protocols from Wayman (2007).

### 3.2.1 Experimental Preparation

The organ culture system components which came into contact with either the artery or the media during the experiment and any tools used to prepare the arteries for culture were sterilized by autoclave the day before artery harvest. Components and tools were placed into plastic autoclave bags and sterilized in a gravity cycle with a 15 minute sterilizing time and a 15 minute drying time. The exceptions to this method were the ultrasound transducers and pressure domes. Due to the vulnerability of the instruments to high heat and pressure and also to ethylene oxide sterilization, the ultrasound transducers and pressure domes were instead thoroughly wiped down with 70% alcohol. All components, including the ultrasound transducers and pressure domes, were then placed in a biological safety hood under ultraviolet light overnight.

Porcine common carotid arteries were harvested from 6-7 month old farm pigs (100-150 kg) at a local abattoir (Holifield Farms, Inc. of Conyers, GA). Artery segments were rinsed with Dulbecco's phosphate buffered saline (PBS, Sigma) immediately after harvest and were transported to the laboratory stored in ice-cold PBS.

Under a laminar flow hood, arteries were trimmed of loose connective tissue and gently inflated with air to identify leaks. Leak-free segments, approximately 30-40 mm in unloaded length, were used for culture. Because the harvested arteries tended to be

approximately 70-90 mm in length, a single artery was cut in half, with each half used either as a control or experimental artery. Arteries were mounted onto the tissue chamber cannula using a single purse-string suture and oriented such that in vivo flow direction was preserved. Warm (37°C) bathing and perfusion medium were added to the assembled flow loop under the hood. The entire flow loop was then transferred to the incubator (maintained at 37°C and 5% $CO_2$) and peripheral equipment was attached and calibrated (peristaltic pump, pressure transducer, pressure controller, ultrasound cable, linear motor/force transducer assembly). Arteries were then set at the unloaded length measured earlier. Once the system was in place, the artery was kept at zero pressure, zero axial stretch, and a minimum flow rate of 30 mL/min for approximately one hour to allow the vessels to acclimate to the organ culture environment.

### 3.2.2 Method for Independently Controlling the Local Parameters

After the acclimation period and before the LabVIEW program was started, the artery was preloaded. In other words, the artery did not begin the experiment in a completely unloaded state since back pressure, flow rate, and axial length were set at values that loaded the artery. This was done for two reasons. First, a loaded artery (pressurized and stretched) was more easily recognized by the ultrasound transducer (i.e. an unloaded artery inhibited the ultrasound transducer's ability to receive an accurate signal describing the artery's dimensions). Second, the "presetting" of the global parameters ensured that the individual rate at which each parameter moved towards its prescribed level would not negatively affect system performance. For example, beginning with an unloaded artery, if pressure increases dramatically faster than the

artery lengthens, there is a possibility the artery will buckle and thus prevent the ultrasound transducer from receiving any signal.

Figure 5 diagrams the process used to control and maintain each of the prescribed local parameters. Note that this schematic displays a general feedback loop which can be interpreted for various hardware setups in any number of organ culture systems. At the onset of each experiment, the shear stress, circumferential stress, and axial stress were prescribed by the user in LabVIEW. Once the program was started, LabVIEW calculated the artery's dimensions using the protocol outlined in Section 3.1.2.1 Method of Calculating the Artery Geometry from Ultrasound Signal.

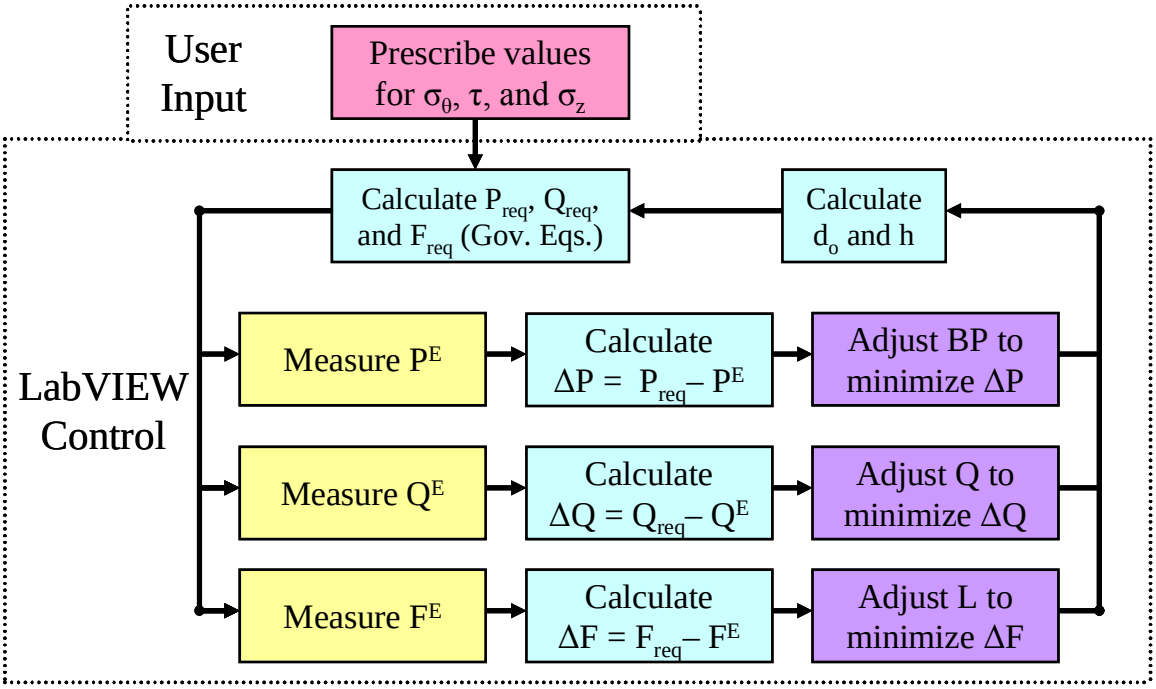


**Figure 5 - Flowchart of Stress Control Method: After prescribing the values for circumferential stress, shear stress, and axial stress, the computer software (in this case LabVIEW) is capable of achieving those values using a simple iterative feedback loop. Typically, to calculate the global parameters needed to satisfy a specified set of local parameters, one would need descriptors of the mechanical response of the artery. The iterative nature of this program eliminates the need to have any information regarding the mechanical response of the artery.**

Using the prescribed stresses and the measured dimensions of the artery, LabVIEW calculated the required pressure ($P_{req}$), required flow rate ($Q_{req}$), and required axial force ($F_{req}$) from the governing equations. The required pressure was calculated using Laplace's Law.

$$\sigma_\theta = \frac{P \cdot r_i}{h} \qquad \text{Eq. 2}$$

or

$$P_{req} = \frac{2 \cdot \sigma_\theta \cdot h}{d_o - 2 \cdot h} \qquad \text{Eq. 3}$$

Assuming Poiseuille flow of a Newtonian fluid, the required flow rate was calculated using:

$$\tau = \frac{32 \cdot \mu \cdot Q}{\pi \cdot (d_o - 2 \cdot h)^3} \qquad \text{Eq. 4}$$

or

$$Q_{req} = \frac{\tau \cdot \pi \cdot (d_o - 2 \cdot h)^3}{32 \cdot \mu} \qquad \text{Eq. 5}$$

where μ represents the fluid viscosity (4 centipoise). The required axial force was calculated using the following definition of stress:

$$\sigma_z = \frac{F}{\pi \cdot (d_o \cdot h - h^2)} \qquad \text{Eq. 6}$$

or

$$F_{req} = \sigma_z \cdot \pi \cdot (d_o \cdot h - h^2) \qquad \text{Eq. 7}$$

The parameters, $P_{req}$, $Q_{req}$, and $F_{req}$, were the values which would satisfy the prescribed stresses given the measured geometry.

Next, the program measured the experimental values of pressure ($P^E$), flow rate ($Q^E$), and axial force ($F^E$) from the pressure transducer, peristaltic pump, and force transducer, respectively. Adjustment factors ($\Delta P$, $\Delta Q$, or $\Delta F$) were defined and calculated as the difference between the required parameters ($P_{req}$, $Q_{req}$, and $F_{req}$) and the experimental parameters ($P^E$, $Q^E$, and $F^E$). The sign of each adjustment factor indicated to the program whether to increase or decrease the respective global parameter, either back pressure (BP), flow rate (Q), or axial length (L). Back pressure was controlled by the pressure controller, flow rate was controlled by the peristaltic pump, and the axial length was controlled by the linear motor. In addition, the magnitude of the adjustment factors indicated the degree to which BP, Q, and L would be adjusted. Because this program attempted to adjust BP, Q, and L even for very small adjustment factors beyond the resolution of the hardware, the program was designed to control the local parameters as accurately and precisely as the hardware would allow.

Any adjustments made to BP, Q, or L tended to alter the artery's geometry due to passive and/or active response. Therefore, the earlier calculations of $P_{req}$, $Q_{req}$, and $F_{req}$ using the artery's initial dimensions did not necessarily satisfy the governing equations given the new geometry. It was therefore necessary for LabVIEW to recalculate the current geometry of the artery in order to determine the actual stresses that the artery was being exposed to and adjust the global parameters accordingly.

First introduced by Wayman et al. (2008), this process is unique in that it can maintain a certain level of stress throughout the duration of an experiment despite an artery's changing geometry or properties, and therefore can prevent the artery from ever restoring baseline values of stress. Therefore, we can maintain an environment that

encourages arterial remodeling and obtain a more accurate depiction of an artery's remodeling capacity. However, unlike Wayman, this method adds the ability to measure the current cross-sectional geometry of the artery at any given point in time and also to prescribe axial stress, all under automated control.

One aim of this research was to examine how various levels of axial stress affect remodeling, independent of shear stress and circumferential stress. Both shear and circumferential stress were maintained at normal physiologic levels (1.5 Pa and 100 kPa, respectively). Preliminary experiments indicated that under an axial stress of approximately 150 kPa, arteries reached and maintained a physiologically normal stretch ratio of approximately 1.5. Therefore, pairs of arteries were tested simultaneously, with one artery exposed to a physiologically normal axial stress of 150 kPa and the other artery exposed to an elevated axial stress of 300 kPa for a total of seven days in organ culture.

### 3.2.3 Mechanical Testing

Two mechanical tests were used to help determine how arteries remodel throughout the culture period. An axial force-length test was used to determine how arteries respond axially to increases in length. A pressure-diameter test was used to gauge the circumferential response of arteries to increased pressures. Both tests were performed prior to and following the culture period.

#### *3.2.3.1 Axial Force-Length Test*

Following the acclimation period, an axial force-length test was performed on each artery. Prior to this test, arteries were stretched through a stretch ratio of

approximately 1.8-2 for 7-10 cycles in order to precondition them. Arteries were kept at zero pressure and a minimum flow rate (30 mL/min) and began the test at a stretch ratio of approximately 1.1 – 1.2. This was done to ensure that there was not any sign of bending in the artery wall, which would have impaired the ultrasound signal used to measure the cross sectional geometry. Arteries were gradually extended in increments of 0.9765 mm until a stretch ratio of at least 1.8 was achieved. A stepwise function that describes the stretching protocol is shown in Figure 6. Note the periodic stretching (at a rate of approximately 1.9 mm/s) between longer intervals of no stretching. During this stretching protocol, the lumen diameter, wall thickness, axial length, and axial force were recorded.

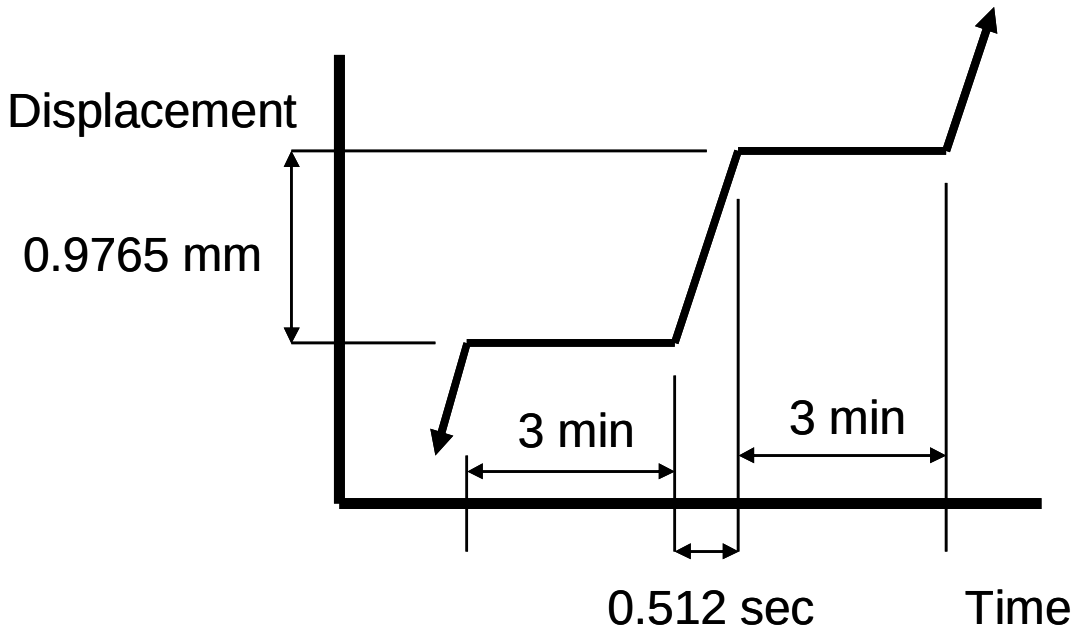


**Figure 6 - Step Wise Displacement Function for Axial Stress-Axial Stress Mechanical Test: Each artery was intermittently stretched at a rate of 1.9 mm/s between longer periods of no stretching**

A similar procedure was used at the conclusion of the organ culture. However, since the unloaded length could not be precisely gauged with the artery still in the tissue chamber, the artery's starting length was set as the shortest length achievable before which the artery would buckle. In other words, the artery was shortened until any part of the artery was no longer parallel to the cannula. The length of the artery at the position just beyond where this buckling occurred was defined as the new unloaded length of the artery and the axial force-length test was repeated.

#### *3.2.3.2 Pressure-Diameter Test*

Following each axial force-length test, a pressure-diameter test was performed. For the pre-culture pressure-diameter test, the artery was maintained at a stretch ratio of 1.5 and a minimum flow rate of 30 mL/min. Pressure in the media reservoir was increased in increments of 10.3 mmHg every three to four minutes while lumen diameter, wall thickness, and intraluminal pressure were recorded.

At the conclusion of the culture period, the second pressure-diameter test was performed. This test was done twice, first at the same length the original pressure-diameter test was performed at, and then at a length equivalent to a stretch ratio of 1.5 at the artery's new length. This was determined using the new artery length obtained in Section 3.2.3.1 Axial Force-Length Test above.

### 3.2.6 End of Experiment

At the conclusion of the experiment, the flow was returned to the minimum flow rate of 30 mL/min, axial stretch was reduced, and transluminal pressure was relieved.

Next, each artery was tested (axial force-length test and pressure-diameter test) as described in 3.2.3 Mechanical Testing.

Following the mechanical tests, the artery was cut from the cannulae and the unloaded length was measured again. The lengths of the segments of artery still sutured onto the cannulae were added to the unloaded length so that the final unloaded length of the artery could be compared to the preliminary unloaded length measured prior to the culture. The artery was then divided into sections for further testing.

### 3.2.7 Biological Endpoints

The following biological markers were used to evaluate changes in the arteries during the culture period. Hematoxylin and eosin staining and a methylthiazol tetrazolium assay gave us a qualitative appreciation of the overall tissue morphology and artery viability, respectively. A $^{3}$H-proline incorporation assay gave us quantitative measures of the arteries' collagen synthesis.

#### *3.2.7.1 Tissue Morphology*

Hematoxylin and eosin (H&E) staining was used to compare the morphology of arterial tissues used in this study. Transverse sections, 5 μm thick, from each sample were deparaffinized and stained for H&E using an auto-stainer (Leica). Hematoxylin stains cell nuclei purple and eosin stains connective tissue pink. Following staining, coverslips were mounted over the sections using Cytoseal 60 mounting medium (Richard-Allan Scientific). Sections were imaged using a Nikon Eclipse E800 microscope.

### *3.2.7.2 Cell Viability*

Methylthiazol tetrazolium (MTT) is a yellowish stain that is converted to a dark blue color by the mitochondria of viable cells. Following culture, arterial ring segments approximately 3 mm in length were statically incubated in 10 mg/mL MTT in deionized water for one hour at 37 degrees Celsius. Pictures were then taken of the ring segments following the incubation period.

### *3.2.7.3 Collagen Synthesis*

Collagen synthesis was measured using a $^{3}$H-proline incorporation assay used by Wayman (2007) who based his method on the method of Peterofsky and Prockop (1962). Proline is an amino acid that is incorporated into cells during the early stages of collagen fiber formation.

Short arterial ring segments approximately 4 mm in length were cut from the artery following organ culture and statically incubated in culture medium supplemented with $^{3}$H-proline (10 μCi/mL). Following a radiolabelling period of 18 hours, segments were washed in a quench solution (PBS supplemented with 0.8 mM sodium sulfate (Sigma) and 1.0 mM L-proline (Sigma)) four times for 30 minutes. Samples were lyophilized and the dry weight was measured. Samples were digested in 0.2-0.4 mg/mL proteinase K (Sigma) in 100 mM ammonium acetate solution (Sigma) overnight at 60 degrees Celsius. The radioactivity was measured using a scinillation counter (Tri-Carb, PerkinElmer) and results were normalized against the tissue sample's dry weight.

# IV. RESULTS AND DISCUSSION

Results demonstrating system performance will be given first in this chapter. The purpose of these data is to demonstrate the ability of both the hardware and software used in this research to achieve and maintain various local mechanical states. The results from two, seven day experiments will also be presented. In these experiments, both the circumferential and shear stresses were maintained at normal physiologic levels while axial stress was experimentally varied. All results will be supplemented with a discussion that includes the significance of the findings.

## *4.1 System Performance*

In order to demonstrate the unique capabilities of this organ culture system, it is important to show that each individual local parameter can be adjusted at will without changing the remaining local parameters. First, results will be given showing the effectiveness of the methodology developed for calculating the arterial geometry (see Section 3.1.2.1 Method of Calculating the Artery Geometry from Ultrasound Signal). The theoretical performance (based on the hardware capabilities) of the system will then be discussed. Finally, the results from a short term experiment will demonstrate the ability of the system to achieve and maintain various levels of stress.

### 4.1.1 Calculation of Artery Geometry

The method of processing the raw ultrasound signals is displayed below in Figure 7. Note that in these sequential graphs, 50 waveforms were summed; however, in the

actual experiments 800 waveforms were summed to enhance the consistency with which the peaks were located. In this example, there are four distinct interfaces which correlate precisely to the four locations where there is a fluid-artery interface. Note how each successive step of the process further differentiates the areas of interest (i.e. the peaks) from the areas not of interest (i.e. the low voltage areas).

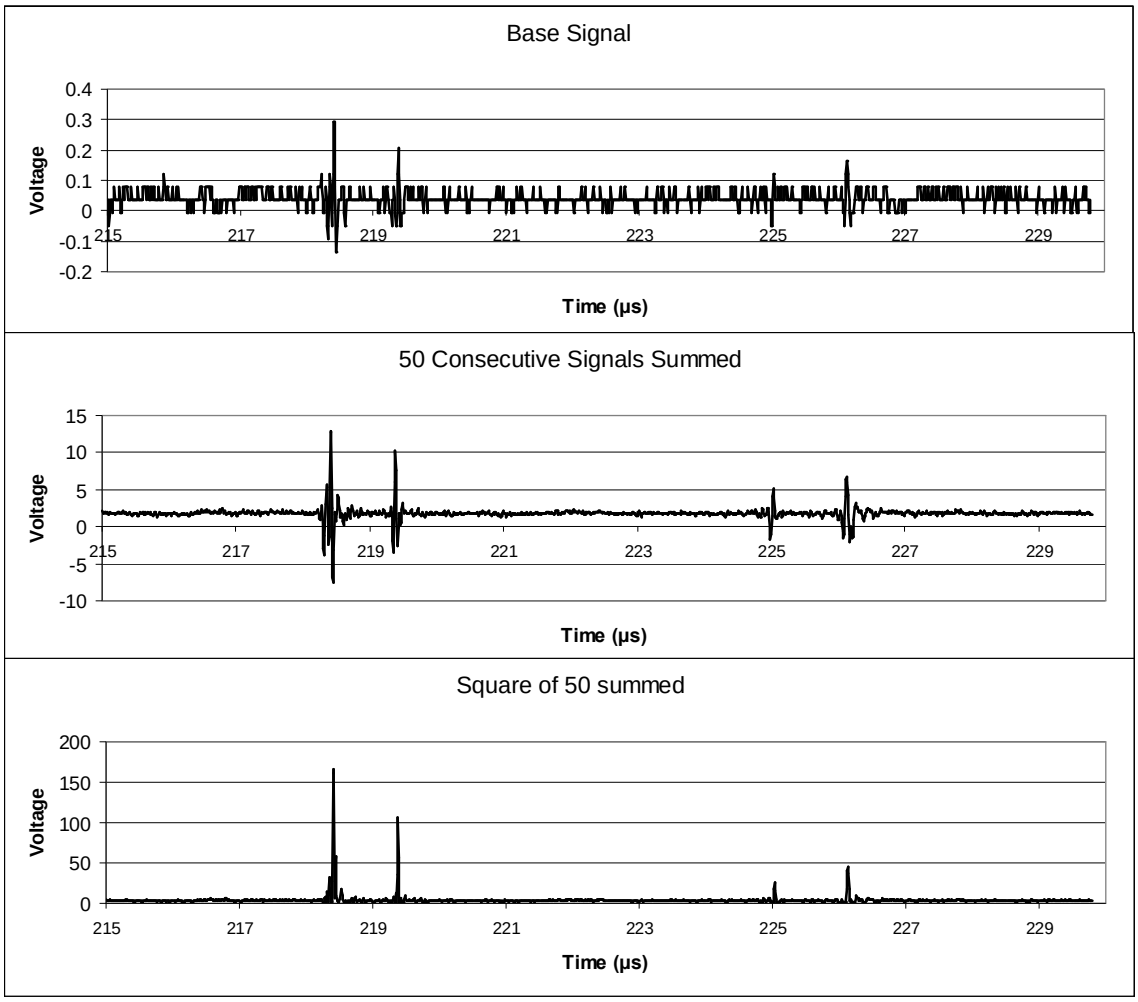


**Figure 7 - Ultrasound Signal Processing: Top, a single raw signal subset showing the maximums and minimums associated with fluid–artery interfaces. Middle, the summation of 50 consecutively sampled raw signals. Notice the clearer differentiation between peaks and noise. Bottom, the square of the middle signal. Notice that the noise is virtually eliminated relative to the height of the four peaks. Note, in the actual experiments, 800 waveforms were summed to ensure the clearest processed signal.**

Figure 8 demonstrates the algorithm of peak detection described above in Section 3.1.2.1 Method of Calculating the Artery Geometry from Ultrasound Signal. The first waveform is the square of the sum of 800 consecutive raw signals. In this case, the fourth peak is the maximum value of this waveform. A peak detection sub-VI notes the time that this peak occurs (x-value) and sets the y-value to zero. In addition, points on either side of the located peak are reduced to zero (the number of points on either side is determined by the user). The second waveform is the resultant waveform after the first peak and its surrounding data points are set to zero. Each successive waveform shown in Figure 8 eliminates one peak from the waveform until all four peak times are located.

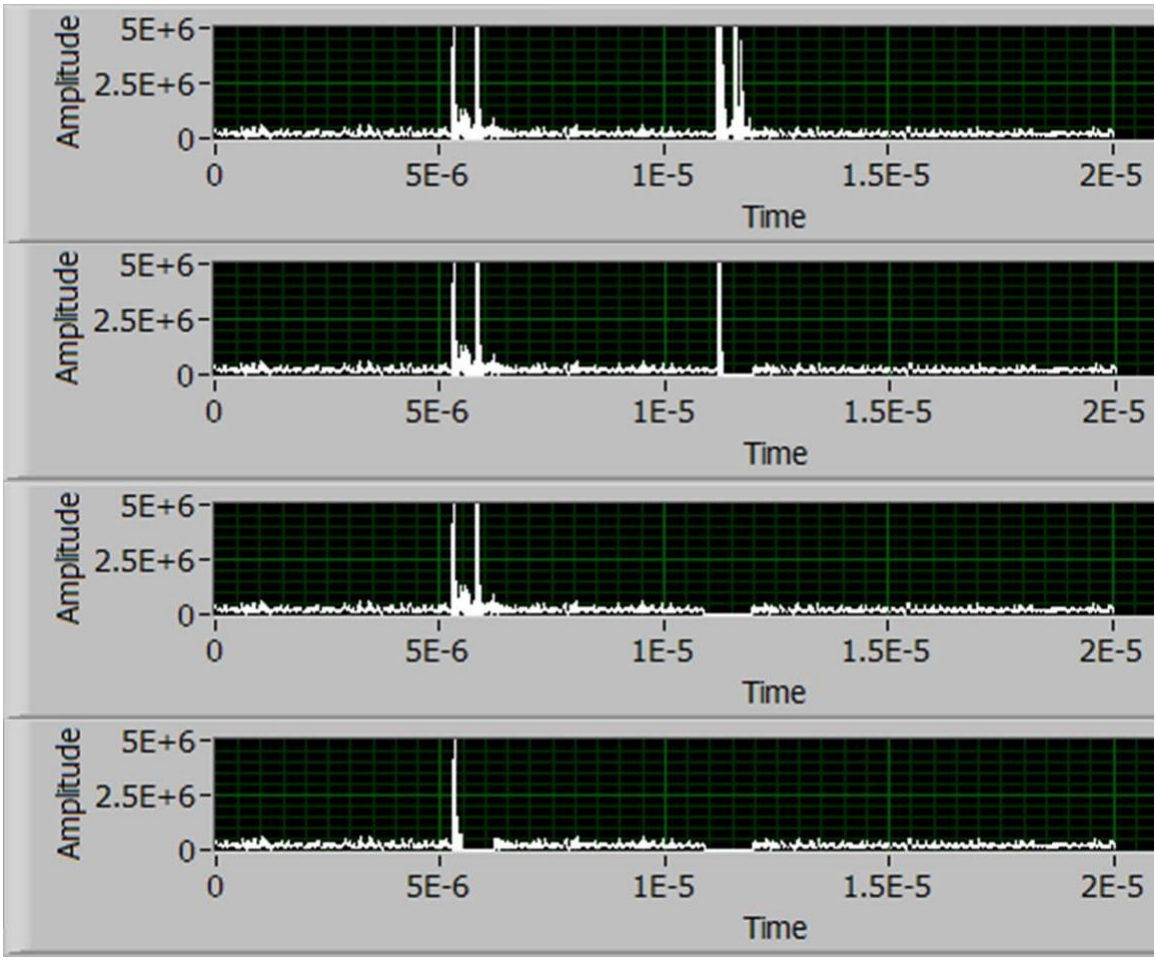


**Figure 8 - Sequential Waveforms Demonstrating Peak Detection Algorithm: Top, the square of 800 consecutively summed raw signals. Second from top, the same waveform after the fourth peak and several surrounding data points are reduced to zero. Second from bottom, the same waveform after the third peak and several surrounding data points are reduced to zero. Bottom, the final waveform after the second peak and several surrounding data points are reduced to zero. The final peak is then determined from this last waveform.**

The four times located above are then used to calculate the artery's geometry using Eq. 1. This process of peak identification and geometry calculation was iterated 8 times during the experiment to obtain an array of dimensions and reduce the possibility of a random error interfering with the system. Figure 9 shows the histograms associated with the array of dimensions (outer diameter on the left, wall thickness on the right). There was typically a high frequency of a specific value with a few occurrences of other

values. All of the values were averaged in order to determine the actual dimension of the artery. Note, that in Figure 9, we iterated the peak detection algorithm 60 times to accentuate the narrow, normal distribution of values that were found.

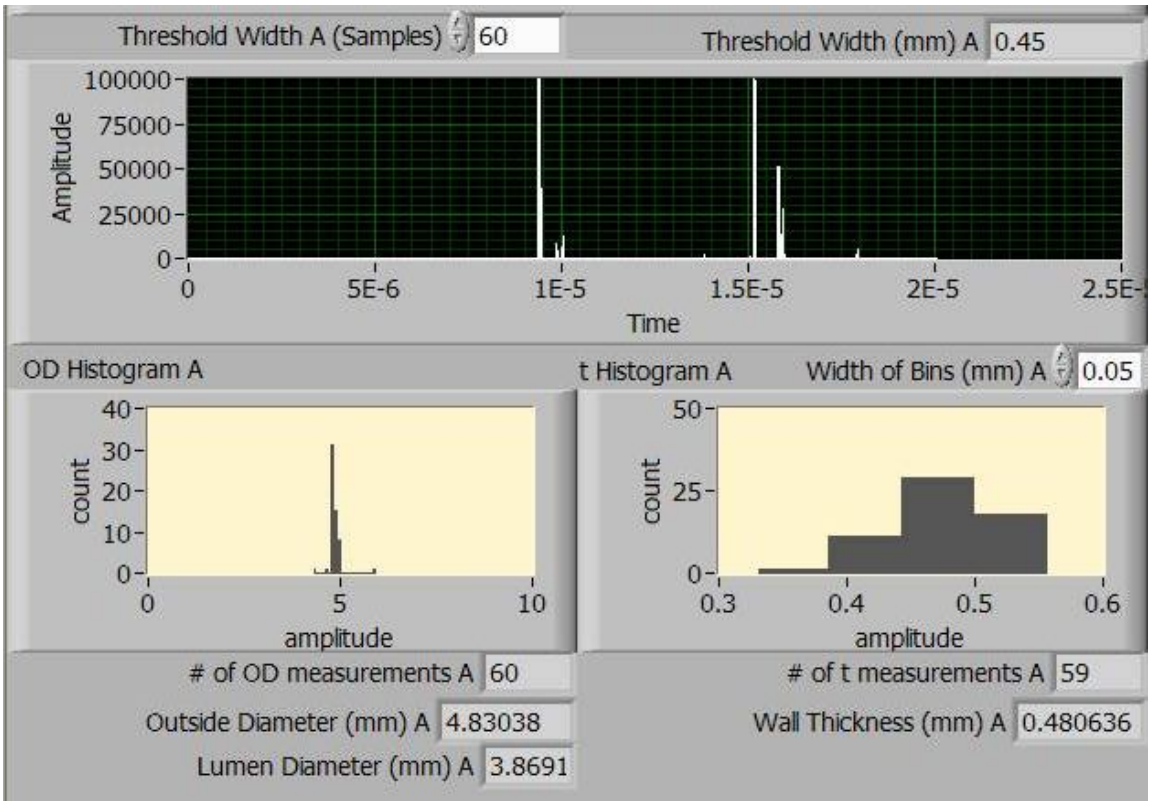


**Figure 9 – Screenshot of LabVIEW Program Showing Waveform and Histograms of Calculated Dimensions: Top, a representative waveform. Middle, histograms of the outside diameters and thicknesses measured from the a total of 60 waveforms. Note the bell shaped distribution. Bottom, the number of usable measurements (out of 60) obtained from the waveforms. Note, how the second peak is relatively small and therefore may not have been detected accurately in one of the iterations (this may be why we have only 59 thickness measurements out of 60 possible). Also, the outside diameter, wall thickness, and lumen diameter are displayed (calculated as the averages of the values in the histograms).**

Table 1 displays the recorded measurements of an artery over a period of approximately 10 minutes. Each successive measurement was made as soon as the hardware would allow. Note the consistency between the measurements. The theoretical

resolution of the ultrasound system (7.5 microns, calculated using the sampling rate of the digitizer and the speed of sound through the various media) is well above the standard deviation witnessed in these measurements.

**Table 1 - Repeatability of Ultrasound Measurements: this table shows the dimensions of an artery as measured using the methodology developed for this research. During these measurements, the global parameters were held constant ($\lambda_z$ = 1.7, Q = 590 mL/min, and P = 90 mmHg). There was approximately 1.5 minutes between measurements. Note that the standard deviation of the measured values is less than the theoretical resolution of the ultrasound system (7.5 microns)**

| | | Lumen Diameter (mm) | Wall Thickness (mm) |
|---|---|---|---|
| Consecutive Measurements | 1 | 6.51035 | 0.39463 |
| | 2 | 6.5065 | 0.39655 |
| | 3 | 6.50458 | 0.39511 |
| | 4 | 6.49976 | 0.39607 |
| | 5 | 6.50073 | 0.39559 |
| | 6 | 6.49976 | 0.39751 |
| Standard Deviation | | 4.3 microns | 1.04 microns |

### 4.1.2 Theoretical System Performance

The following table describes the theoretical limitations of the system based on the minimum and maximum capabilities of the hardware. For these calculations, an artery with a 7 mm outer diameter and 0.4 mm wall thickness was assumed. However, because these dimensions are representative only, actual system performance may differ slightly. The physiologic values for the circumferential, shear, and axial stress are 100 kPa, 15 dyn/cm$^2$, and 150 kPa, respectively.

**Table 2 - Theoretical Performance of the Experimental System: The minimum and maximum achievable stresses are given on the right, based on the minimum and maximum capabilities of the hardware, given an artery with a 7 mm outer diameter and 0.4 mm wall thickness.**

| | Hardware Capabilities | | | Corresponding Stresses | |
|---|---|---|---|---|---|
| | Minimum | Maximum | | Minimum | Maximum |
| Pressure | 0 mmHg | 258 mmHg | Circumferential Stress | 0 kPa | 267 kPa |
| Flow Rate | 30 mL/min | 1000 mL/min | Shear Stress | 0.1 $dyn/cm^2$ | 28.49 $dyn/cm^2$ |
| Axial Force | 0 N | 44.5 N | Axial Stress | 0 kPa | 5365 kPa |

### 4.1.3 Control of Local Parameters

To ensure that the system is capable of achieving and maintaining various levels of stress, a short term (approximately 8 hours) experiment was performed. In this experiment, three stress levels were prescribed for each local parameter. The first condition was a physiologically normal state – 150 kPa for axial stress, 1.5 Pa for shear stress, and 100 kPa for circumferential stress. The second condition was defined as 50% below physiologically normal levels – 75 kPa for axial stress, 0.75 Pa for shear stress, and 50 kPa for circumferential stress. The final condition was defined as 50% above physiologically normal conditions – 225 kPa for axial stress, 2.25 Pa for shear stress, and 150 kPa for circumferential stress. After normal physiologic levels were achieved for all three local parameters, each local parameter was changed to 50% above and below its physiological normal level. The time course for this experiment can be seen in Figure 10. In this figure and all figures following, each local parameter was normalized by its respective physiologically normal level (150 kPa for axial stress, 1.5 Pa for shear stress, and 100 kPa for circumferential stress.)

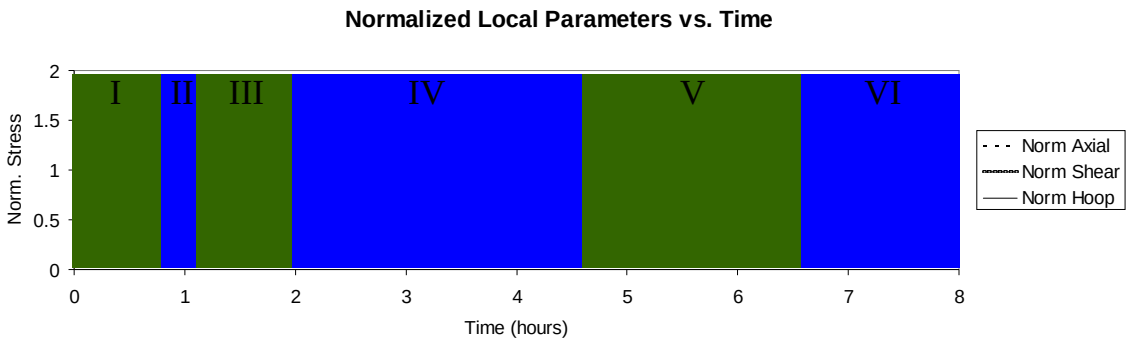


**Figure 10 - Time Course of Normalized Local Parameters: Each local parameter was individually changed through 50% above and below its physiologically normal state. Each local parameter was normalized by its physiologically normal level (150 kPa for axial stress, 1.5 Pa for shear stress, and 100 kPa for axial stress).**

A more detailed look at the individual regions shown in Figure 10 will allow a more complete examination of the system's capabilities. Figure 11 shows a closer look at Regions I and II from Figure 10. At the start of this experiment, the artery was pressurized to approximately 80 mmHg and a shear stress of 300 mL/min. It was also lengthened to 60mm (from an unloaded length of 44mm). The justification of this "preloading" is described in Section 3.2.2 Method for Independently Controlling the Local Parameters. Because of this preloading, the axial stress, shear stress, and circumferential stress all begin at a nonzero level. However, all three parameters are below their prescribed levels of stress. In Region I, all three local parameters move towards achieving their prescribed local parameters. In Region II, all three parameters have achieved their prescribed levels of stress, and maintain this level through Region II.

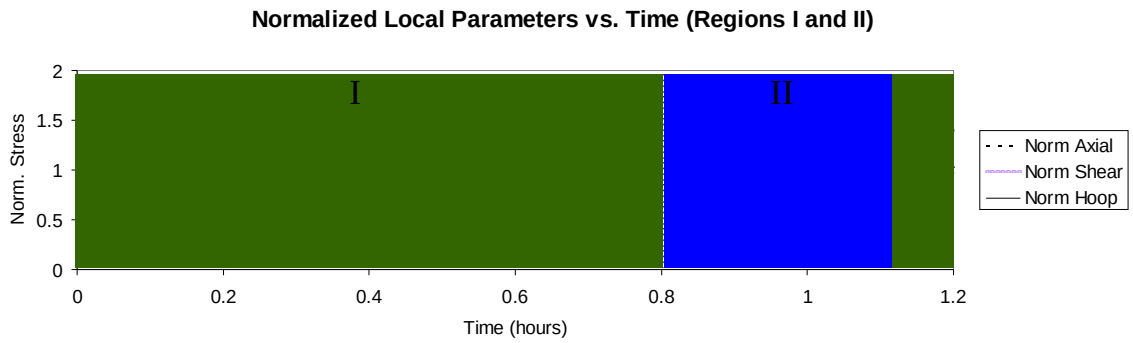


**Figure 11 - Time Course of Normalized Local Parameters, Regions I and II: Region I is the adjustment period. At the beginning of the experiment, values of stress were prescribed. However, because the artery began the experiment at some state other then the desired stress state, a period of adjustment was necessary. Region II shows the local parameters after they have achieved the prescribed level of stress.**

Figure 12 shows Regions III and IV in detail (from Figure 10). At the start of Region III, shear stress was prescribed to a superphysiologic level (50% above normal). Once this level was achieved, it a subphysiologic level (50% below normal) was prescribed. Once this was achieved and maintained, shear stress was returned to a normal level. Region IV is the result of a similar change to the axial stress.

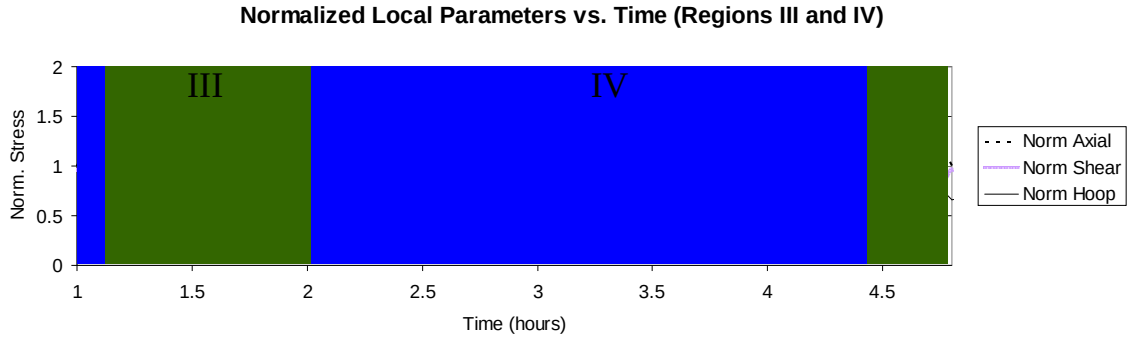


**Figure 12 - Time Course of Normalized Local Parameters, Regions III and IV: In Region III, shear was first adjusted to 50% above its physiologically normal level. Once this was achieved, it was adjusted to 50% below its physiologically normal level. Finally, shear stress was returned to its physiologically normal level. A similar protocol was performed during Region IV, except axial stress was the local parameter being adjusted.**

Figure 13 is a detailed view of Regions V and VI from Figure 10. In Region V, circumferential stress is first reduced (to 50% below physiologic levels). After circumferential stress is maintained at this reduced level of stress, it is increased to 50% above physiologic levels. Finally it is returned to a normal level. In Region VI, all three local parameters are returned to their physiologically normal levels and held there until the end of the experiment.

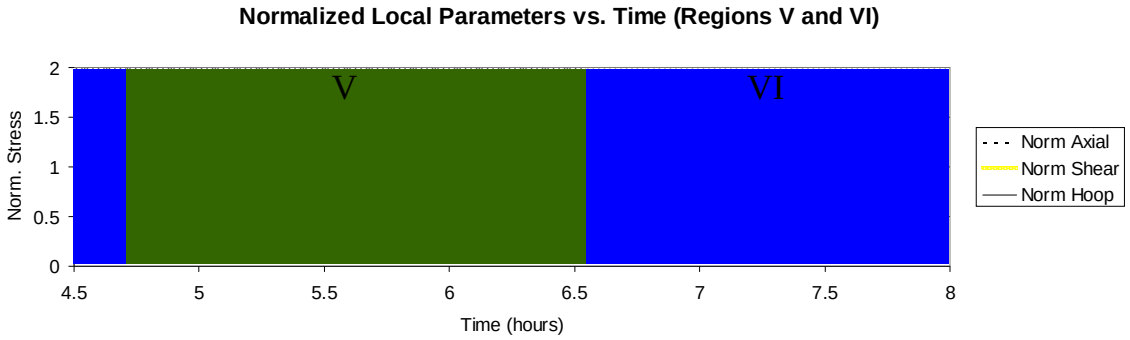


**Figure 13 - Time Course of Normalized Local Parameters, Regions V and VI: Region V shows circumferential stress as it is adjusted from a normal level to a subphysiologic level, a superphysiologic level, and finally returned to normal. Region VI shows the conclusion of the experiment where all three parameters were returned to and held at their normal levels.**

Note that in all of the preceding figures, the parameters which were not being adjusted were maintained at all times. This is not the same thing as keeping the global parameters constant. From Figure 14, it is apparent that the global parameters must cooperatively vary quite a bit in order to maintain specific levels of stress. For example, while shear stress is typically associated the control of flow, we do not see a direct correlation. In Figure 10, shear stress is maintained at a normal physiologic level from hours 2-8. However, in Figure 14, flow rate varies dramatically over that period in order

to accommodate changing arterial geometry caused by the adjustment of other global parameters.

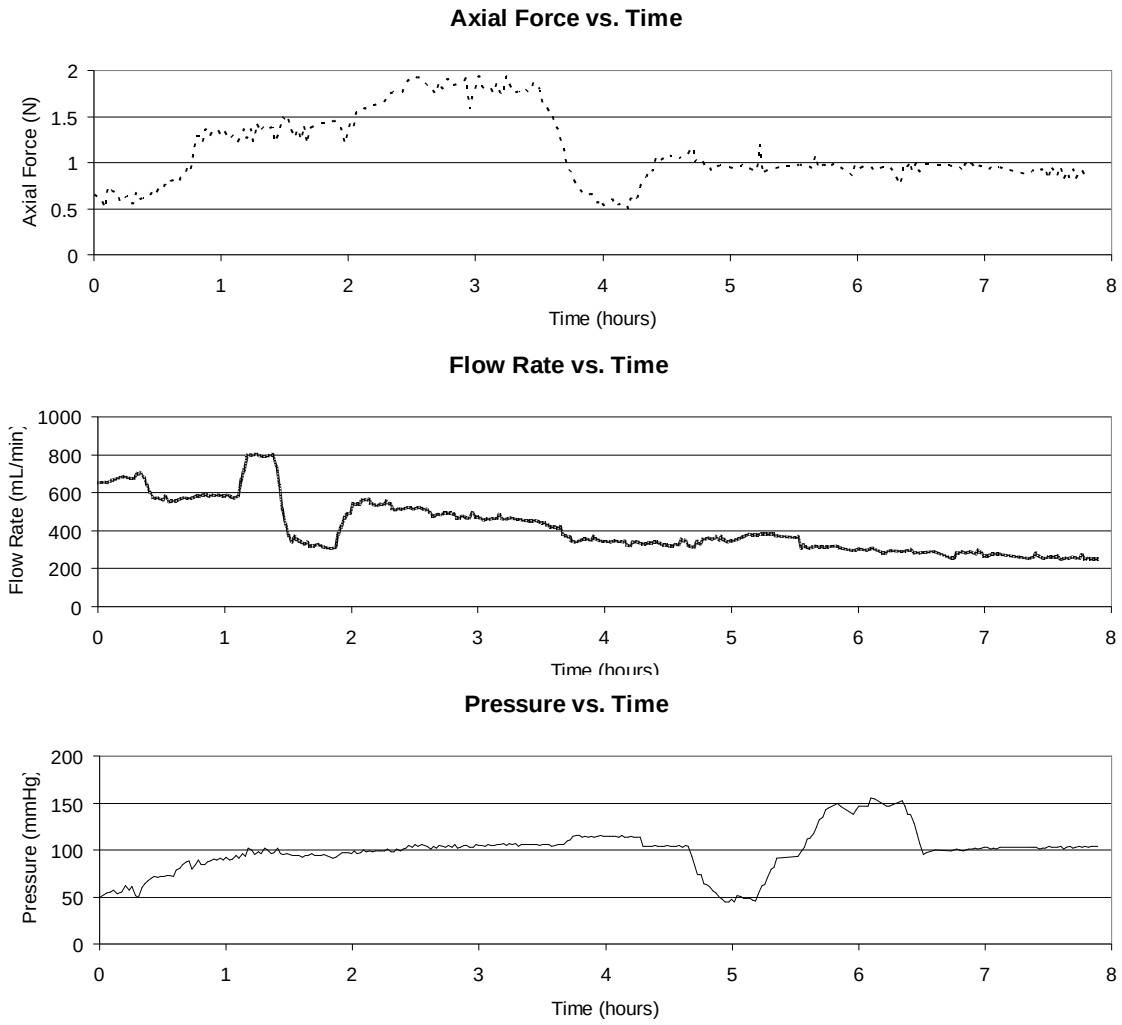


**Figure 14 - Time Course of Global Parameters: This figure shows how the global parameters were adjusted through the course of the experiment described above. Note that while shear stress was maintained at a constant level from hours two through eight, the flow rate changed significantly.**

Table 3 quantifies the ability of the experimental system in maintaining specified levels of stress. After eliminating periods of adjustment (Region I and any area where the stress was moving towards achieving a new level of stress), each value for each local

parameter was categorized as subphysiologic, physiologic, or superphysiologic. At each level, the average and standard deviation of the local parameter values were calculated. All three parameters were fairly successful in achieving their prescribed level of stress, as well as maintaining them within a small deviation.

**Table 3 - Ability of Experimental System in Achieving Desired Local Parameters: The average value and standard deviation of all three local parameters was calculated three times, once for each level of stress that was prescribed. The adjustment period (Region I in Figure 10) was not included in these calculations. Also, the periods of time when the stresses were changing to a new level were ignored. While the prescribed levels of stress were not achieved exactly, the difference between the average value and prescribed value is very small for all local parameters.**

| | Subphysiologic Level | | Physiologic Level | | Super-physiologic Level | |
|---|---|---|---|---|---|---|
| | Ave. | St. Dev. | Ave. | St. Dev. | Ave. | St. Dev. |
| Axial Stress (kPa) | 75.74 | 5.26 | 155.21 | 8.59 | 222.91 | 8.17 |
| Shear Stress ($dyn/cm^2$) | 8.10 | 0.21 | 14.97 | 0.93 | 21.29 | 0.16 |
| Circumferential Stress (kPa) | 51.17 | 2.95 | 99.07 | 2.29 | 148.02 | 3.93 |

There are a number of potential reasons why the local parameters did not more accurately achieve the prescribed levels. For shear stress, the resolution of the peristaltic pump (increments of 10 mL/min) was not ideal. This meant that if the required flow rate fell on any number that was not an increment of 10 mL/min, the pump could only round to the nearest 10. At most, this would account for a 5 mL/min discrepancy; and considering experimental flow rates typically reached a few hundred mL/min of fluid, this would explain a few percentage points of error. Another likely culprit is inherent in the calculation of shear stress. Shear stress is inversely proportional to the cube of the lumen diameter. Therefore, a slight change in the geometry of the artery would result in

a dramatic change in the shear stress. All else being the same, a decrease in lumen diameter from 5 mm to 4.95 mm (a 1% change) would result in a 3.1% increase in calculated shear stress. Slight changes in lumen diameter are not only possible but extremely likely due to the vasomotor response of the artery. Lastly, this issue may be the result of a programming choice. Flow rate is controlled in LabVIEW by first reading the output voltage of the peristaltic pump and then converting that voltage into a flow rate. A new flow rate is determined and converted back into a voltage which is then sent to the peristaltic pump. While this approach seems logical enough, it warrants further examination as to whether this introduces too much error into the calculations. Because each conversion (from voltage to flow or flow to voltage) requires an equation that only approximates the actual voltage/flow relationship, each conversion equation is associated with a small error. Because the program utilizes two such conversions in its flow rate algorithm, we may be introducing twice the error than necessary.

The probable culprits for errors in the axial stress are likely the method used in calculating the force or the hardware problems with the cannula seal. Because there are several assumptions made in calculating the axial force (see Section 3.1.2.2 Method of Calculating the Axial Force for a complete discussion on the limitations of this method), the axial force measurement introduces some error. Also, this observation prompted us to try to reduce the friction at the seal as much as possible. One way this was done was to keep the seal as loose as possible without causing any leaks. However, in doing so, sometimes a small leak would develop. As the seal leaked, the media would tend to dry, and cause the sliding cannula to stick in certain locations. While typically less than 1 mL

of media was lost this way, it may have had a significant effect on the axial force readings for all experiments.

While the preceding paragraphs point to possible causes of the errors seen in this experiment, it also acts to prove the resiliency of the system. Despite all potential difficulties in accurately achieving various levels of stress, this system was able to do so within a small percentage of error.

Through the entire process described above, no user interaction was necessary, other than to change the prescribed stress values as desired. This is a significant advantage over previous organ culture systems which required more human involvement to adjust the global parameters. Despite the automation of the feedback loop, the process must be monitored periodically to ensure that the ultrasound signal being used to calculate artery dimensions accurately depicts the artery's cross section. One other organ culture study has used ultrasound transducers to measure the wall thickness of arteries. Zulliger et al. (2002) used an ultrasonic transducer and experienced some difficulties in measuring the dimensions of the artery at high pressures (when the lateral movement of the artery wall reduced the ultrasound signal) or if the artery wall 'fluttered.' Such difficulties were overcome with this system (specifically the signal processing described in Section 3.1.2.1 Method of Calculating the Artery Geometry from Ultrasound Signal); however, similar difficulties existed at high pressures when the ultrasound signal was reduced. Therefore, a more complex signal processing scheme may be required to more accurately and consistently extract the dimensions of the arteries from the ultrasound signals.

Despite the small errors in achieving the desired levels of stress, no past research has attempted to independently control all three local parameters. This novel system can therefore facilitate complete control of the local mechanical environment in organ culture studies. The independent effect of any local parameter can be examined without any confounding results that arise from studies that use systems incapable of controlling the remaining two local parameters. Additionally, the interaction between multiple parameters can be studied. Because complete control over the local mechanical parameters (which ultimately drive remodeling) can be realized, it is possible to obtain a more thorough understanding of the growth and remodeling phenomenon.

## *4.2 Elevated Axial Stress Experiments*

Two experiments were performed, each comparing two artery segments exposed to different levels of axial stress, but identical levels of shear stress and circumferential stress. This was done to further gauge the ability of the organ culture system to maintain a specific local mechanical environment as well as examine the effect that an independent change on axial stress has on arterial remodeling. For a period of approximately seven days, two segments of the same artery were maintained at physiologically normal levels of shear stress (1.5 Pa) and circumferential stress (100 kPa). The control artery was maintained at a physiologically normal level of axial stress (150 kPa). The experimental artery was maintained at a physiologically elevated level of axial stress (300 kPa). For the purposes of the following discussion, the experiments will be referred to as experiment 1 and experiment 2. For each experiment, the artery exposed to normal levels of axial stress (150 kPa) will be referred to as the control artery and the artery exposed to high levels of axial stress (300 kPa) will be referred to as the experimental artery.

All experiments began with an initial adjustment period, where the local parameters were given time to achieve their prescribed levels. During this period, data was taken and the global parameters were adjusted approximately every 3-5 minutes per chamber. After the user felt the local parameters were satisfactorily achieved, the duration between iterations was increased to approximately 2.5 hours. This increased time between iterations limited the workload on the hardware and software. Also, because remodeling occurs on a time scale of days to months, such limited sampling of the data was deemed justifiable.

### 4.2.1 System Performance

For both experiments, the ability of the system to achieve and maintain various levels of stress will be discussed, similar to Section 4.1.3 Control of Local Parameters. In this section, the main purpose is to provide further evidence that the experimental system developed for this research is capable of achieving and maintaining a specific local mechanical environment despite changes in the artery's geometry throughout a seven day culture. This section will detail the time course of the global parameters and artery dimensions to give a better understanding of how the local mechanical environment was maintained and also give insight into the behavior of the deformed artery through culture. Note that the changes in arterial dimensions mentioned in this section are not necessarily attributable solely to remodeling, as the global parameters are changing throughout the experiment.

#### *4.2.1.1 Experiment 1: Control Artery*

Figure 15 and Figure 16 display the time course of the control artery from experiment 1. Figure 15 shows the entire experiment while Figure 16 focuses on the initial few hours of adjustment. In this experiment, the control artery was exposed to an axial stress of 150 kPa, a shear stress of 1.5 Pa, and a circumferential stress of 100 kPa. In Figure 15, notice that the shear stress was at zero during the first day. This was because during the first night of the experiment, the peristaltic pump overheated and the system did not perfuse any media. Once this was noticed the following morning, the problem was corrected and flow was allowed to increase to the level defined by the system algorithm. Despite this setback during the experiment, the data taken was still determined to be useful since remodeling driven by altered levels of shear stress generally occur on a long time scale (relative to the experiment) on the order of weeks to months. In other words, the low shear conditions should not have impacted the remodeling of the artery in the time span of this experiment, especially considering how quickly flow was returned.

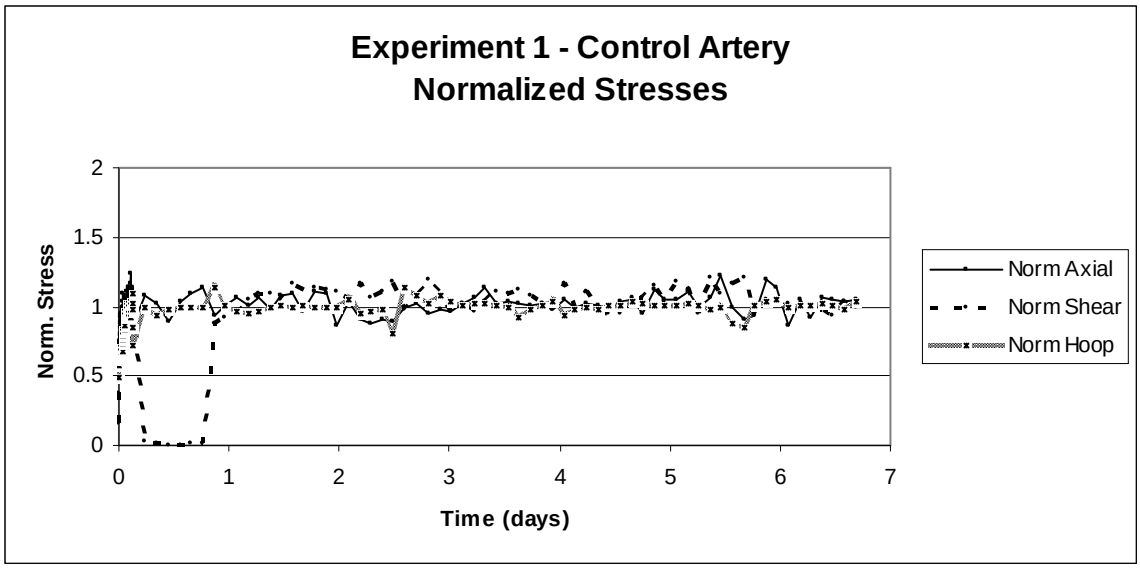


**Figure 15 - Time Course of Local Parameters, Control Artery: This graph shows how each of the three local parameters was achieved and maintained throughout the culture period. During this experiment, axial stress, shear stress, and circumferential stress were prescribed values of 150 kPa, 1.5 Pa, and 100 kPa. During the first night of the experiment, the peristaltic pump overheated and did not perfuse any media (the shear stress was zero during this period). However, once this was noticed the following morning, shear stress was quickly restored to its prescribed level.**

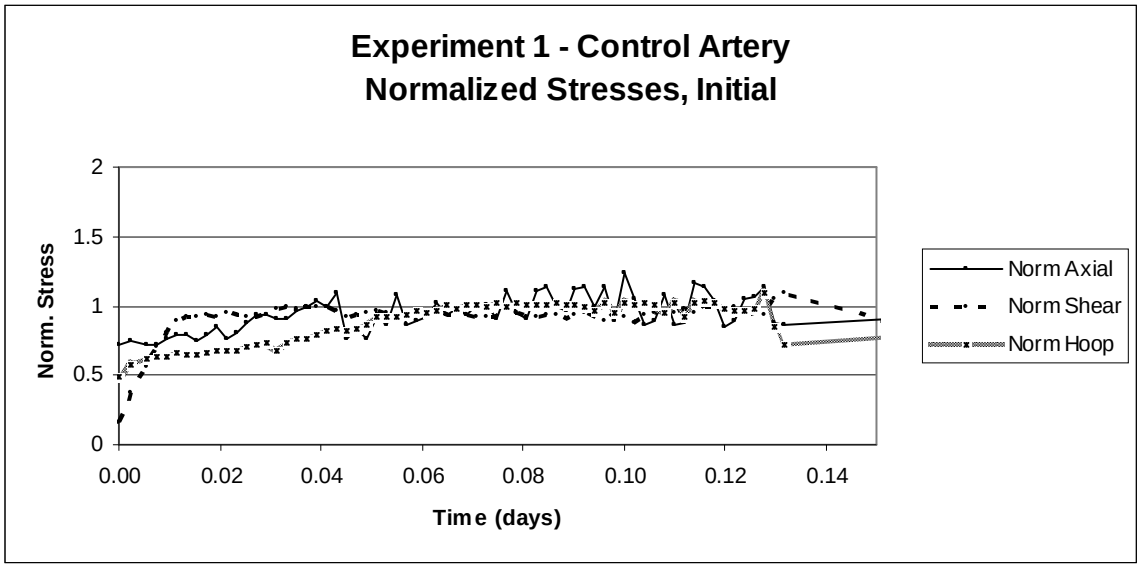


**Figure 16 - Time Course of Local Parameters, Control Artery, Initial Adjustment Period: This graph is a close up look at the initial few hours of the experiment depicted in Figure 15. Note that the local parameters were initially below their prescribed values (less than 1), but soon achieved and maintained steady values near 1.**

Table 4 summarizes the system's ability to maintain the prescribed local parameters throughout the experiment. These values were calculated after the initial adjustment period when the local parameters were below their prescribed values. If we examine the standard deviation as a percentage of the prescribed value, we see relatively little deviation of the circumferential stress (5.01/100 or about 5%), axial stress (11.47/150 or 7.6%) and shear stress (1.16/15 or 7.7%).

**Table 4 - Average and Standard Deviation of Local Parameters, Control Artery: The following data were collected after the initial adjustment period. Also, because the flow was stopped during the first night of the experiment, shear stress values that were calculated during this time were not included in the average and standard deviation shown here.**

| | Prescribed | Average | Standard Deviation |
|---|---|---|---|
| Axial Stress (kPa) | 150 | 152.89 | 11.47 |
| Shear Stress (dyn/cm$^2$) | 15 | 15.90 | 1.16 |
| Circumferential Stress (kPa) | 100 | 99.72 | 5.01 |

Figure 17, Figure 18, and Figure 19 display the artery's dimensions throughout the experiment. Note that all these dimensions were taken during the experiment, and therefore represent the artery's dimensions in its loaded state. The changes in the diameters of the artery seem to correspond to the changes seen in the wall thickness (e.g. an increase in diameter(s) leads to a decrease in wall thickness). However, it is important to note that the dramatic changes in cross sectional geometry witnessed during the first two days of this experiment were atypical. However, this could likely be explained by the pump malfunction described earlier. If we examine the period of time at the beginning of the experiment when the shear stress was zero, it appears that the artery was dilating, and the wall thickness decreasing. This was possibly the artery's attempt to restore baseline levels of shear stress in its low shear stress environment. However, once

shear stress was restored, approximately 18 hours into the experiment, the artery began constricting and behaving more generally like the arteries in other experiments. During the first two days of the experiment, the artery appeared to exhibit significant creep (Figure 19). However, after day two, the artery length remained virtually unchanged. During this same time period (days two through seven), the artery's diameters were increasing and wall thickness were decreasing. This suggests some "softening" of the artery, considering the artery's volume did not change throughout the experiment (see Section 4.2.2 Artery Dimensions).

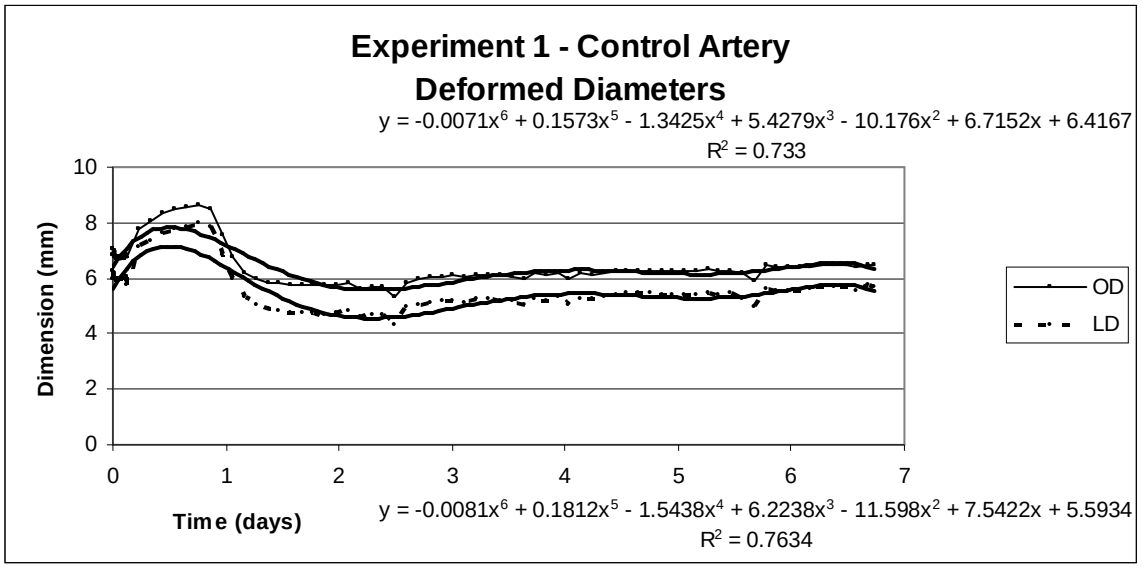


**Figure 17 - Time Course of Deformed Lumen Diameter and Outer Diameter, Control Artery: These two data sets represent the outer diameter (top plot) and lumen diameter (lower plot). The polynomial trend lines (top equation for outer diameter, bottom equation for lumen diameter) show how the artery does not maintain a constant geometry throughout the culture period.**

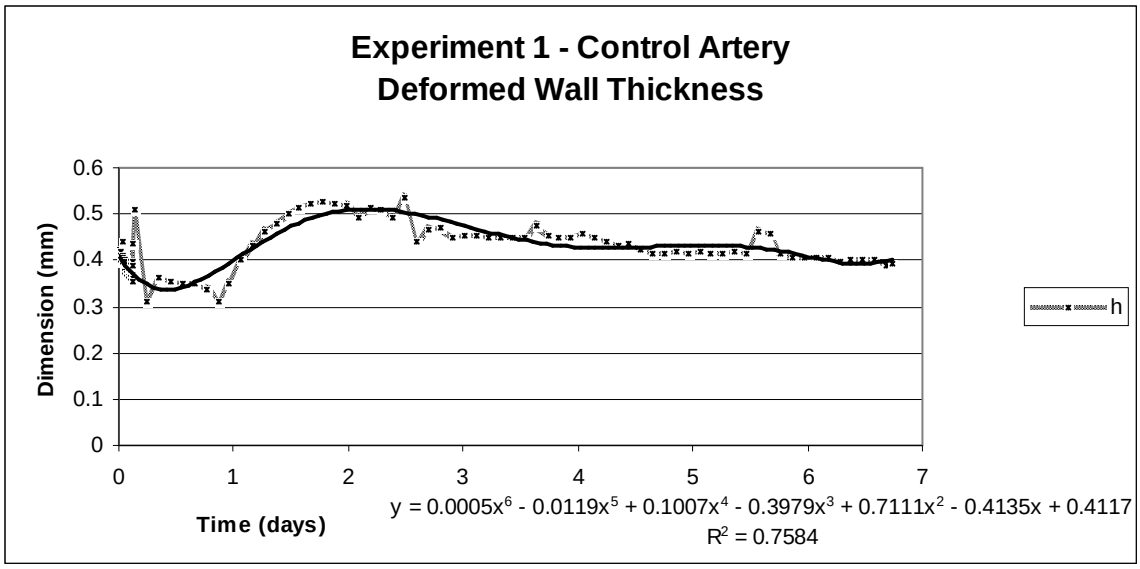


**Figure 18 - Time Course of Deformed Wall Thickness, Control Artery: The polynomial trend line gives a better perspective on the overall tendency of the wall thickness over time. The dramatic changes in geometry seen in the beginning of the experiment correspond to the changes seen in the diameters (Figure 17) under the assumption of incompressibility.**

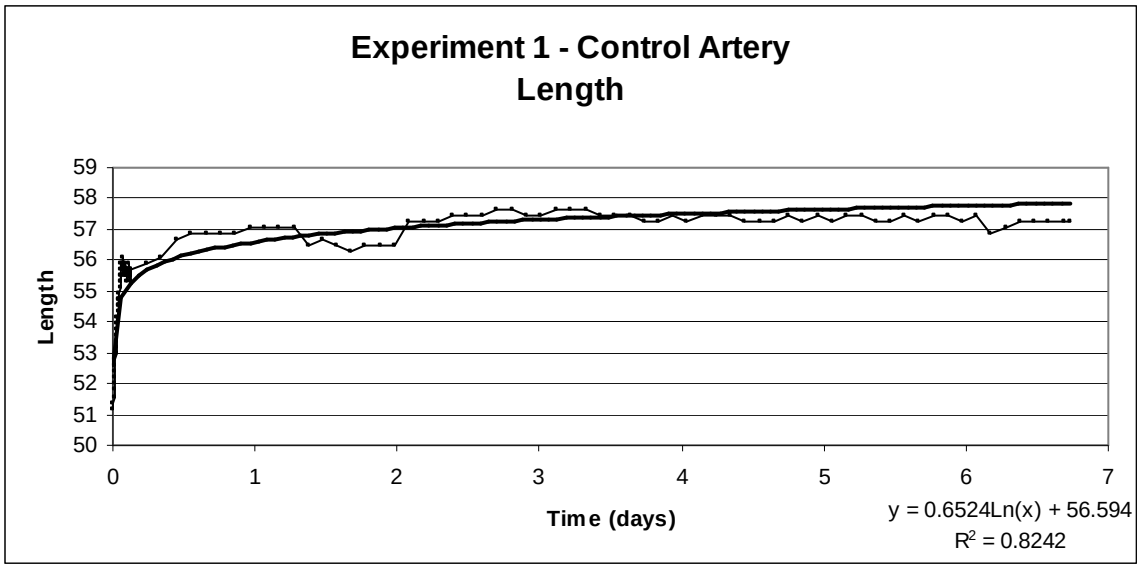


**Figure 19 - Time Course of Artery Length, Control Artery: The artery lengthens logarithmically, with a more dramatic increase in length seen earlier in the experiment. The lengthening seen here may be creep since arteries tend to behave as viscoelastic materials. Note the axial force (Figure 20) does not change much during the experiment.**

Figure 20 contains three plots of the global parameters throughout the experiment. In order for the local parameters to be maintained in as narrow a range as is depicted in Figure 15, the global parameters needed to be adjusted significantly – specifically the flow and pressure. At the beginning of day two the flow rate and pressure were approximately 250 mL/min and 160 mmHg, respectively. By the end of the experiment, these values had changed to 400 mL/min and 110, respectively. These changes occurred in response to the geometrical changes shown in Figure 17, Figure 18, and Figure 19.

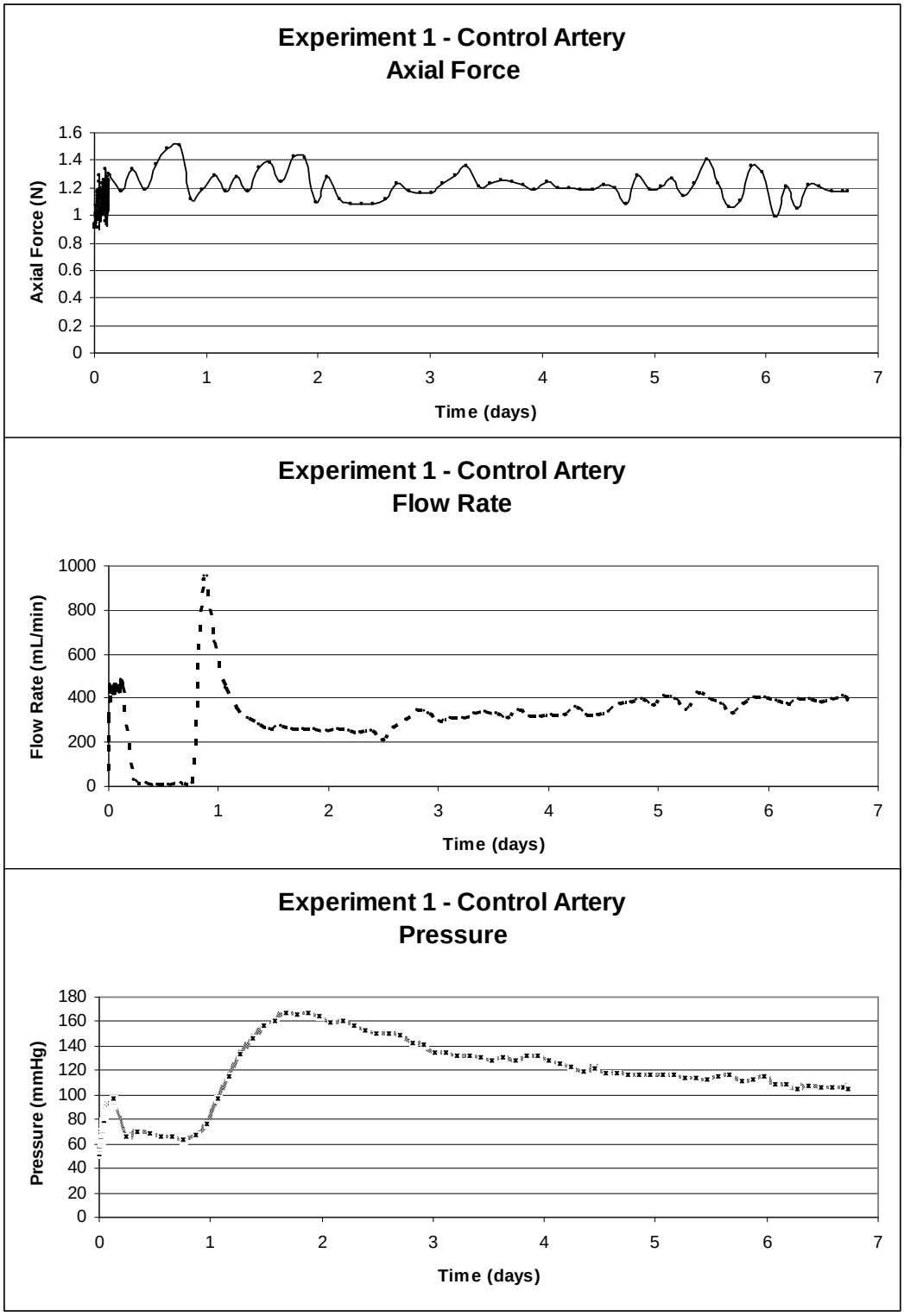


**Figure 20 - Time Course of Global Parameters, Control Artery: Note how each of the global parameters needed to be changed throughout the course of the experiment in order to maintain the levels of the local parameters. Due to the changing artery geometry, pressure and flow needed to be adjusted significantly in order to maintain the prescribed levels of stress.**

#### *4.2.1.2 Experiment 1: Experimental Artery*

Figure 21 shows the time course of the local parameters throughout the entire experiment. Because axial stress was elevated in this experiment, the axial stress plot converges toward 2 (300 kPa normalized by 150 kPa). Figure 22 depicts the first few hours of this same experiment. During the first few hours, we once again see how the local parameters moved toward their prescribed values after beginning the experiment well below these values.

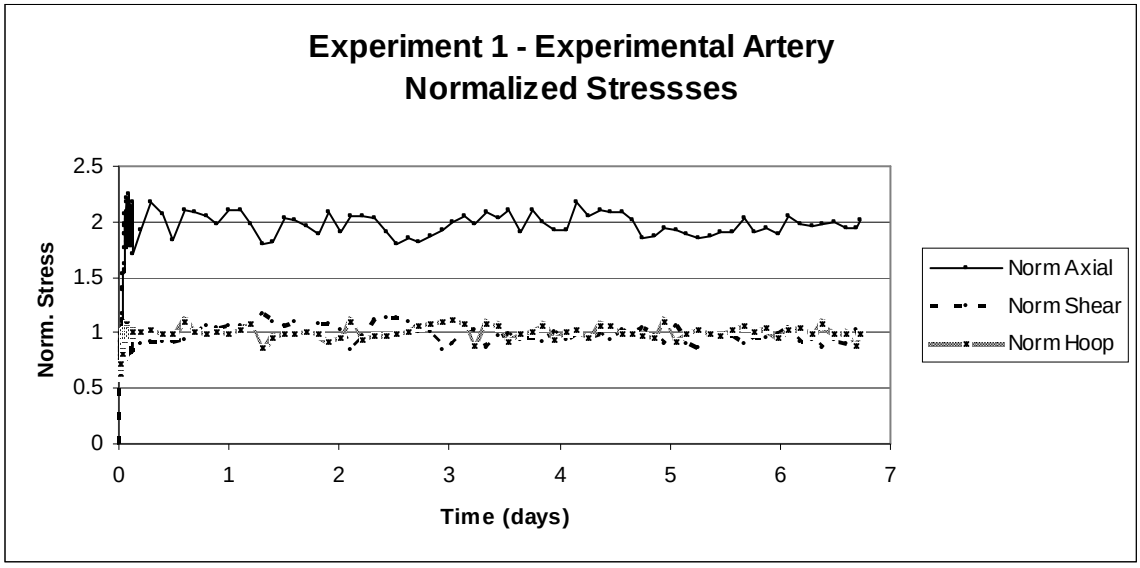


**Figure 21 - Time Course of Local Parameters, Experimental Artery: This graph shows how each of the three local parameters was achieved and maintained throughout the experiment. During this experiment, acial stress, shear stress, and circumferential stress were prescribed values of 300 kPa, 1.5 Pa, and 100 kPa. Note that the axial stress for this artery was doubled relative to the control artery (held at 150 kPa axial stress).**

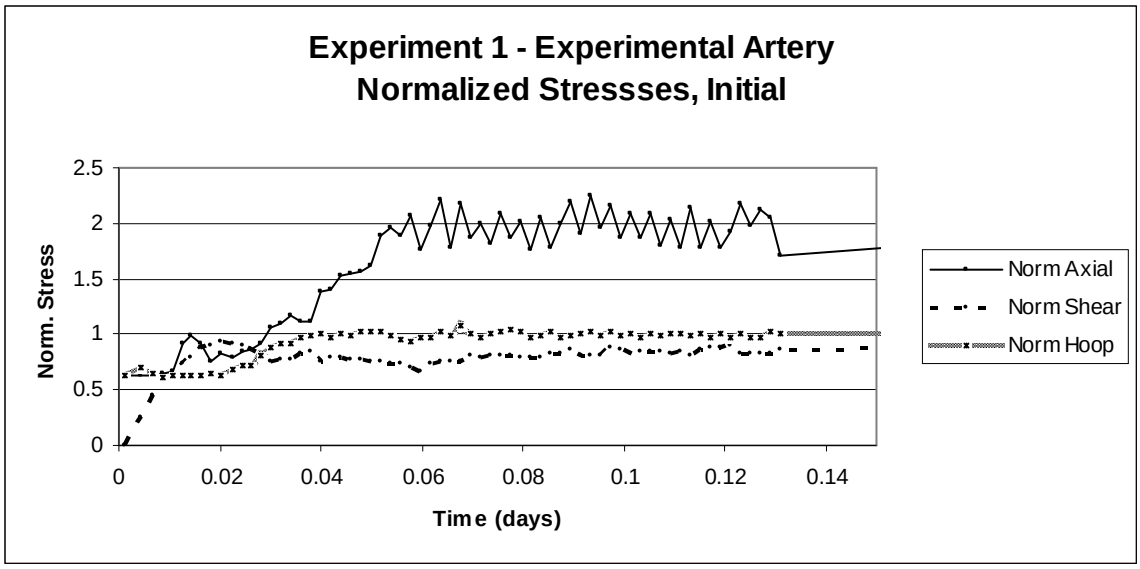


**Figure 22 - Time Course of Local Parameters, Experimental Artery, Initial Adjustment Period: This graph is a close up look at the initial few hours of the experiment depicted in Figure 21. Once again, the local parameters began the experiment below the prescribed values, but were able to achieve and maintain them relatively quickly.**

Table 5 summarizes the system's performance. This artery exhibited similar deviation from the prescribed values as the control artery in this same experiment. This validates the system's ability to maintain two different, constant stress environments simultaneously.

**Table 5 - Average and Standard Deviation of Local Parameters, Experimental Artery: The following data were collected after the initial adjustment period. Note the similar deviation between these data and the data from the control artery (Table 4)**

| | Prescribed | Average | Standard Deviation |
|---|---|---|---|
| Axial Stress (kPa) | 300 | 296.32 | 14.25 |
| Shear Stress (dyn/cm$^2$) | 15 | 14.75 | 1.16 |
| Circumferential Stress (kPa) | 100 | 100.46 | 5.68 |

Figure 23 and Figure 24 show the cross sectional dimensions of the artery over time. Note the similarity to the control artery (Figure 17 and Figure 18) with the

exception of the initial dilation. If we assume the dilation seen at the beginning of the control artery experiment was due to the low shear conditions, both the control artery and experimental artery exhibit similar behavior through the culture. Initially, there is a constriction, followed by a slower less pronounced dilation. Figure 25 shows the artery length over time during culture. While there is a similar viscoelastic creep seen at the beginning of the experiment, there appears to be little change of length throughout the experiment.

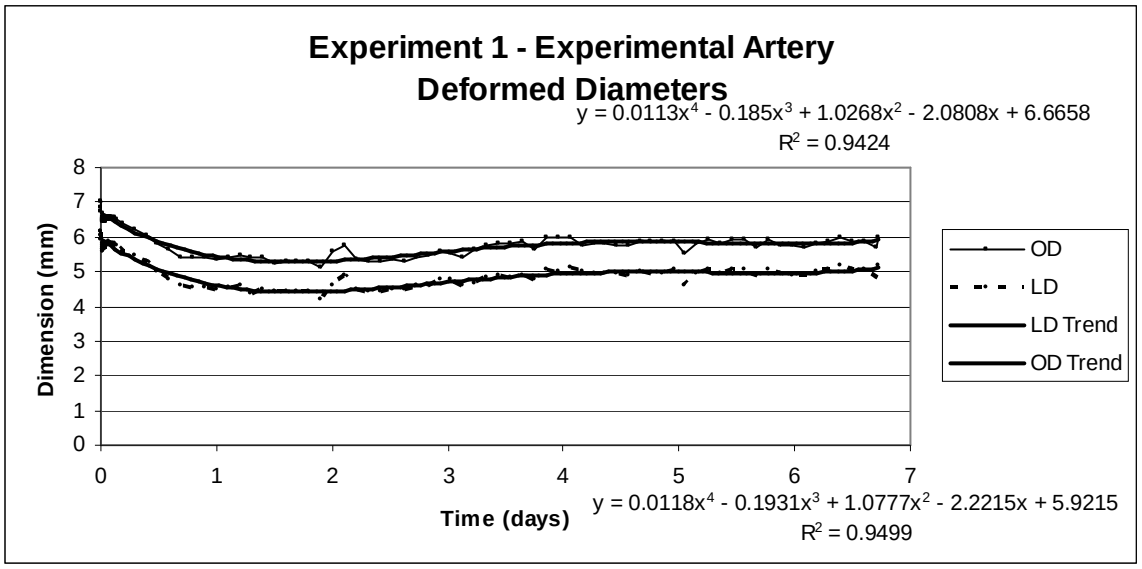


**Figure 23 - Time Course of Deformed Lumen Diameter and Outer Diameter, Experimental Artery: These two data sets display the measured outer diameter (top) and lumen diameter (bottom) of the experimental artery. The polynomial trend lines show the general behavior of the artery throughout the experiment. The equation for outer diameter trendline is on top of the graph, while the equation for the lumen diameter trendline is located below the graph.**

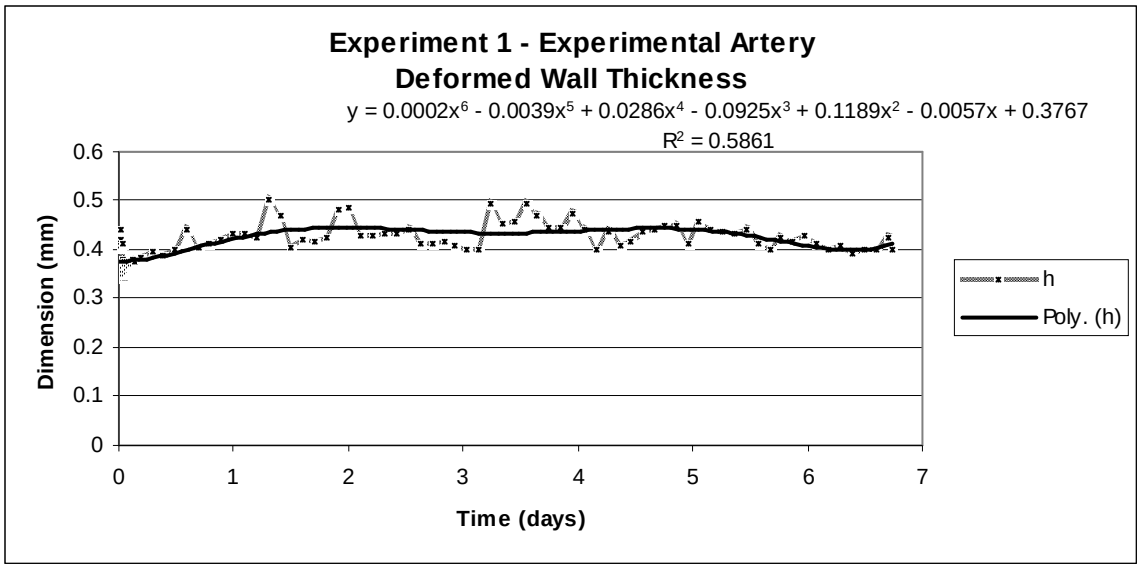


**Figure 24 – Time Course of Deformed Wall Thickness, Experimental Artery: The polynomial trend line which overlays the data set displays the general behavior of the artery through the culture period. Once again, the changes seen here correspond to the changes seen in the diameters (Figure 23**

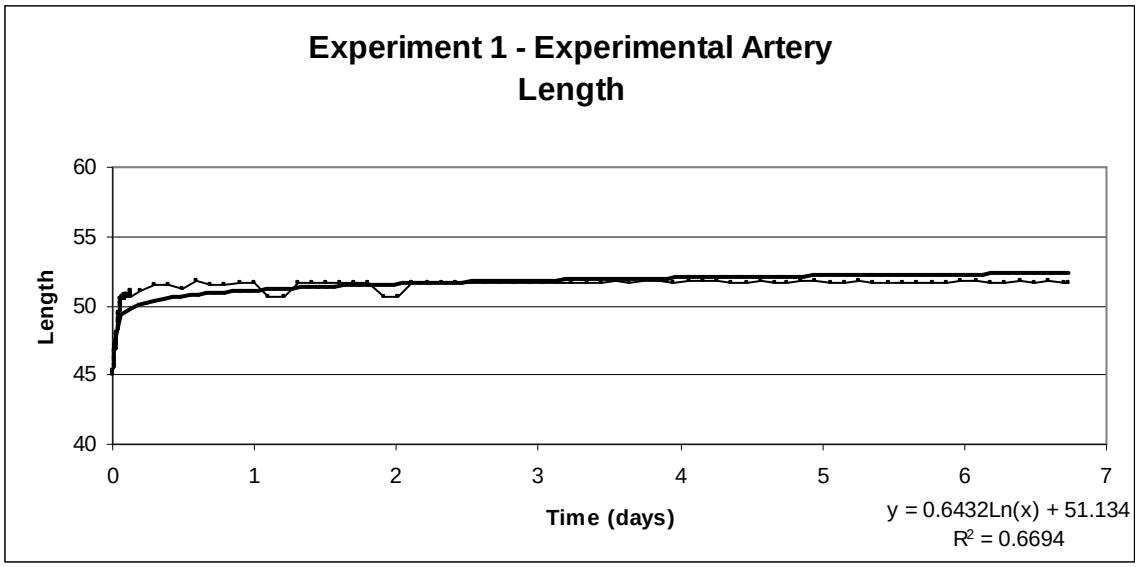


**Figure 25 - Time Course of Artery Length, Experimental Artery: The artery lengthens logarithmically, similar to the control artery. However, in general, there is relatively little change in length throughout the experiment.**

Figure 26 shows the corresponding time course of the global parameters through the culture period. Similar to the control artery, there is a need to change the global parameters such that the local mechanical environment is maintained. This is further evidence that a system which is capable of selecting global parameters that satisfy the local parameters given an ever changing arterial geometry is necessary for studies on arterial remodeling.

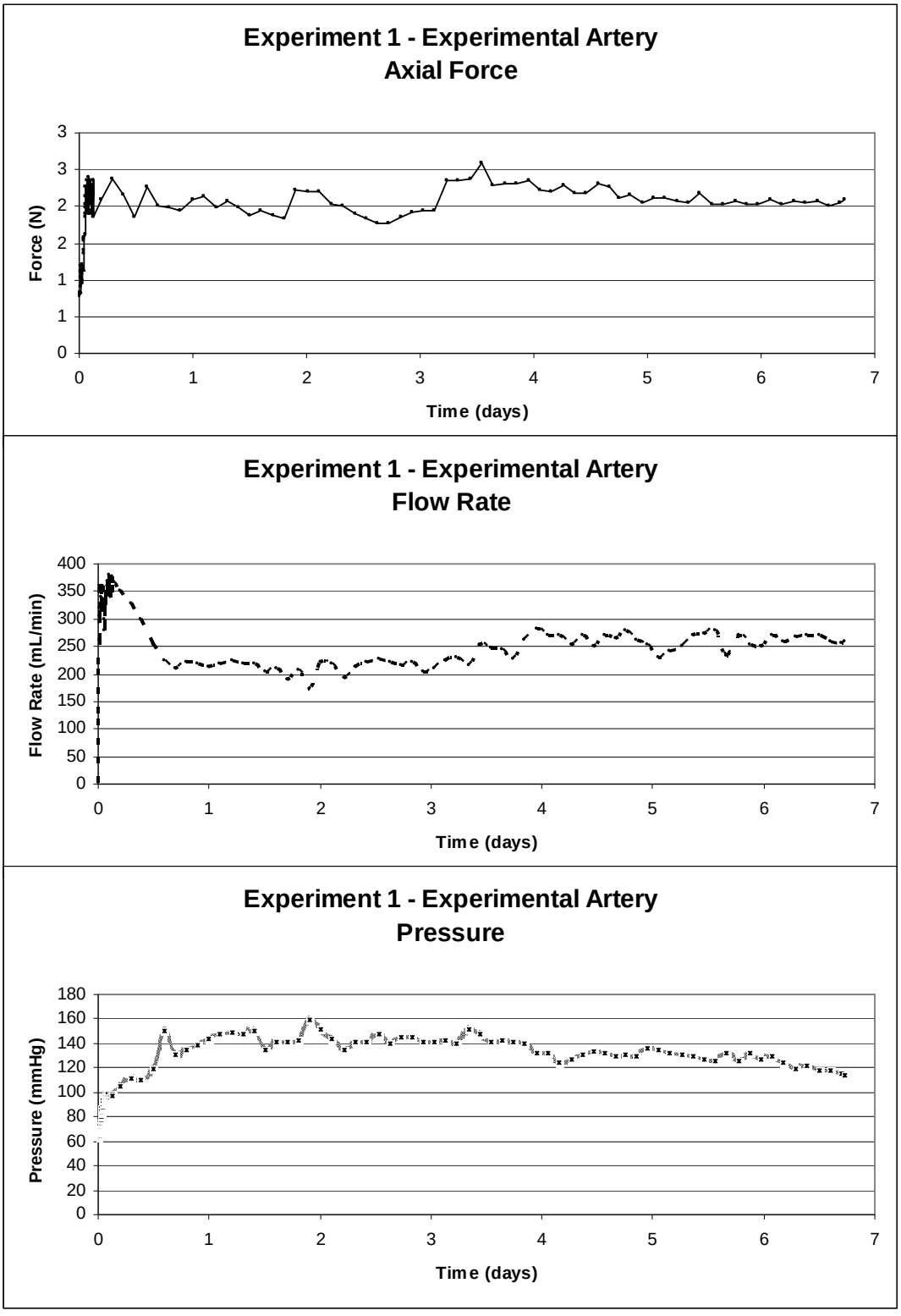


**Figure 26 - Time Course of Global Parameters, Experimental Artery: Once again, through the culture period, significant changes needed to be made to the global parameters, specifically flow rate and pressure in order to maintain a constant level stress environment.**

#### *4.2.1.3 Experiment 2: Control Artery*

Figure 27 shows the normalized stresses experienced by the control artery in the second experiment. Once again, note the convergence to a normalized value of 1 throughout the experiment. Figure 28 gives a detailed view of the first few hours of the experiment. This view shows the period of adjustment where the local parameters gradually moved towards their prescribed values.

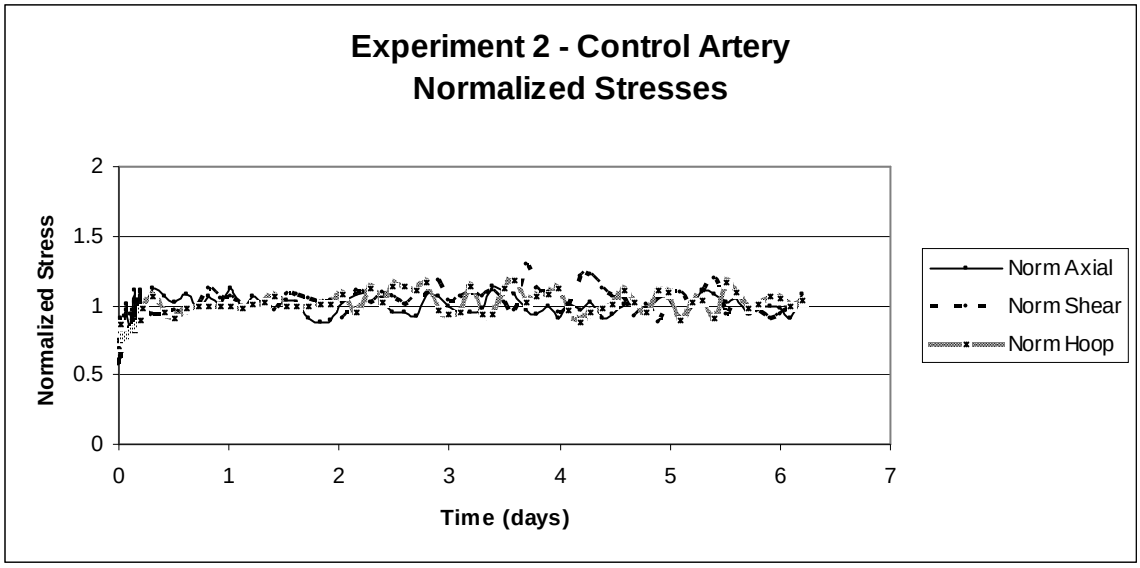


**Figure 27 - Time Course of Local Parameters, Control Artery: This graph shows the three local parameters over time. During this experiment, axial stress, shear stress, and circumferential stress were prescribed values of 150 kPa, 1.5 Pa, and 100 kPa, respectively.**

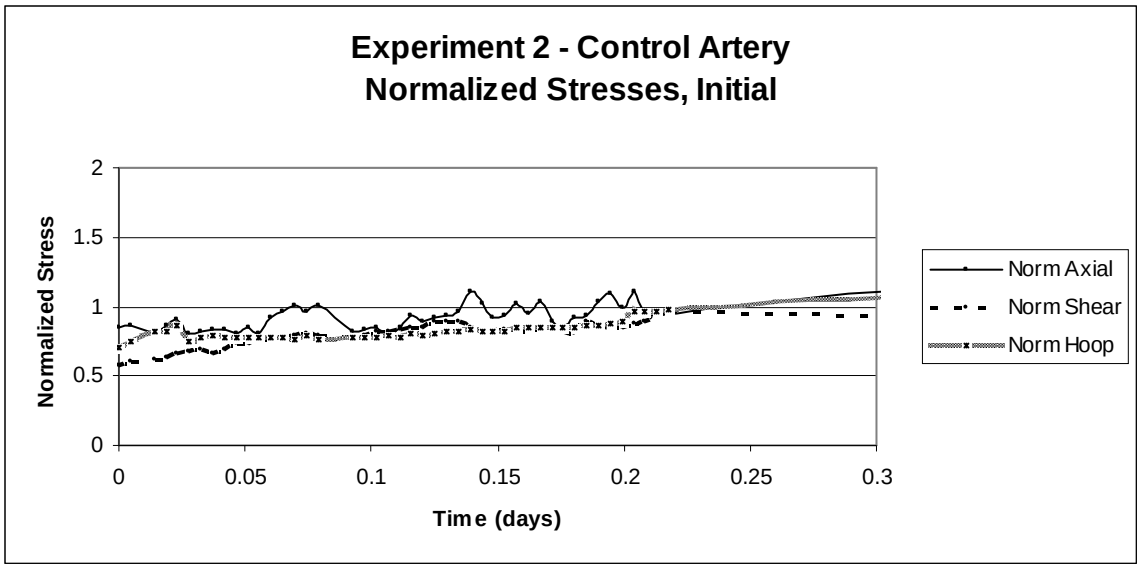


**Figure 28 - Time Course of Local Parameters, Control Artery, Initial Adjustment Period: This graph shows the first few hours of the experiment shown in Figure 27. All three stresses begin the experiment as values less than their prescribed level, but achieve their prescribed level within the first few hours.**

Table 6 is a quantitative summary of the system's ability to maintain the prescribed local parameters throughout the experiment. Note how similar these data are to the data from experiment 1.

**Table 6 – Average and Standard Deviation of Local Parameters, Control Artery: The following data were collected after the initial adjustment period. Specifically, note that the deviations are small relative to the prescribed values of stress.**

| | Prescribed | Average | Standard Deviation |
|---|---|---|---|
| Axial Stress (kPa) | 150 | 151.17 | 9.91 |
| Shear Stress (dyn/cm$^2$) | 15 | 15.62 | 1.26 |
| Circumferential Stress (kPa) | 100 | 102.30 | 7.38 |

Figure 29 displays the diameters of the control artery. Once again, the artery's diameters shrink at the beginning of the experiment, but increase after about day one through the end of the experiment. As a corollary, the wall thickness (Figure 30)

thickens at the beginning of the experiment and thins somewhat from day one through the end of the experiment. There is also an increase in length seen at the beginning of the experiment (Figure 31) that is similar to the results from experiment 1. This is followed by a long period of relatively little change in length.

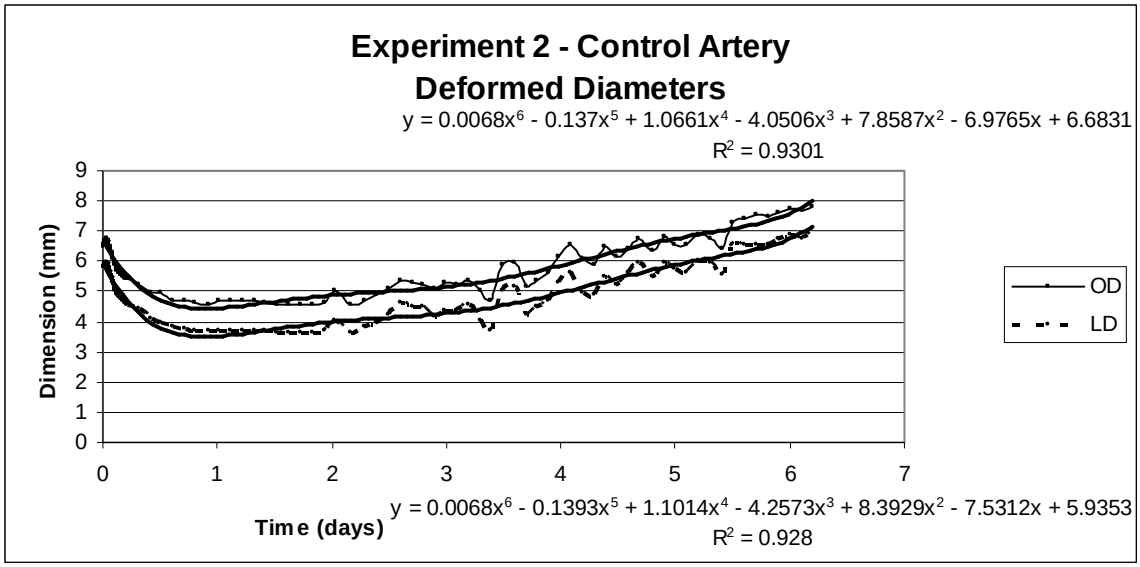


**Figure 29 - Time Course of Deformed Lumen Diameter and Outer Diameter, Control Artery: These two data sets represent the outer diameter (top plot) and lumen diameter (lower plot). The polynomial trend lines (top equation for outer diameter, bottom equation for lumen diameter) show how the artery does not maintain a constant geometry throughout the culture period. Note how similar the behavior is to experiment 1 (an initial reduction in diameter followed by an increase until the end of the experiment).**

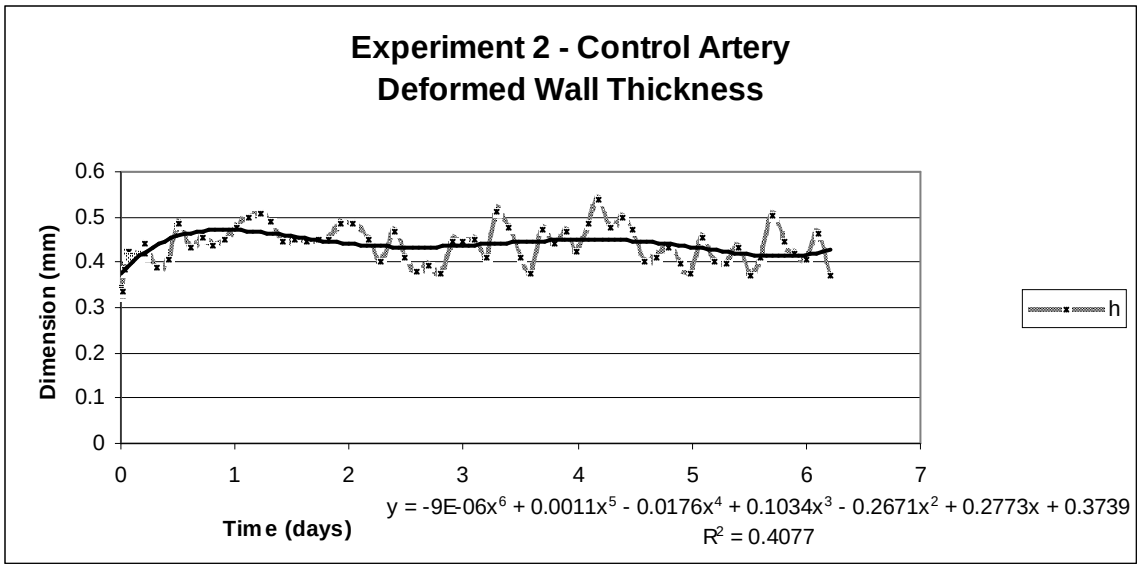


**Figure 30 - Time Course of Deformed Wall Thickness, Control Artery: The polynomial trend line gives a better perspective on the overall tendency of the wall thickness over time. Note that at the beginning of the experiment when the diameter is dramatically shrinking, the wall is thickening. Also, as the diameters increase, the wall tends to shrink, as evidenced by the trend line.**

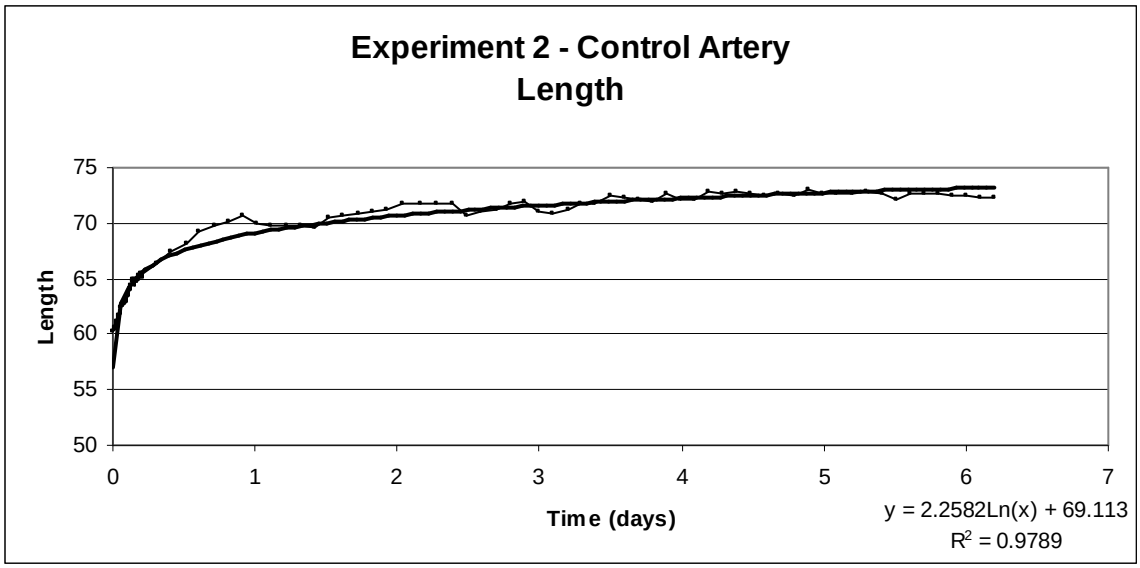


**Figure 31 - Time Course of Artery Length, Control Artery: The artery lengthens logarithmically, with a more dramatic increase in length seen earlier in the experiment. The lengthening seen here may be creep since arteries tend to behave as viscoelastic materials. However, since the axial force does not remain constant during the experiment, it may not necessarily be creep.**

Figure 32 displays the global parameters that created the desired local environment. For this artery, all three global parameters changed significantly in order to maintain a constant level of stress. This is because of the changes in the artery's geometry over that same period of time. Because shear stress is inversely proportional to the cube of the inner diameter, the flow rate was significantly different throughout the experiment, increasing nearly eight-fold between days two and seven. A method that maintained constant global parameters throughout organ culture would tend to cause changes in the local parameters as dramatic as the changes in the global parameters seen here.

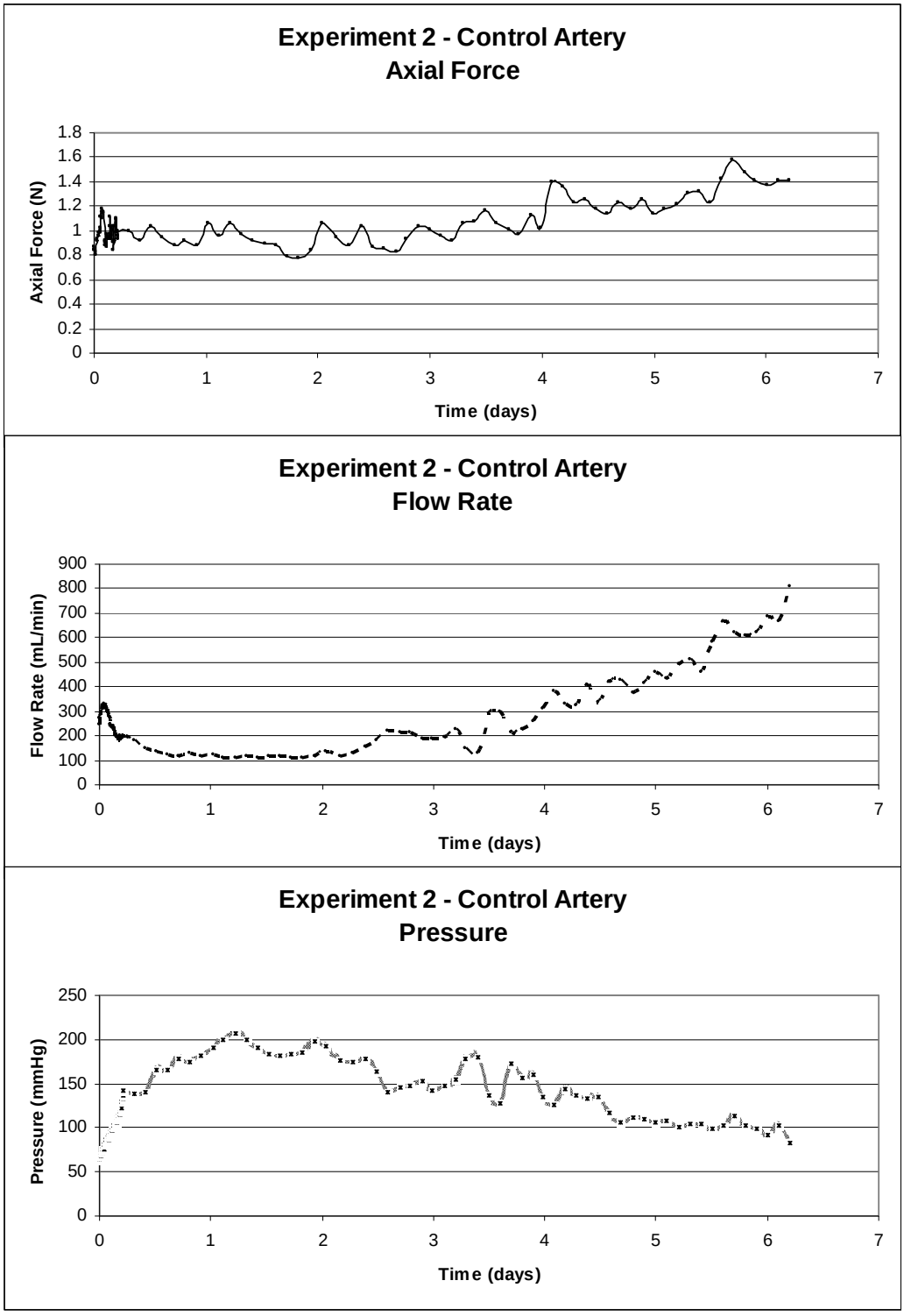


**Figure 32 - Time Course of Global Parameters, Control Artery: Note how dramatically all three global parameters must change throughout the experiment in order to maintain constant levels of stress.**

#### *4.2.1.4 Experiment 2: Experimental Artery*

Figure 33 shows the time course of the local parameters throughout the entire experiment. Because axial stress was elevated in this experiment, the axial stress plot converges towards 2 (300 kPa normalized by 150 kPa). Figure 34 depicts the first few hours of this same experiment. During the first few hours, the local parameters move toward their prescribed values and maintain them through the experiment once achieved.

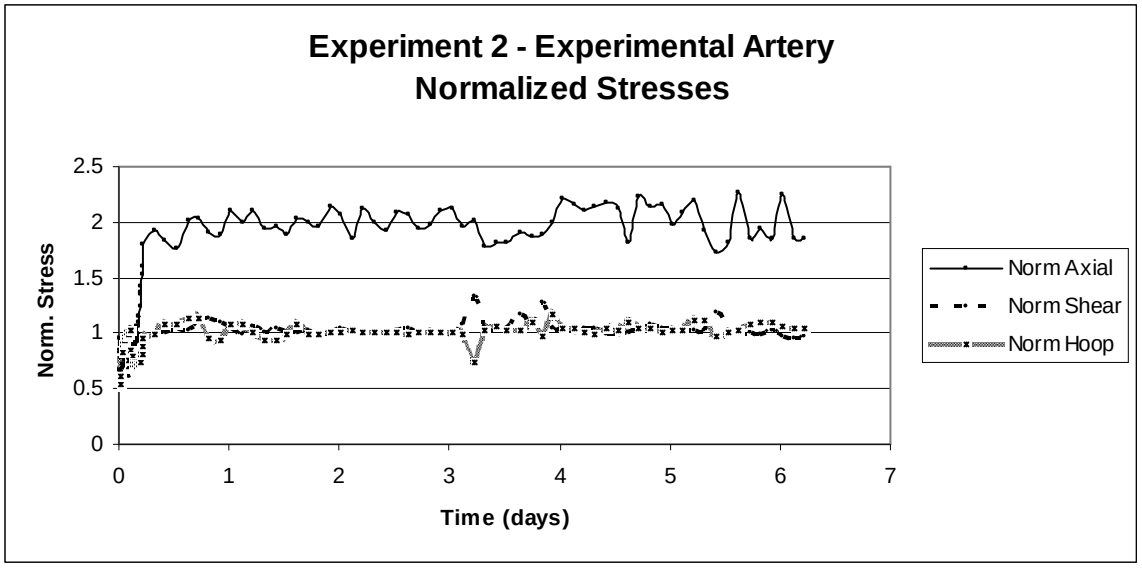


**Figure 33 - Time Course of Local Parameters, Experimental Artery: This graph shows how each of the three local parameters was achieved and maintained throughout the experiment. During this experiment, axial stress, shear stress, and circumferential stress were prescribed values of 300 kPa, 1.5 Pa, and 100 kPa. Note that the axial stress for this artery was doubled relative to the control artery (held at 150 kPa axial stress).**

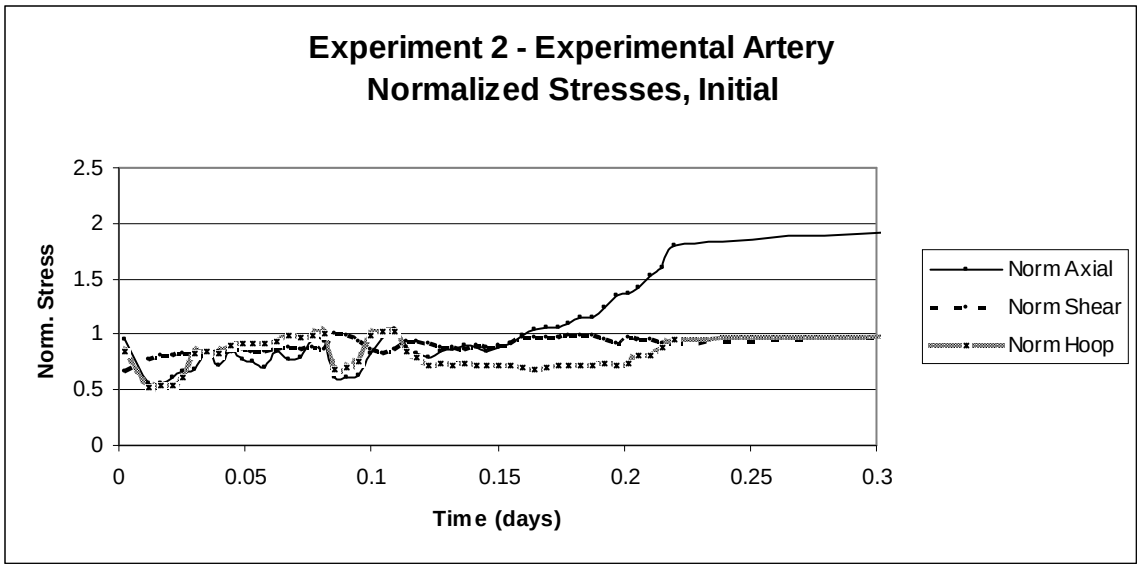


**Figure 34 - Time Course of Local Parameters, Experimental Artery, Initial Adjustment Period: This graph is a close up look at the initial few hours of the experiment depicted in Figure 33Figure 21. Once again, the local parameters began the experiment below the prescribed values, but were able to achieve and maintain them relatively quickly.**

Table 7 summarizes the system's performance. While the deviation in axial stress is highest in this experiment compared to all others, the deviation as a percentage of the prescribed value is (20.29/300 or 6.7%) is comparable and well within an acceptable range.

**Table 7 – Average and Standard Deviation of Local Parameters, Experimental Artery: The following data were collected after the initial adjustment period. Note the similar deviation between these data and the data from the control artery experiment 1.**

| | Prescribed | Average | Standard Deviation |
|---|---|---|---|
| Axial Stress (kPa) | 300 | 299.22 | 20.29 |
| Shear Stress (dyn/cm$^2$) | 15 | 15.58 | 1.00 |
| Circumferential Stress (kPa) | 100 | 102.57 | 6.23 |

The diameters (Figure 35) of the experimental artery underwent similar decreases during the first day of culture. However, unlike previous experiments, the diameters did

not appear to increase through the culture period. As a result, the wall thickness tended to remain relatively stable through the culture (note that the polynomial trend line in Figure 36 did not fit the data well, but it is apparent from the individual data points that the wall thickness did not appear to change significantly. Figure 37 however is very similar to all of the other experiments run (both control and experimental arteries) in that there is a logarithmic shape to the change in length over time.

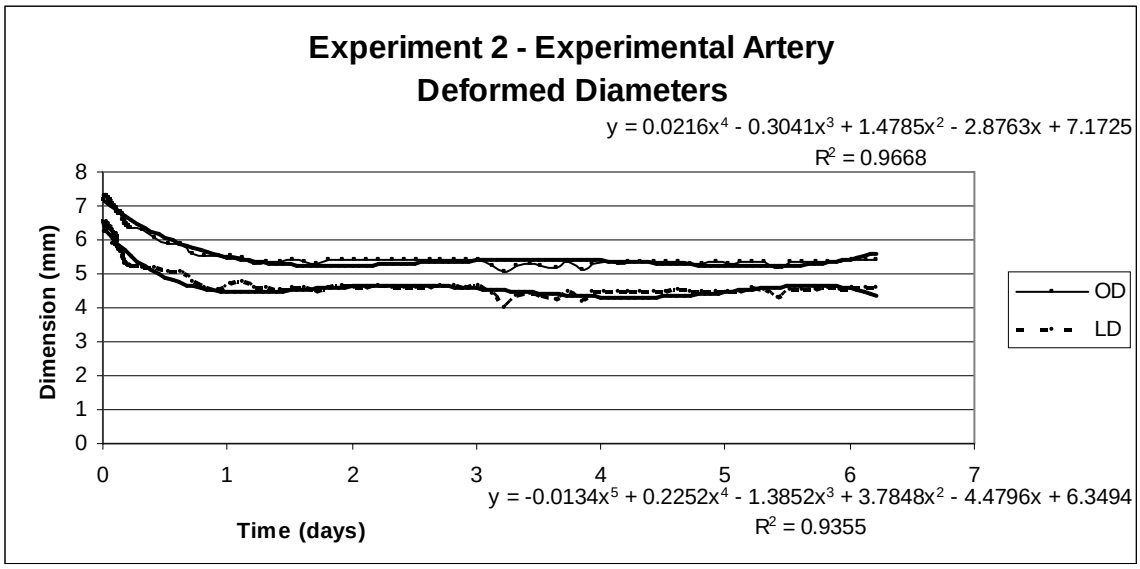


**Figure 35 - Time Course of Deformed Lumen Diameter and Outer Diameter, Experimental Artery: These two data sets display the measured outer diameter (top) and lumen diameter (bottom) of the experimental artery. The polynomial trend lines show the general behavior of the artery throughout the experiment. The equation for outer diameter trendline is on top of the graph, while the equation for the lumen diameter trendline is located below the graph.**

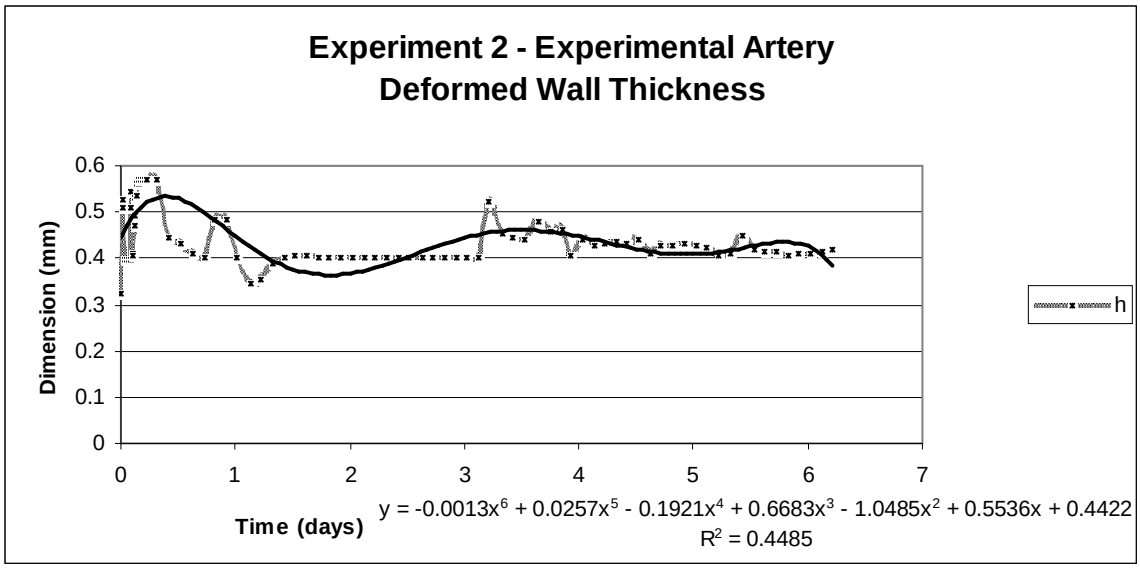


**Figure 36 - Time Course of Deformed Wall Thickness, Experimental Artery: The polynomial trend line which overlays the data set displays the general behavior of the artery through the culture period. Once again, the changes seen here correspond to the changes seen in the diameters (Figure 35).**

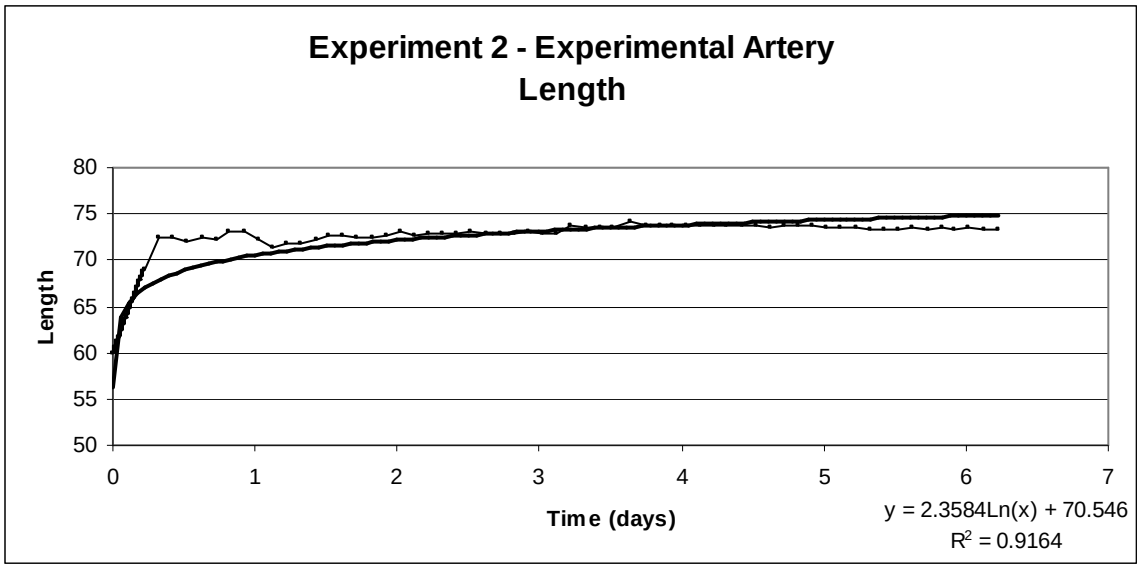


**Figure 37 - Time Course of Artery Length, Experimental Artery: The artery lengthens logarithmically, similar to the control artery. However, in general, there is relatively little change in length throughout the experiment.**

The global parameters (Figure 38) during this experiment remained relatively stable, especially toward the end of the experiment when there was very little change in arterial geometry. However, at the beginning of the experiment when there was a change in arterial geometry, the global parameters were adjusted accordingly in order to maintain the local mechanical environment.

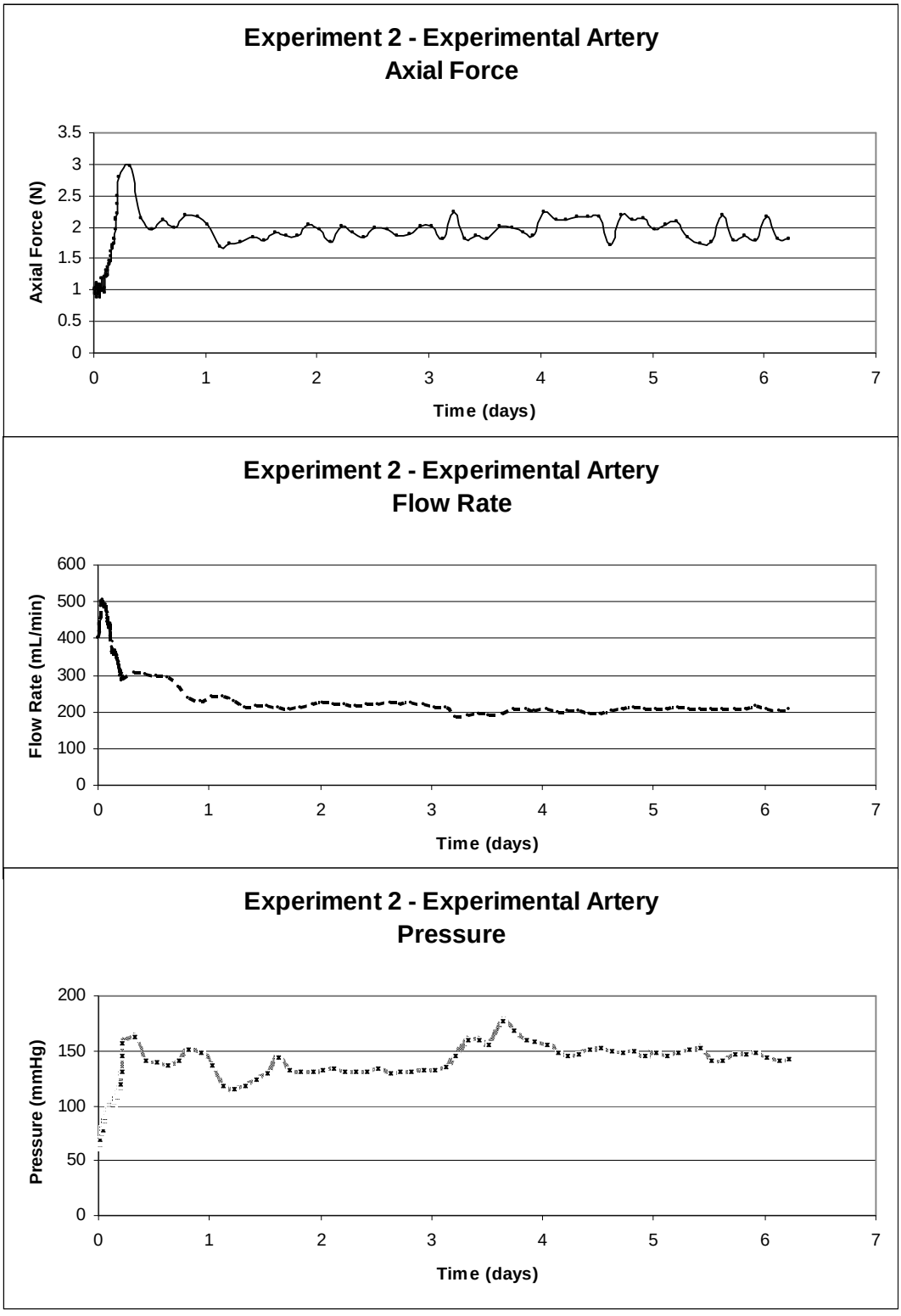


**Figure 38 - Time Course of Global Parameters, Experimental Artery: The most significant changes to the global parameters occurred at the beginning of this experiment. Because the artery's cross sectional geometry did not change significantly during this experiment, the global parameters did not change significantly (relative to the other experiments).**

Overall, all four arteries displayed similar traits. The active response seen by the arteries early in the culture was qualitatively similar to the strong active response witnessed by Wayman et al. (2008) in their organ culture studies. These time course data also reinforce the need for continuously monitoring arterial geometry such that the local parameters can be maintained.

### 4.2.2 Artery Dimensions

The unloaded dimensions (wall thickness, outer diameter, and length) of both the control and experimental arteries were noted before (initial) and after (final) each culture period. From these values, the pre-culture and post-culture volume of the artery was calculated. This data is displayed in Table 8.

**Table 8 – Summary of Dimension Changes: The change in undeformed outer diameter, wall thickness, length, and volume is given below for each artery tested. Note the dramatic changes in outer diameter and wall thickness, yet the relative stability of both length and volume.**

| | | Experiment 1 | | Experiment 2 | |
|---|---|---|---|---|---|
| | | Control | Experimental | Control | Experimental |
| Undeformed Outer Diameter (mm) | Initial | 5.78 | 6.22 | 5.28 | 5.33 |
| | Final | 4.87 | 4.70 | 4.58 | 4.63 |
| | % Change | - 15.6% | - 24.4% | - 13.3% | - 13.2% |
| Undeformed Wall Thickness (mm) | Initial | 0.84 | 0.73 | 0.71 | 0.86 |
| | Final | 1.04 | 1.07 | 0.86 | 1.05 |
| | % Change | 23.5% | 45.2% | 21.8% | 22.4% |
| Unloaded Length (mm) | Initial | 34 | 30 | 39 | 41 |
| | Final | 35 | 30 | 40 | 41 |
| | % Change | 2.9% | 0% | 2.6% | 0% |
| Volume ($mm^3$) | Initial | 444.58 | 379.98 | 396.39 | 494.35 |
| | Final | 439.33 | 365.84 | 402.48 | 483.90 |
| | % Change | - 1.2% | - 3.7% | 1.5% | - 2.1% |

Following culture, neither the control nor the experimental artery's unloaded length differed significantly from their respective initial unloaded lengths. Although the control artery lengthened by 1 mm in two of the experiments, this may be the result of the measurement technique employed and not an actual lengthening of the artery. A ruler with increments of 1 mm was used to visually measure the length of the artery. Although this method lacks some precision, it would be more than sufficient in measuring the many millimeter increases seen in other studies. Although in vivo studies have described artery lengthening when exposed to super physiologic stresses or stretches, these results are in agreement with existing organ culture studies.

Jackson et al. (2002) found that rabbit carotid arteries exposed to elevated stretch showed permanent elongation in as little as 3 days in vivo. However, ex vivo studies have generated different results. Davis et al. (2005) applied a constant axial force on arteries and found that when cultured above a threshold stretch ratio of 2.14, there was permanent length change; however, below that threshold, no permanent length change was seen. While Davis did witness some biological markers signaling the beginning of some positive remodeling changes, he also acknowledged that the overall length change is likely mostly due to structural damage within and plastic deformation of the tissue. Clerin et al. (2003) applied gradually lengthened arteries over a period of nine days and found permanent increases in artery length for stretch ratios of 2.25 and above, similar to Davis's findings. It should be noted that these high levels of stretch were not approached in this study. The high levels of axial stress applied to experimental arteries resulted in stretch ratios of approximately 1.7. Therefore, one would not expect any permanent increase in length. Gleason et al. (2007) witnessed significant permanent lengthening of

mice carotid arteries in two days, but once again attributed at least some of this lengthening to organ culture effects. They did witness significantly more lengthening at higher stretch ratios (1.95), but once again, this is beyond the stretch ratios seen in this experiment.

Also note that neither artery experienced significant volume change during the experiment. This contradicts the findings of Wayman et al. (2008), which described a decrease in volume, most noticeably during the first 15 hours of the experiment. Wayman calculated the initial volume of arteries and then again at 15 hour intervals. There was a decrease in volume between the first and second data point (i.e. first 15 hours). While Wayman attributes the volume change to the first day, it is unclear as to whether the change occurred in a matter of hours or an entire day. This experiment required a more complicated initial setup and a number of mechanical tests prior to each culture period which extended the period of time before which any measurements were taken. It is possible that the volume change that Wayman attributed to the first 24 hours may have occurred within the few hours before which measurements in this study were taken.

Although no length change or overall volume change was noted, there was a significant change in the cross sectional dimensions of both control and experimental arteries. In all arteries, the wall tended to thicken and the outer diameter tended to decrease. However, the combination of these changes did not change the volume of the arteries. This suggests two possibilities. First, it is possible that the organ culture system caused some reorganization of the structural components of the tissue within the artery. In other words, no tissue growth occurred, but there was a reorganization of the tissue

structure which resulted in the dimensional changes observed. Because the carotid arteries used in this study are relatively large (compared to smaller arteries or carotid arteries from smaller animals), it is possible that they are more prone to diffusion and other transport phenomenon that may alter the cross sectional geometry of the artery. The second possibility is that the observed dimensions are the result of a myogenic response of the arteries causing a sustained increase in muscular tone. When arteries exhibit a contractile response, their diameters reduce and walls thicken. Also, because there is no tissue addition or subtraction during contraction, there is no volume change. The pre-culture dimensions of the arteries were taken after a significant period of time during which the arteries were not loaded (transport to the laboratory, preparation of artery, insertion into organ culture, acclimation period in organ culture system – approximately 4-6 hours). However, the post-culture dimensions of the arteries were taken after seven days of loading. The post-culture arteries which are relatively quickly unloaded and measured may undergo some myogenic response which accounts for the geometry changes described above. This may also explain why the experimental arteries seemed to exhibit a greater degree of outer diameter and wall thickness change (i.e. a greater contractile response).

Although there was no measurable change in volume of any arteries during the experiment, remodeling changes tend to manifest themselves on a macroscopic level on much longer time scales than our experimental setup provided. Also, organ culture environments do not drive remodeling as effectively or as fast as in vivo environments. Despite the fact that no remodeling changes were found by measuring the dimensions of the artery, it is possible that we observed some restructuring of the artery, or at the very

least, an altered basal tone, which accounts for the change in cross sectional geometry of both the control and experimental arteries.

### 4.2.3 Mechanical Testing

As described above in Section 3.2.3 Mechanical Testing, multiple mechanical tests were performed on the arteries both prior to and following the culture period. The first subsection will examine the axial stress-axial strain response of the artery. The following subsection will examine the circumferential stress-circumferential strain response of the artery. In both cases strain is defined as the Green strain, defined as:

$$E = \frac{1}{2} \cdot \left( \lambda^2 - 1 \right) \qquad \text{Eq. 8}$$

For the axial response, λ is defined as the axial stretch ratio, or:

$$\lambda_z = \frac{l}{L_0} \qquad \text{Eq. 9}$$

For the circumferential response, λ is defined as the circumferential stretch ratio, or:

$$\lambda_\theta = \frac{OD - h}{OD_0 - h_0} \qquad \text{Eq. 10}$$

#### *4.2.3.1 Axial Stress-Axial Strain Response*

The axial stress-axial strain response of the arteries was calculated using data from the axial force-length test described in Section 3.2.3.1 Axial Force-Length Test. During this test, both arteries are exposed to zero pressure and low flow (30 mL/min). Figure 39 shows the axial stress-axial strain response of the control artery from experiment 1. For this and all arteries described in the mechanical testing section, solid lines represent the pre-culture behavior, while dashed lines represent the post-culture

behavior. Qualitatively, both response functions appear similar. However, in order to quantitatively compare the two functions, a simple linearized model was used.

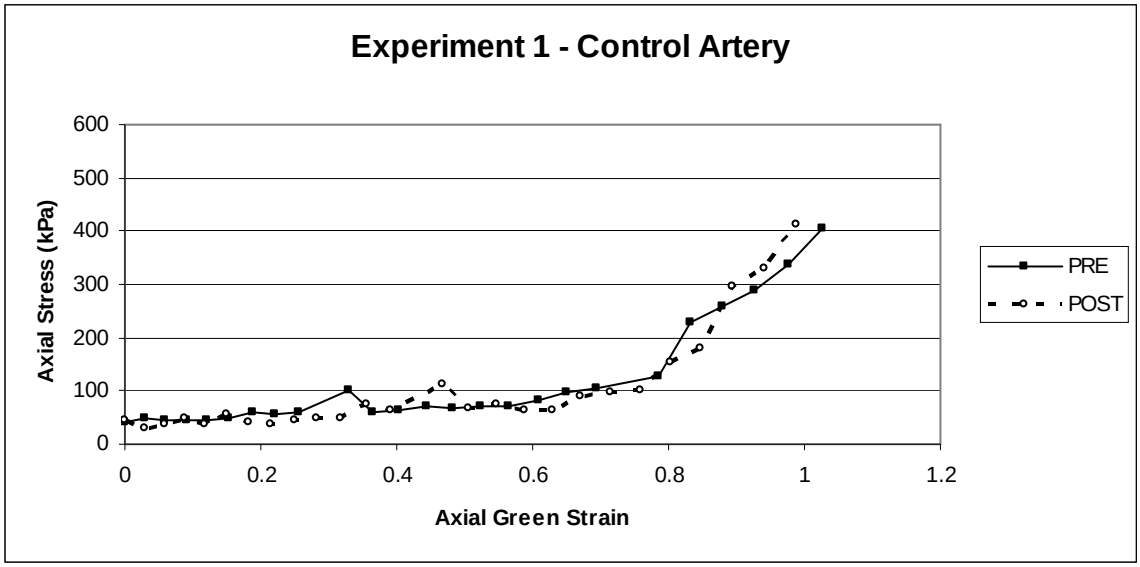


**Figure 39 - Axial Stress-Axial Strain Response, Control Artery: This experiment was performed under no pressure and low flow (30 mL/min). The pre-culture behavior of the artery is shown as a solid line, while the post-culture behavior is shown as a dotted line. Note the similar pre-culture and post-culture behavior of the artery.**

Note that the axial stress-axial strain response curves seem to fit a bilinear model when divided at a strain of 0.8 (this strain corresponds to a stretch ratio of approximately 1.6). Because this (as well as all subsequent) response curve exhibited similar characteristics, a strain value of 0.8 was used to divide all data. Therefore each response curve was split into two data sets that could be roughly approximated with two linear trend lines. The slope of these trend lines would represent the approximate modulus of the material over that range of strains. Figure 40 displays the linear trend lines calculated from the data in Figure 39. The linear trend lines were fit using a least squares method of

regression. Although this approach is not the most sophisticated method, it does provide valuable insight into the general behavior of the artery over various ranges.

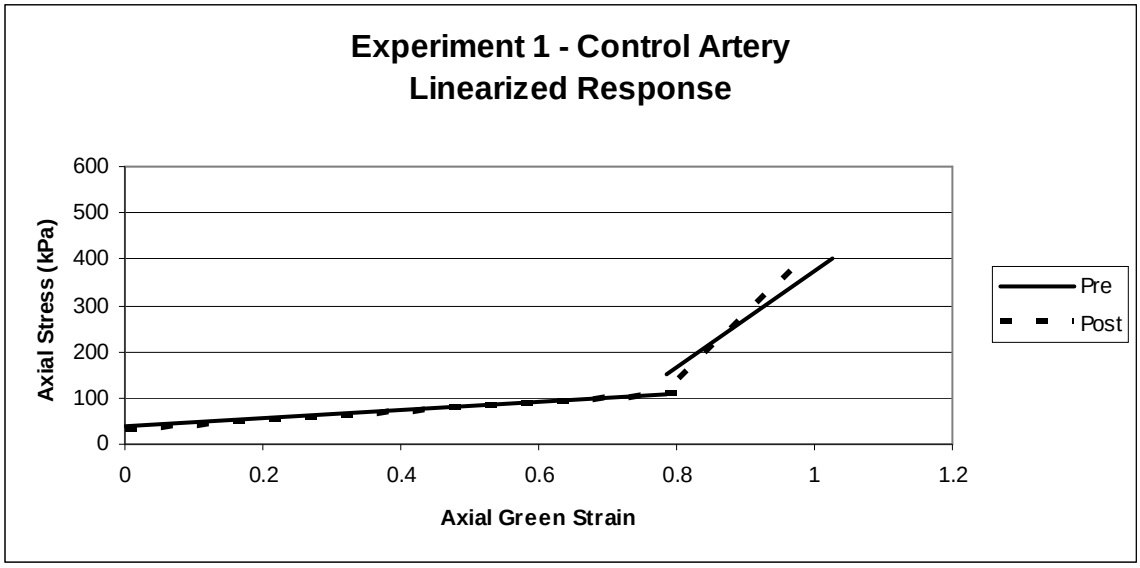


**Figure 40 - Linearized Approximation of Axial Stress-Axial Strain Response, Control Artery: The data from Figure 39 was divided at a strain of 0.8. Each data set was then fit with a linear trend line using least squares regression. The slope of this line was used to approximate the modulus of the material over these ranges.**

A similar method was employed on the experimental artery. Figure 41 shows the axial stress-axial strain response of the experimental artery, while Figure 42 shows the linearized approximation of this behavior.

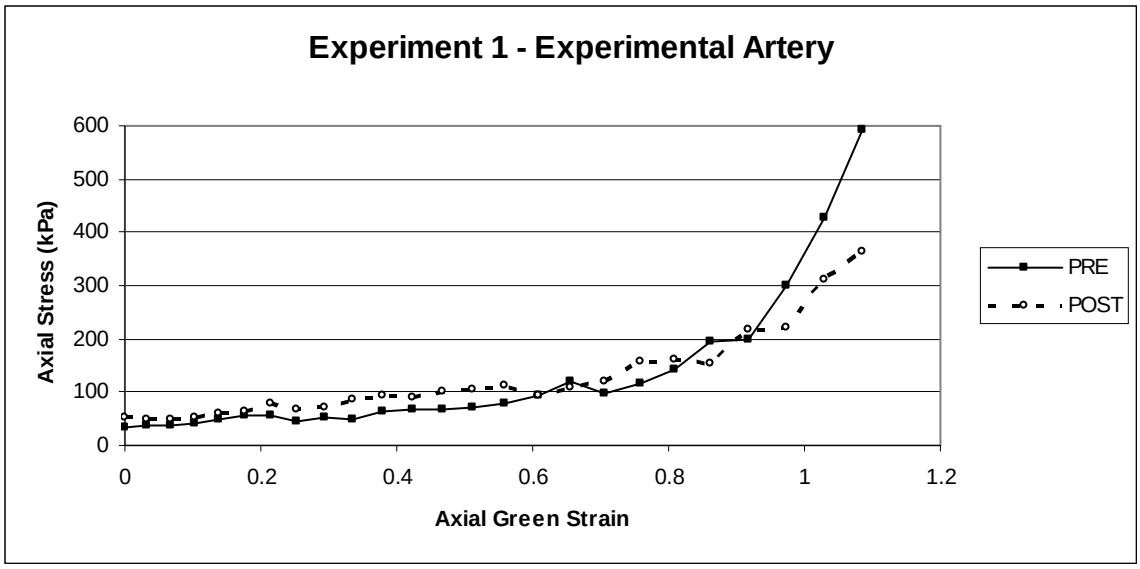


**Figure 41 - Axial Stress-Axial Strain Response, Experimental Artery: This experiment was performed under no pressure and low flow (30 mL/min). The pre-culture behavior of the artery is shown as a solid line, while the post-culture behavior is shown as a dotted line.**

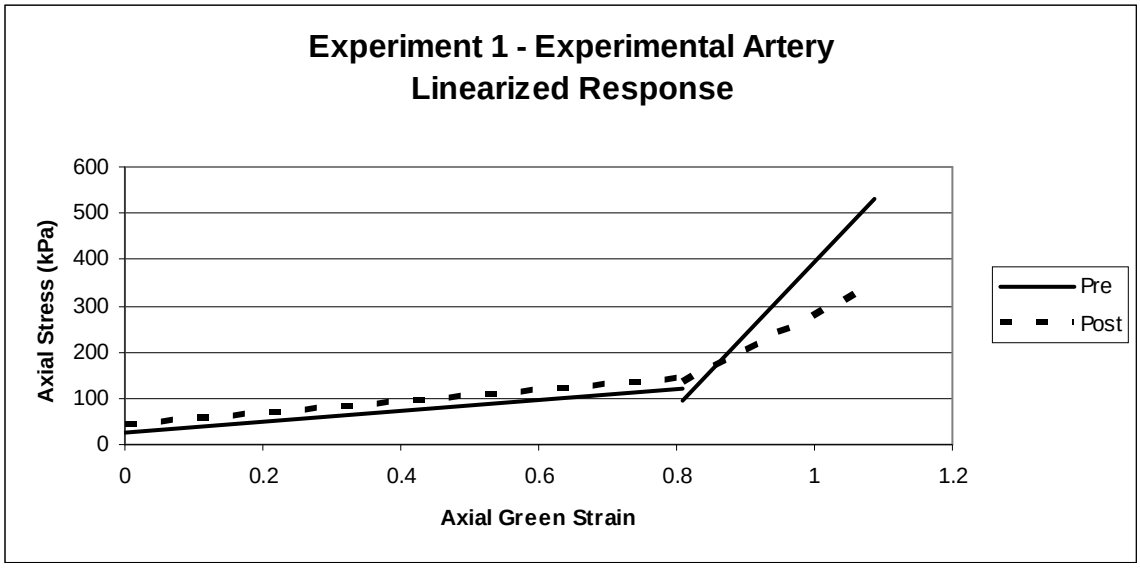


**Figure 42 - Linearized Approximation of Axial Stress-Axial Strain Response, Experimental Artery: The data from Figure 41 was divided at a strain of 0.8. Each data set was then fit with a linear trend line using least squares regression. The slope of this line was used to approximate the modulus of the material over these ranges.**

Using the linearized response curves of both the control and experimental artery from experiment 1, we can obtain approximations of the modulus over two ranges, for E < 0.8 and for E > 0.8. This data is summarized in Table 9. For low strains (E < 0.8), there appears to be relatively little change of arterial stiffness axially. For high strains (E > 0.8), the tissue of the control artery stiffens slightly, while the tissue of the experimental artery softens significantly (50% decrease in the linearized modulus).

**Table 9 - Linearized Modulus for Experiment 1: This table shows the modulus (i.e. slope) of the linearized response curves (Figure 40 and Figure 42). It also displays the percentage change from pre-culture to post-culture of this modulus measure.**

| | | Linearized Modulus (kPa) | |
|---|---|---|---|
| | | For E < 0.8 | For E > 0.8 |
| Control Artery | Pre-culture | 85.3 | 1029.4 |
| | Post-culture | 96.5 | 1364.4 |
| | % Change | 13.2% | 32.5% |
| Experimental Artery | Pre-culture | 115.0 | 1575.0 |
| | Post-culture | 122.7 | 772.8 |
| | % Change | 6.7% | - 50.9% |

These same calculations were performed during experiment 2. The control artery's axial stress-axial strain response curves and associated linearized response curves are shown in Figure 43 and Figure 44, respectively. Once again, note the relative similarity between the pre-culture (solid line) and post-culture (dashed line) behavior, especially at low strains (E < 0.8). The experimental artery's axial stress-axial strain response curves and associated linearized response curves are shown in Figure 45 and Figure 46, respectively.

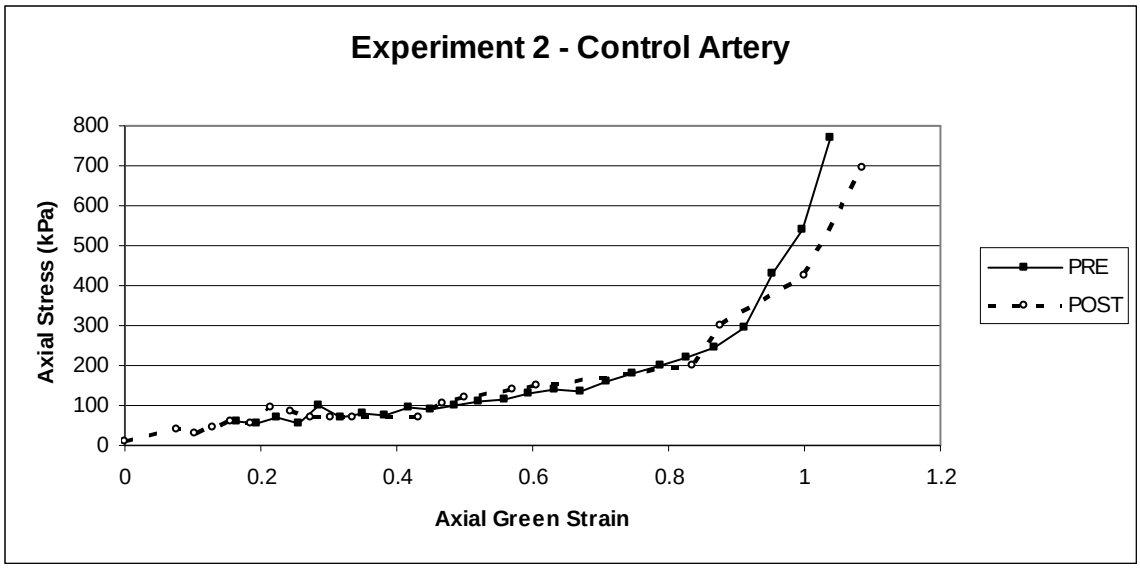


**Figure 43 - Axial Stress-Axial Strain Response, Control Artery: This experiment was performed under no pressure and low flow (30 mL/min). The pre-culture behavior of the artery is shown as a solid line, while the post-culture behavior is shown as a dotted line. Note the similar pre-culture and post-culture behavior of the artery.**

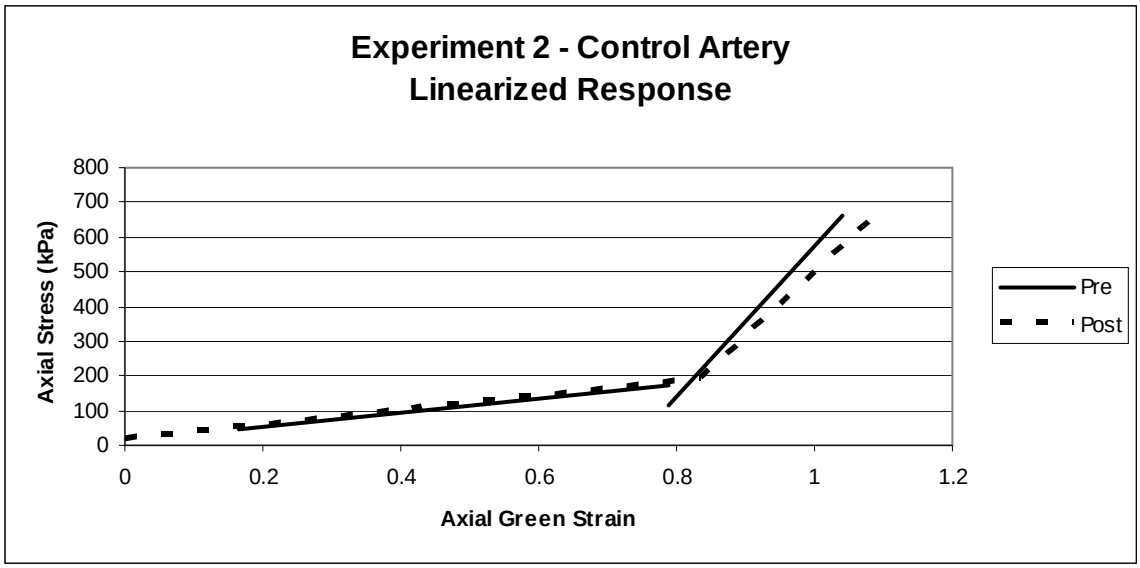


**Figure 44 - Linearized Approximation of Axial Stress-Axial Strain Response, Control Artery: The data from Figure 39 was divided at a strain of 0.8. Each data set was then fit with a linear trend line using least squares regression. The slope of this line was used to approximate the modulus of the material over these ranges.**

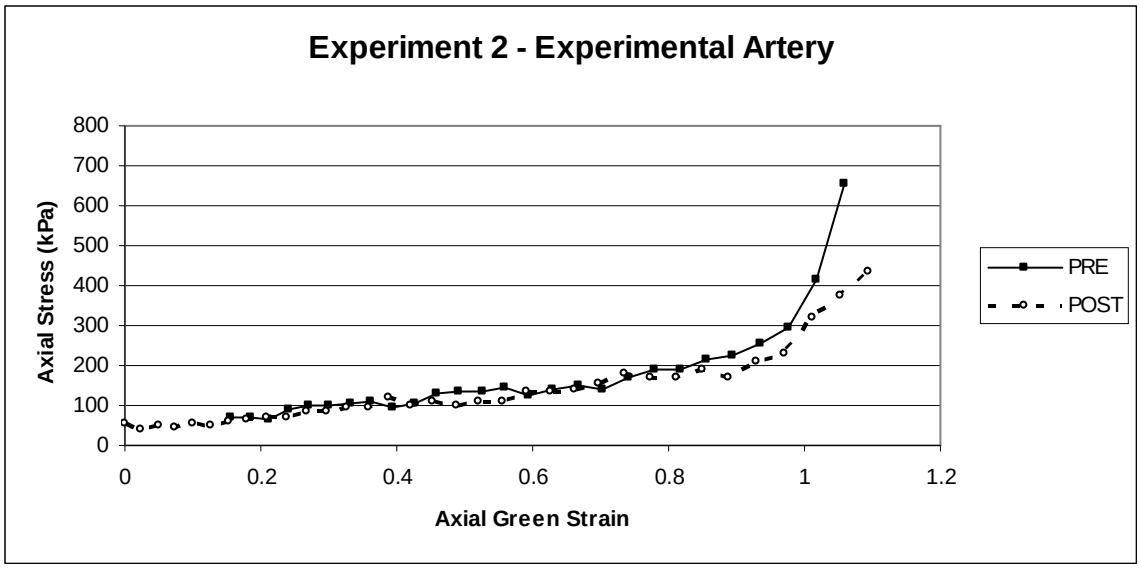


**Figure 45 - Axial Stress-Axial Strain Response, Experimental Artery: This experiment was performed under no pressure and low flow (30 mL/min). The pre-culture behavior of the artery is shown as a solid line, while the post-culture behavior is shown as a dotted line. Note the similar pre-culture and post-culture behavior of the artery.**

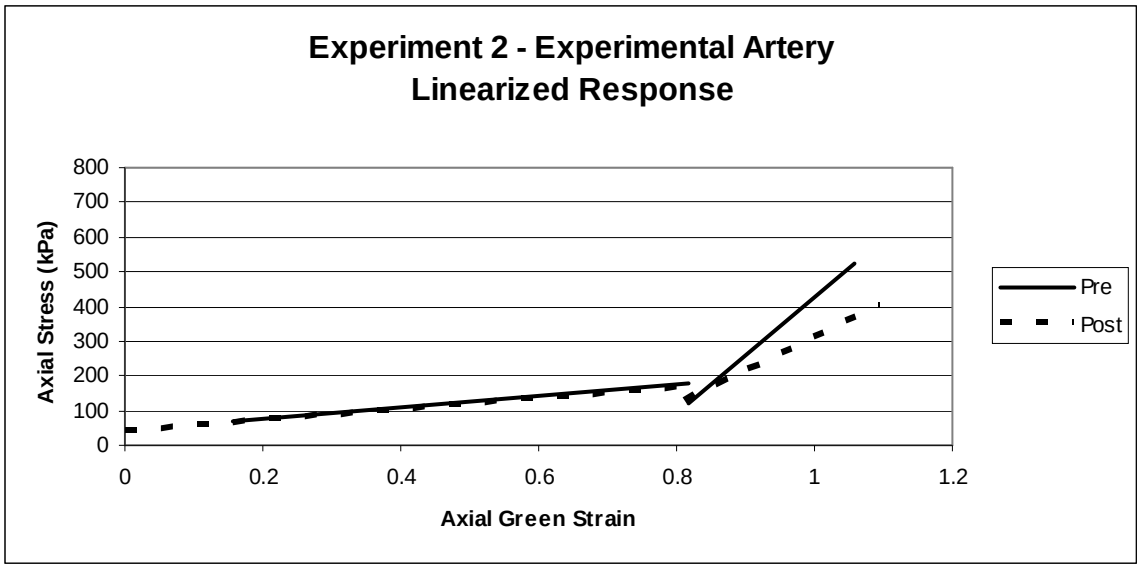


**Figure 46 - Linearized Approximation of Axial Stress-Axial Strain Response, Experimental Artery: The data from Figure 45 was divided at a strain of 0.8. Each data set was then fit with a linear trend line using least squares regression. The slope of this line was used to approximate the modulus of the material over these ranges.**

Table 10 summarizes the data from the linearized response curves (Figure 44 and Figure 46) for experiment 2. Similar to experiment 1, there was essentially no change in the modulus of the tissue over small strains ($E < 0.8$). Both experiments (see Table 9 for data on experiment 1) also saw a significant decrease in axial stiffness (50.9% decrease for experiment 1, 42.5% decrease for experiment 2) of tissue for arteries subjected to higher levels of axial stress throughout the experiment.

**Table 10 - Linearized Modulus for Experiment 2: This table shows the modulus (i.e. slope) of the linearized response curves (Figure 44 and Figure 46). It also displays the percentage change from pre-culture to post-culture of this modulus measure.**

| | | Linearized Modulus (kPa) | |
|---|---|---|---|
| | | For $E < 0.8$ | For $E > 0.8$ |
| Control Artery | Pre-culture | 205.3 | 2157.5 |
| | Post-culture | 205.2 | 1825.8 |
| | % Change | 0.0% | -15.4% |
| Experimental Artery | Pre-culture | 169.3 | 1669.1 |
| | Post-culture | 162.2 | 959.1 |
| | % Change | - 4.2% | - 42.5% |

Because the axial stress-axial stretch relationship describes a material response (as opposed to a structural response), the changed cross sectional geometry described above would not be the cause of such changes in modulus. Also, the only consistent change in modulus is seen in the experimental arteries (i.e. the arteries exposed to elevated axial stresses). This finding differs from the results of Gleason et al. (2007). This group found no significant difference between the axial stress-axial stretch response of cultured mouse arteries. However, it should also be noted that Gleason et al. did not attempt to maintain target values of stress. In fact, they calculated hoop stress and axial stress throughout the two day culture period and found that hoop stress varied as much 25% from its initial

level and axial stress varied as much as 88% from its initial level. Therefore the data presented in Gleason et al. (2007) and presented here in this study should not be seen as mutually exclusive, but rather results that are unique to the methodology employed.

#### *4.2.3.2 Circumferential Stress-circumferential Strain Response*

The circumferential stress-circumferential strain response data was obtained from the pressure-diameter tests performed as described in Section 3.2.3.2 Pressure-Diameter Test. During these tests, flow was kept at a minimum level (30 mL/min) and axial stretch was kept at an axial stretch ratio of 1.5, as calculated using the unloaded length of the artery. The circumferential stress-circumferential response curves for experiment 1 are shown in Figure 47 (control artery) and Figure 48 (experimental artery). Because the response curves exist over such a wide range of strain values, it is not possible to employ the method used above in Section 4.2.3.1 Axial Stress-Axial Strain Response, where data sets were divided at a specific strain value. However, such an analysis is not necessary here since the differences in behavior between the pre-culture and post-culture arteries is more apparent. The tissue of both arteries exhibited significant softening in the circumferential direction.

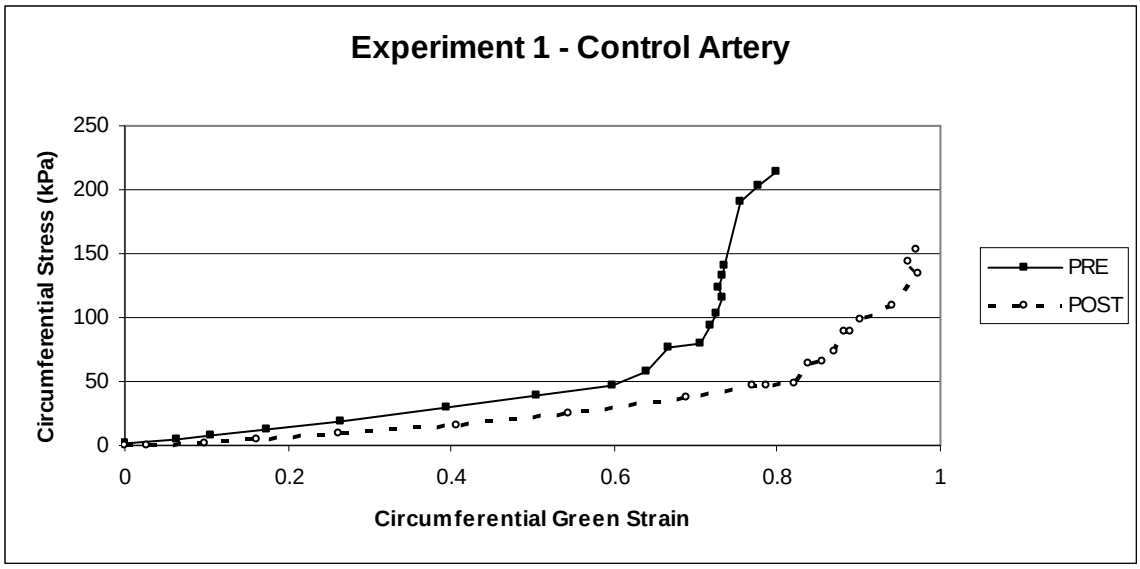


**Figure 47 - Circumferential Stress-Circumferential Strain Response, Control Artery: This experiment was performed under low flow (30 mL/min) and an axial stretch ratio of 1.5. The pre-culture behavior of the artery is shown as a solid line, while the post-culture behavior is shown as a dotted line.**

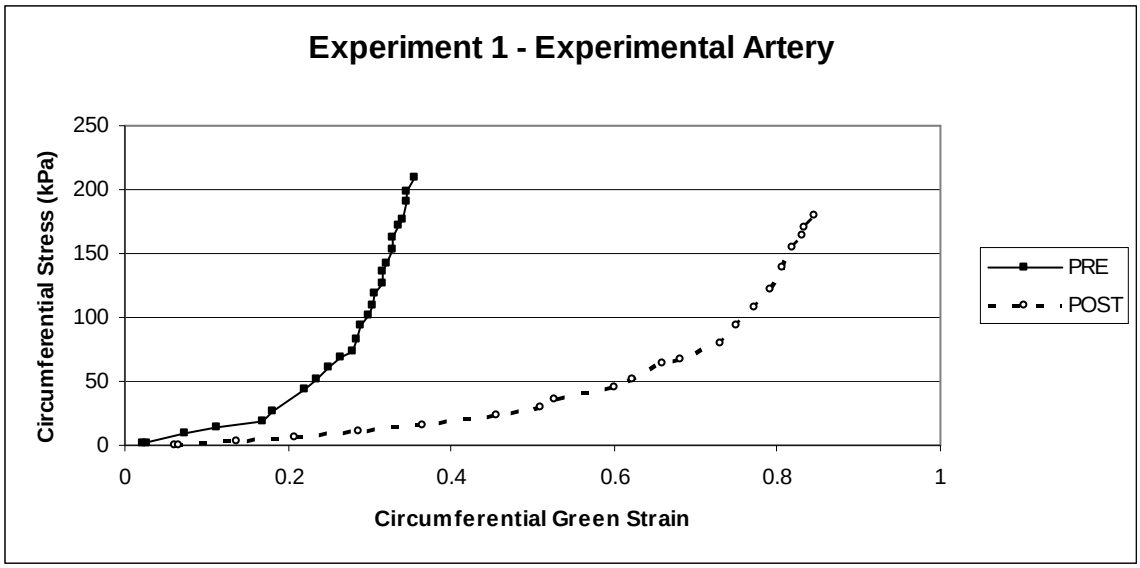


**Figure 48 - Circumferential Stress-Circumferential Strain Response, Experimental Artery: This experiment was performed under low flow (30 mL/min) and an axial stretch ratio of 1.5. The pre-culture behavior of the artery is shown as a solid line, while the post-culture behavior is shown as a dotted line.**

If we examine the pre-culture behavior of the arteries from experiment 1 (solid lines in Figure 47 and Figure 48), it is apparent that even at the beginning of the experiment, that material response of the tissue of the arteries was quite different. The arteries used in this experiment are both segments of the same longer carotid artery. Therefore, such differences are not the result of animal to animal variation, but rather the variation that occurs naturally along the length of the same artery. Such differences make comparison of control and experimental arteries more difficult since they both start at different baseline levels. However, the relatively simple method used here to quantify the behavior of the arteries focuses on the percentage change of the arteries through culture, thereby eliminating the need to have identical material response at the start of the experiment.

In order to quantify this softening, the strains at a given circumferential stress were compared. Because the physiologically normal level of circumferential stress is 100 kPa, this value was chosen to compare pre-culture and post-culture strain. Table 11 shows the strain values experienced by each artery under a 100 kPa circumferential stress and an axial stretch ratio of 1.5. Because the pressure was incremented by approximately 10 mmHg during this test, it is unlikely that the artery ever experienced 100 kPa exactly. To approximate the strain experienced by the artery under a 100 kPa circumferential load, the values closest to 100 kPa on either side were used to linearly interpolate the data. Though the control artery softens circumferentially through the culture period (a 35.7% increase in strain), the experimental artery undergoes significantly more softening (a 159.6% increase in strain).

**Table 11 – Strain Values for Experiment 1 (Figure 47 and Figure 48): This table compares the Green strain for each artery at 100 kPa circumferential stress and an axial stretch ratio of 1.5. Because it is unlikely that the artery was ever at exactly 100 kPa of circumferential stress, the closest values on either side were used and the value at 100 kPa was interpolated linearly.**

| | | Green Strain @ $\sigma_\theta$ = 100 kPa and $\lambda_z$ = 1.5 |
|---|---|---|
| Control Artery | Pre-culture | 0.72 |
| | Post-culture | 0.91 |
| | % Change | 25.7% |
| Experimental Artery | Pre-culture | 0.30 |
| | Post-culture | 0.77 |
| | % Change | 159.6% |

Another way to examine the pre-culture and post-culture behavior of the arteries is to look at the material response of the vascular tissue from each artery over relevant physiologic pressures (80-120 mmHg). Figure 49 and Figure 50 show the data from Figure 47 and Figure 48, respectively, only over the range of pressures from 80 mmHg to 120 mmHg. A least squares linear regression line was then fit over these subsets of data, the slope of which can be used to approximate the modulus of the tissue over the physiologic range of pressures.

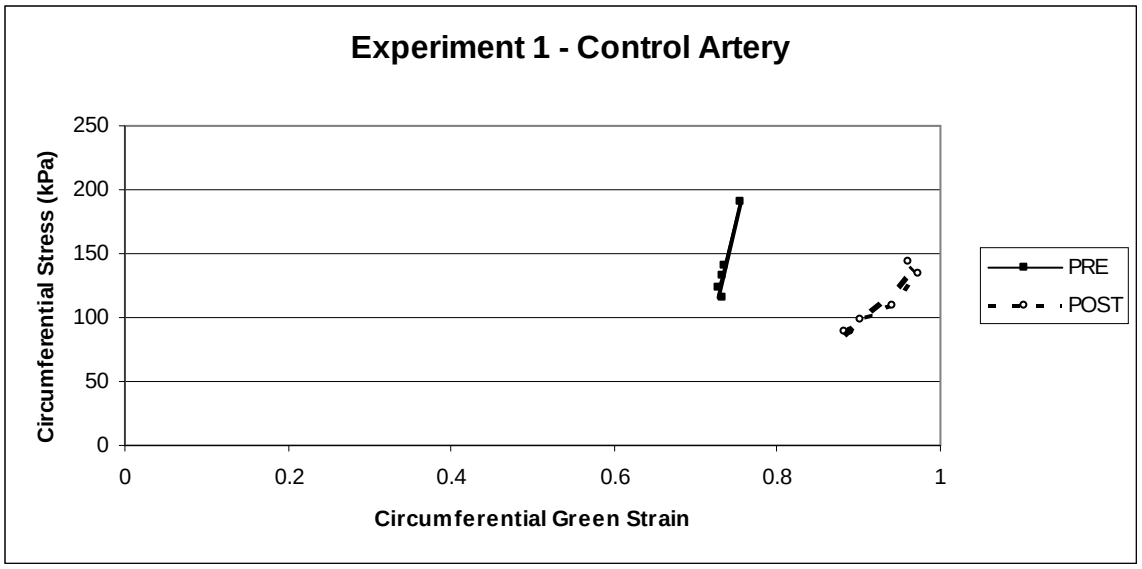


**Figure 49 - Circumferential Stress-Circumferential Strain Over Physiologic Pressures, Control Artery: A subset of data from Figure 47 corresponding to the pressures from 80 mmHg to 120 mmHg are shown here. A least squares regression fit line is shown on top of the data which is then used to calculate the linearized modulus over this range.**

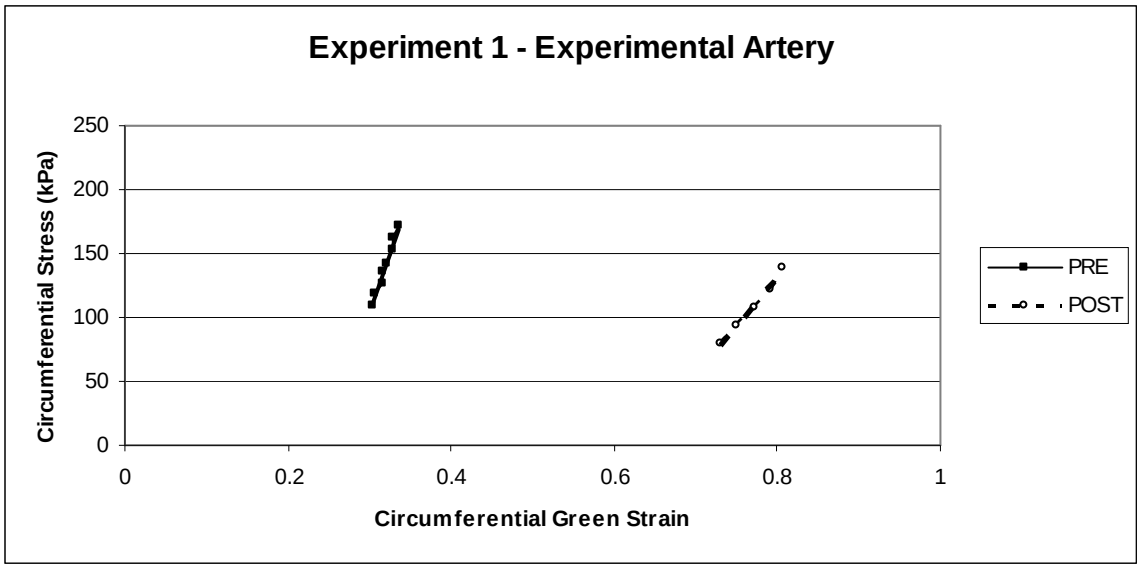


**Figure 50 - Circumferential Stress-Circumferential Strain Over Physiologic Pressures, Experimental Artery: A subset of data from Figure 48 corresponding to the pressures from 80 mmHg to 120 mmHg are shown here. A least squares regression fit line is shown on top of the data which is then used to calculate the linearized modulus over this range.**

Table 12 lists the linearized moduli calculated from the slopes of the linear trend lines in Figure 49 and Figure 50. The tissue in both the control and experimental artery experiences softening over this range, with the control artery actually experiencing slightly more softening than the experimental artery (control artery softening by 80% vs experimental artery softening by 59%).

**Table 12 – Linearized Modulus for Experiment 1: The slopes of the regression lines from Figure 49 and Figure 50 were used as approximations of the modulus over pressures ranging from 80 mmHg to 120 mmHg. Note the similar decreases in stiffness.**

| | | Linearized Modulus (kPa) @ Physiologic pressure (80-120 mmHg) |
|---|---|---|
| Control Artery | Pre-culture | 2891.31 |
| | Post-culture | 576.50 |
| | % Change | - 80.1% |
| Experimental Artery | Pre-culture | 1816.56 |
| | Post-culture | 750.96 |
| | % Change | - 58.7% |

Figure 51and Figure 52 show the circumferential stress-circumferential strain response of the control and experimental artery, respectively, from experiment 2. As in experiment 1, both arteries exhibit gross softening in the circumferential direction through the entire range of stresses. Also as in experiment 1, the pre-culture behavior of the arteries is different, though both segments are taken from the same carotid artery.

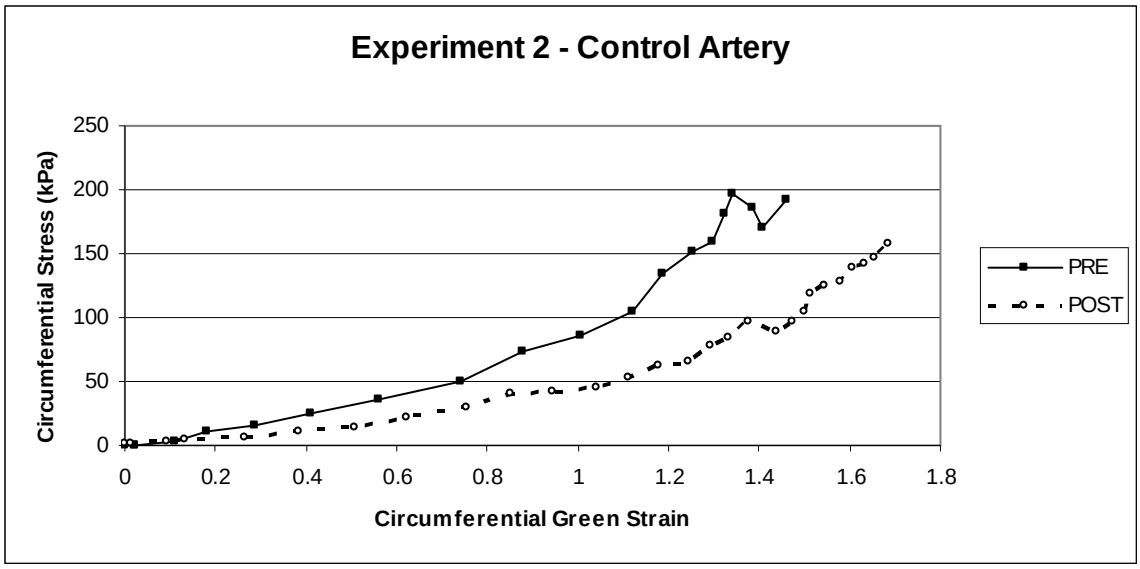


**Figure 51 - Circumferential Stress-Circumferential Strain Response, Control Artery: This experiment was performed under low flow (30 mL/min) and an axial stretch ratio of 1.5. The pre-culture behavior of the artery is shown as a solid line, while the post-culture behavior is shown as a dotted line.**

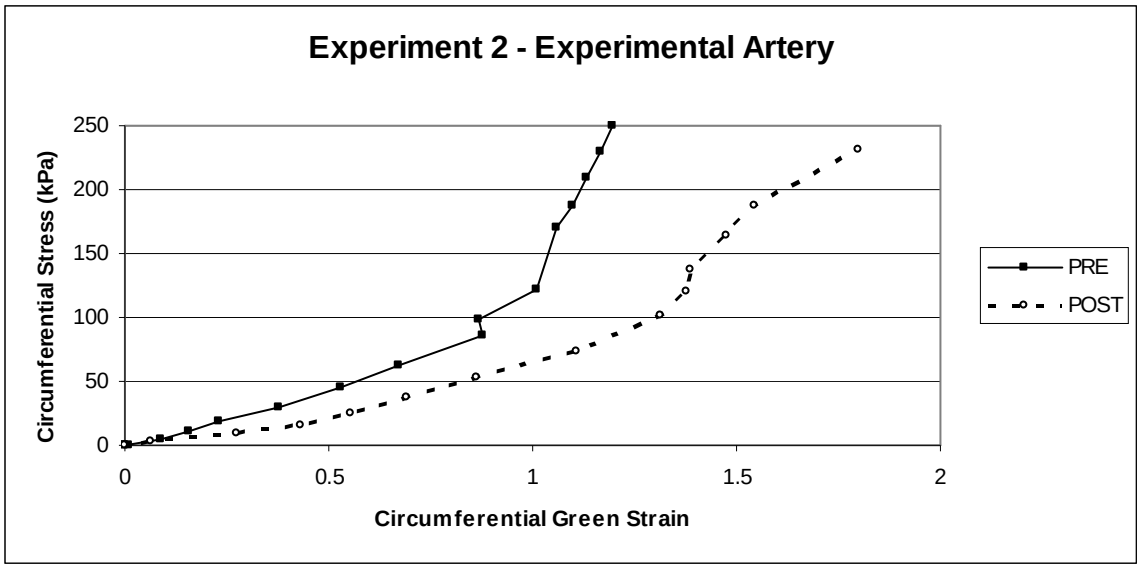


**Figure 52 - Circumferential Stress-Circumferential Strain Response, Experimental Artery: This experiment was performed under low flow (30 mL/min) and an axial stretch ratio of 1.5. The pre-culture behavior of the artery is shown as a solid line, while the post-culture behavior is shown as a dotted line.**

A similar method was used to quantify the degree to which the tissue of each artery softened through the culture period. This data can be found in Table 13. As in experiment 1, both arteries, under an identical circumferential stress and axial stretch ratio, experienced higher strains at the end of the culture period relative to the beginning of the culture. The control artery experienced a 36.3% increase in strain while the experimental artery experienced a 49.5% increase in strain. These results are similar to the results from experiment 1 in that the tissue in the experimental artery underwent more softening than the tissue in the control artery.

**Table 13 - Strain Values for Experiment 2 (Figure 51 and Figure 52): This table compares the Green strain for each artery at 100 kPa circumferential stress and an axial stretch ratio of 1.5. Because it is unlikely that the artery was ever at exactly 100 kPa of circumferential stress, the closest values on either side were used and the value at 100 kPa was interpolated linearly.**

| | | Green Strain @ $\sigma_\theta$ = 100 kPa and $\lambda_z$ = 1.5 |
|---|---|---|
| Control Artery | Pre-culture | 1.09 |
| | Post-culture | 1.49 |
| | % Change | 36.3% |
| Experimental Artery | Pre-culture | 0.87 |
| | Post-culture | 1.31 |
| | % Change | 49.5% |

The data from Figure 51 and Figure 52 is shown in Figure 53 and Figure 54, respectively, but only over a range of pressures that correspond to physiologically normal pressures (80-120 mmHg). Linear, least squares, regression lines were fit over these data subsets and the slope was calculated. Each slope represents the approximate circumferential modulus of the artery's tissue over this range of pressures.

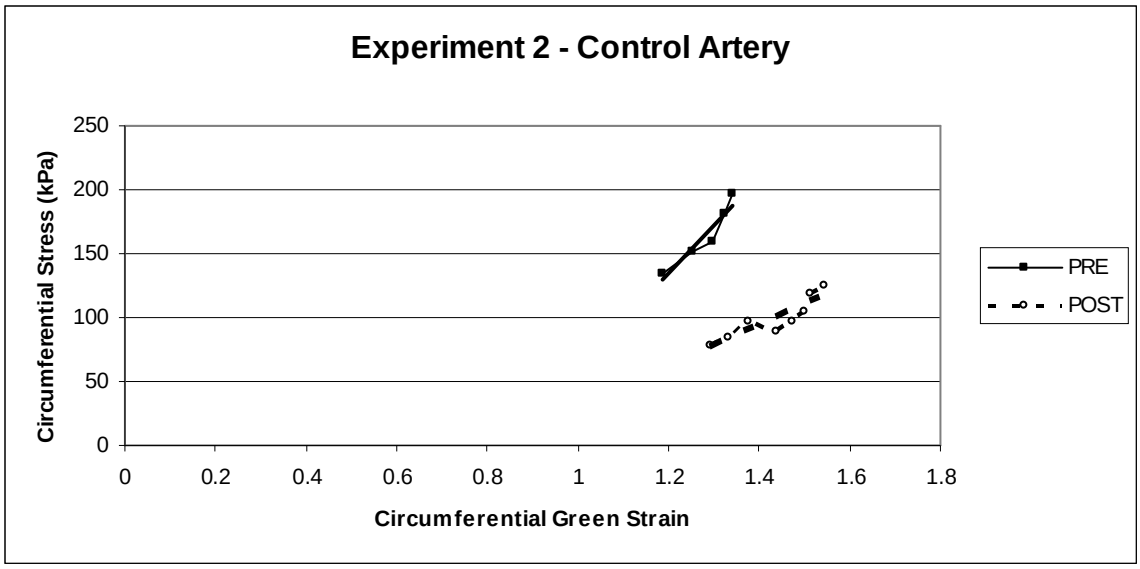


**Figure 53 - Circumferential Stress-Circumferential Strain Over Physiologic Pressures, Control Artery: A subset of data from Figure 51 corresponding to the pressures from 80 mmHg to 120 mmHg are shown here. A least squares regression fit line is shown on top of the data which is then used to calculate the linearized modulus over this range.**

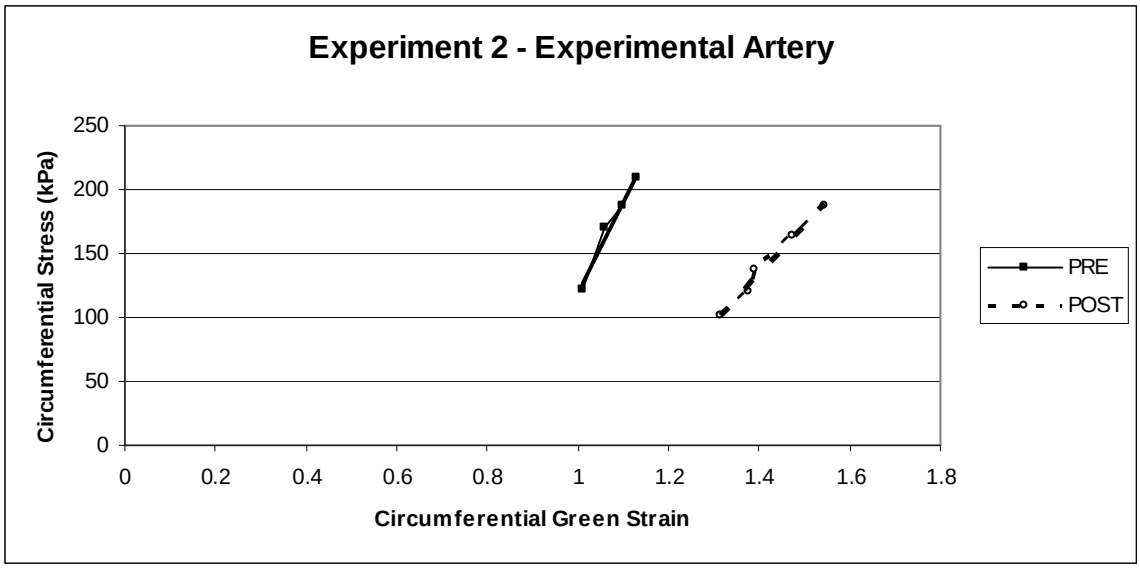


**Figure 54 - Circumferential Stress-Circumferential Strain Over Physiologic Pressures, Control Artery: A subset of data from Figure 52 corresponding to the pressures from 80 mmHg to 120 mmHg are shown here. A least squares regression fit line is shown on top of the data which is then used to calculate the linearized modulus over this range.**

The slopes are given in Table 14. Similar to experiment 1, both arteries experienced softening in the circumferential direction, with the control artery softening only slightly more than the experimental artery. However, in this case, both arteries softened a similar amount (56.1% vs. 45.2%).

**Table 14 - Linearized Modulus for Experiment 1: The slopes of the regression lines from Figure 53 and Figure 54 were used as approximations of the modulus over pressures ranging from 80 mmHg to 120 mmHg. Note the similar decreases in stiffness.**

| | | Linearized Modulus (kPa) @ Physiologic pressure (80-120 mmHg) |
|---|---|---|
| Control Artery | Pre-culture | 366.08 |
| | Post-culture | 160.83 |
| | % Change | - 56.1% |
| Experimental Artery | Pre-culture | 687.74 |
| | Post-culture | 376.72 |
| | % Change | - 45.2% |

### 4.2.4 Biological Markers

The hematoxylin and eosin (H&E) staining protocol was used to examine the general morphology of cultured artery segments. In this staining protocol, cell nuclei are stained purple while connective tissue is stained pink. As seen in Figure 55, both control arteries and experimental arteries are qualitatively similar to a freshly harvested artery. The intimal layer appears similar in all arteries, smooth muscle cells in the media maintained their circumferential orientation, and overall the arteries were free of any ruptures.

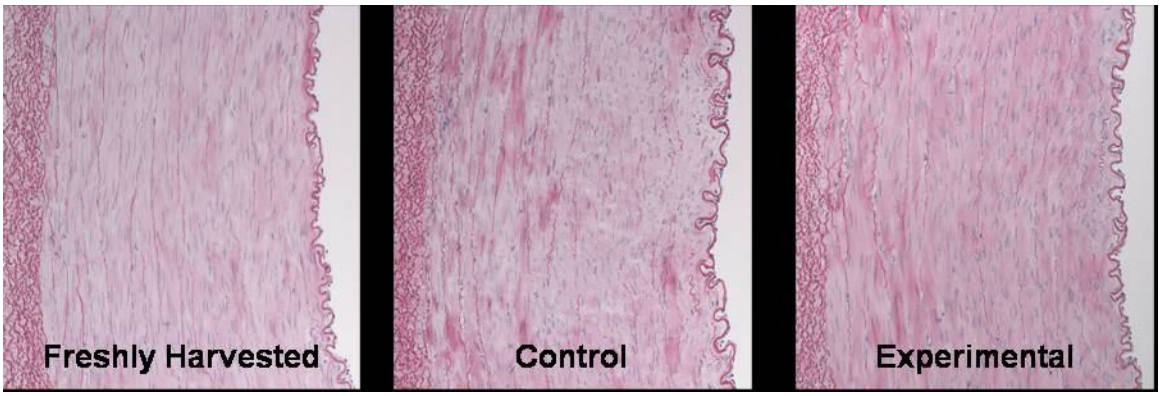


**Figure 55 - Hematoxylin and Eosin Stain: Left, a freshly harvested artery; center, a control artery following a 7 day culture; right, an experimental artery. Notice the similarity between the freshly harvested artery and the post-culture arteries.**

Cell viability was determined using an MTT assay which stains viable tissue a dark blue color. As demonstrated in Figure 56, viable tissue is easily differentiable from nonviable tissue. This is a qualitative measure of an artery's viability. It also shows that arteries remain viable after removal from the organ culture system such that further biological tests can be performed during static incubation (e.g. $^{3}$H-Proline collagen synthesis assay).

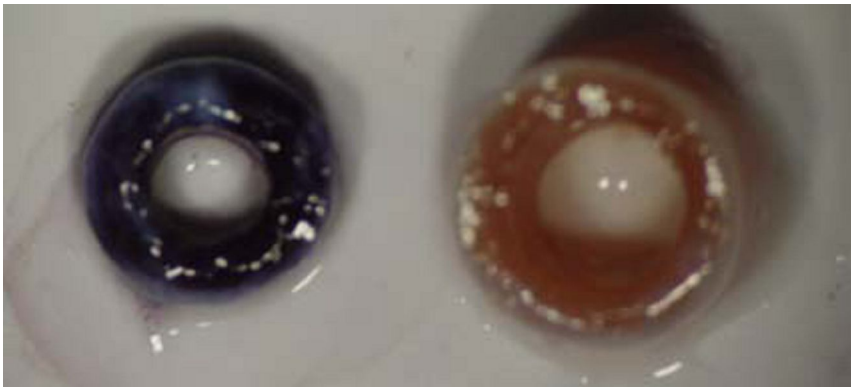

**Figure 56 - Viability From MTT Assay: Representative image showing two arteries incubated in MTT solution. The artery on the left represents a viable artery segment while the artery on the right has been exposed to a series of freeze-thaw cycles to lyse cells. (Image from Wayman, 2007).**

This test was performed on both the control and experimental arteries. Figure 57 compares MTT incorporation between control and experimental arteries. Qualitatively, both arteries display similar viability and all arteries appear similar to the fresh arteries incubated in MTT.

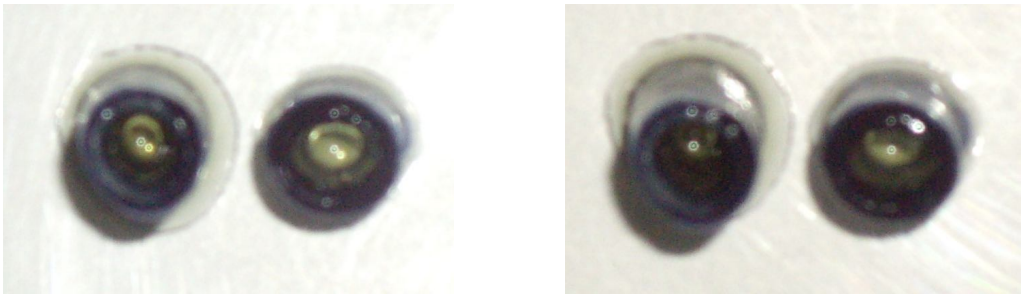

**Figure 57 – Viable Artery Segments: four representative artery segments (control arteries on the left and experimental arteries on the right in each image) demonstrating that both control and experimental arteries remained viable following the seven day culture. Note that the non-blue colorations are a combination of imaging artifacts and shadows.**

Table 15 compares the $^{3}$H-proline incorporation between control and experimental arteries. It appears that experimental arteries exhibited more proline incorporation, thereby suggesting more collagen synthesis. In both experiments collagen synthesis was approximately 10% greater in the experimental arteries than in the control arteries. However, this slight increase needs to be verified further before any assumptions on the significance of such a finding can be drawn. Because the sample size is so small (n=2), a t-test will not give us any valuable information regarding the significance of this data.

**Table 15 – Mean $^{3}$H-Proline incorporation: Experimental arteries exhibited slightly increased proline incorporation. However, due to the limited number of experiments, this slight difference is not statistically significant.**

| | Experiment 1 | | Experiment 2 | |
|---|---|---|---|---|
| | Control | Experimental | Control | Experimental |
| $^{3}$H-proline Incorporation (DPM/mg) | 264.7 | 275.3 | 292.8 | 305.0 |

This assay is limited in that it measures proline incorporation during a small timeframe at the conclusion of the experiment. Also, this is a gross measure of collagen synthesis, without regard to the alignment or organization of collagen. Because of this, one can only infer what is occurring in the artery using these data and the mechanical response curves.

## *4.3 Discussion*

The local mechanical environment that the control arteries were exposed to was identical to physiologically normal stresses seen in vivo. Therefore, one would expect no significant changes in the material response of the tissue of these control arteries. While the control arteries exhibited similar pre-culture and post-culture behavior in the axial direction, there was significant softening of the tissue in the circumferential direction. Because the local parameters were kept at normal baseline levels, this may be attributed to the effects of organ culture.

The organ culture system does not exactly mimic the environment within the human body, so it is reasonable to assume that such a system would have an effect on the artery over a seven day culture. Also, because relatively large arteries were used in this system (as opposed to smaller porcine arteries or carotid arteries from smaller animals), it

is possiblt that diffusion or other transport mechanisms have an effect on the circumferential stiffness of the tissue, regardless of the local parameters.

However, despite any organ culture effects on the arterial tissue, there still exists some differences between the control and experimental arteries. In the axial direction, the tissue of the experimental arteries softened at high strain values relative to the tissue of the control arteries. In the circumferential direction, the tissue of the experimental arteries softened more than the tissue of the control arteries softened. Therefore, it appears that the tissue of arteries cultured at an elevated axial stress experienced reduced stiffness compared to the tissue of arteries kept at a normal axial stress.

Because the material response (stress-strain) was plotted and because no volume change was seen through the culture period, one can assume that the changes witnessed in the mechanical behavior of the arteries was the result of the collagen or elastin changing. Elastin dominates the small strain mechanical behavior of arteries, while collagen dominates the large strain mechanical behavior. Since the axial stress-axial strain response of control and experimental arterial tissue was similar for low strains both pre-culture and post-culture, it is likely that elastin is not changing significantly. However, since the axial stress-strain response of control and experimental arterial tissue was different at high strains, one can assume that collagen is playing a major role in the changes observed.

Based on the results of this study, a mechanism through which the observed softening behavior could be explained was postulated. At the beginning of the experiment, let us assume we start with two arteries of identical collagen structural organization. If held at a physiologically normal local mechanical environment, both

arteries will exhibit identical structural organization. For our experiment, the control artery was maintained at a physiologically normal local mechanical environment, while the experimental artery was maintained at an axial stress above the physiological norm, which stretched the artery beyond its in-situ length. Therefore, the control artery and experimental artery exhibited a different structural organization of the collagen since the experimental artery was stretched more than the control artery.

The mechanism described here hinges on one basic assumption. Let us assume that the collagen turnover (i.e. the degradation and synthesis of collagen that continually occurs in healthy arteries) is driven by the circumferential stress. Because collagen is highly directional and mainly oriented along the circumferential direction, it is likely that circumferential stress (as opposed to axial or shear stress) is the dominant driver of collagen synthesis and degradation. In our experiments, both the control and experimental artery are exposed to identical levels of circumferential stress. This would imply that the structural organization of the collagen that is being synthesized during the organ culture period will be identical in both arteries, despite the fact that the experimental artery is at a larger axial stretch ratio than the control artery.

At the conclusion of the experiment, the control artery and experimental are brought to a physiologically normal stretch ratio of 1.5 (based on the unloaded length of the artery) for the pressure-diameter test. The experimental will shorten from its cultured length more than the control artery since the experimental artery was held at a higher axial stress. Therefore, during the pressure-diameter test, when the arteries are brought to identical axial stretch ratios, the structural organization between the two arteries will be different.

The structural organization of the collagen changed in the experimental artery such that the vascular tissue of the experimental artery was softer than that of the control artery. This can be achieved numerous ways on a microscopic level. Collagen fibers are crimped and composed of many collagen fibrils. There is also a distribution of collagen throughout the arterial wall such that described the amount of crimping in the collagen fibers. If the collagen becomes more crimped such that it is not recruited into the overall mechanical response until higher strains are achieved, the tissue will appear softer. Additionally, a change to the number of collagen fibrils in each collagen fiber can also affect the mechanical behavior of individual collagen fibers, and thus, the mechanical behavior of the vascular tissue. A shift in the distribution curve or a change in the shape of the distribution curve of collagen crimping will also affect the amount and degree to which collagen is recruited as the artery is strained. This, in turn, affects the gross mechanical response of the tissue.

The combination of organ culture effects along with altered collagen structural organization are both plausible explanations which offer insight into how the arteries in this study responded to the organ culture system and experimental setup.

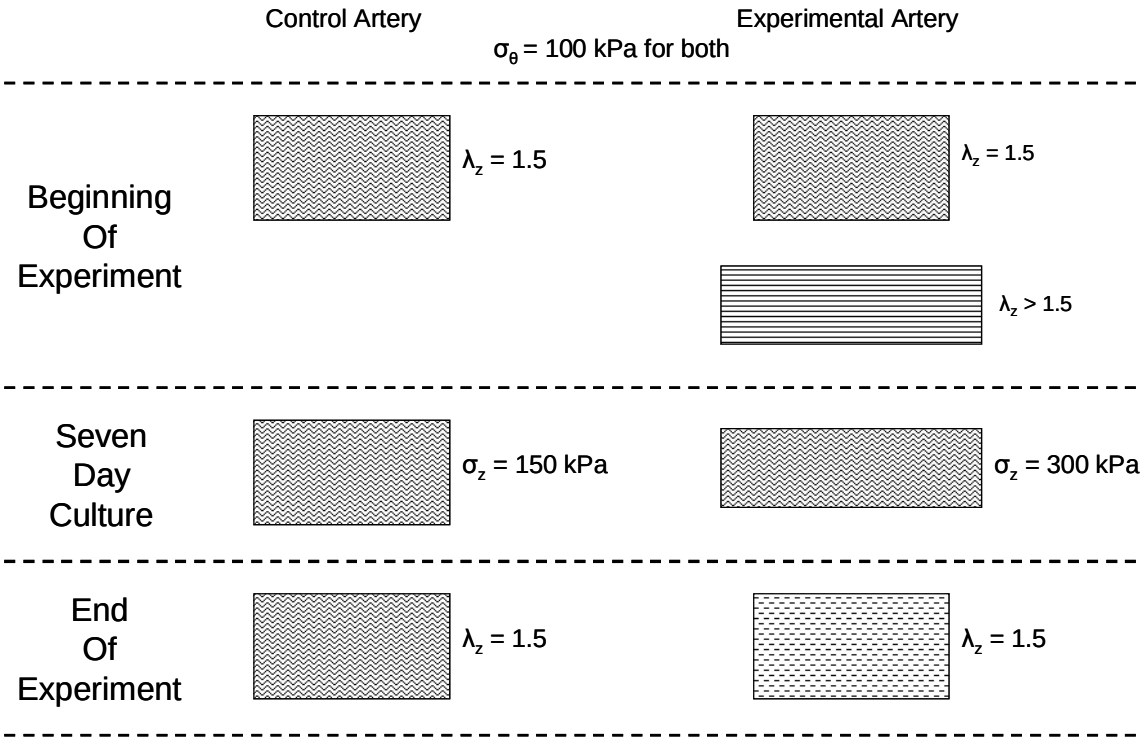


**Figure 58 – Schematic of the Structural Organization of Collagen in Experiments: Each pattern represents a unique collagen structural organization. At the beginning of the experiment, both arteries exhibit identical structural organizations. However, when stretched above a physiologically normal axial stretch ratio, the experimental artery displays a different structural organization. During culture, because both arteries are maintained at identical levels of circumferential stress, the structural organization of the collagen being synthesized is identical. Following the culture period, both arteries are brought to a physiological relevant axial stretch ratio of 1.5. Because the arteries had an identical structural organization of collagen at different axial stretch ratios, they had a different structural organization of collagen at identical axial stretch ratios.**

# V. CONCLUSIONS AND RECOMMENDATIONS

## *5.1 Conclusions*

A novel approach to study arterial remodeling was developed. This approach combined a system capable of computer monitoring and control of hardware with an algorithm designed to automatically achieve and maintain various levels of axial stress, circumferential stress, and shear stress. Because the cross sectional geometry of the artery could be measured throughout the culture period, there was no need to define a strain energy function. The algorithm utilized an iterative feedback loop that did not require any future knowledge regarding how changing any of the parameters would deform the current geometry of the artery. This proves to the major advantage over previous organ culture systems, and this was made capable because of our ability to measure the wall thickness using ultrasound.

In all system performance evaluations, the organ culture system developed in this study was capable of achieving and maintaining a user prescribed level of stress. After the initial adjustment period, the average value of stress only varied from the target value by a maximum of 6.7%. Not only were the prescribed values of the local parameters achieved, but they were achieved with relatively little user interaction. While not fully automated, the system was capable of reducing user interaction to simple monitoring of the data as opposed to manual control of any of the hardware.

No cultured arteries exhibited any significant change in length, despite the prescribed level of axial stress. There was a dramatic increase in wall thickness and

decrease in outside diameter seen in all arteries. However, this combination of geometry changes resulted in essentially zero volume change. This type of geometric change implies either an altered basal tone, a reorganization of the arterial structure, or some sort of organ culture effect (since the effect was seen in both control and experimental arteries).

Experimental arteries experienced an increased compliance, both axially and circumferentially, at higher stretch ratios. It was hypothesized that this change in stiffness was the result of an altered collagen structure. This was not confirmed microscopically, but inferred based on the gross mechanical behavior of the arteries. Because even control arteries softened circumferentially, it is likely that organ culture effects played an additional role in the softening seen in this study.

## *5.2 Limitations and Future Work*

While this study resulted in the creation of a novel organ culture system, there still exists many avenues for further research. This study was limited by time in that only two axial stress experiments were conducted. The most logical work to follow from this study is a more thorough examination of increased axial stress and its effect on arterial remodeling. Future studies will be able to increase the number of experiments such that one can derive statistical significance from the data and evaluate the trends mentioned here in more detail. Also, a more in depth biological analysis may prove useful in identifying the precursors to remodeling. In order to eliminate the possibility of confounding the results due to the active myogenic response of arteries during mechanical testing, it is necessary to develop a method of comparing pre-culture and post-culture arteries which have similar basal tone. It may be beneficial to compare

arterial mechanical response under states of maximal contraction and maximal relaxation so as to ensure that pre-culture and post-culture arteries are under the same mechanical conditions. Additional biological assays including but not limited to matrix degradation, cell function, and cell death may prove useful as well.

While the function of endothelial cells and smooth muscle cells were tested in preliminary experiments to ensure that a seven day culture period was feasible, such tests were not performed on tested arteries due to the possibility of the agonists used in those assays to interfere with the $^{3}$H-proline assay performed following culture. Because the protocols used in this research were previously reported in published work by members of our lab (Han and Ku, 2001; Han et al., 2003; Davis et al., 2005) who maintained organ culture systems for similar lengths of time, it is likely that cell function was maintained. In addition, the active mitochondria evidenced by MTT incorporation suggests retained functionality. However, future work may seek to identify alternative functionality assays that would be more compatible with the biological markers tested for in this research.

While the system itself has proven adequate in achieving and maintaining a user specified local mechanical environment, there is room for improvement. The most novel aspect of the system (the ultrasound transducer and related programming) is also the area which would benefit most from a potential redesign. The signal processing techniques used here were relatively simple to develop and simple to program; however, they may not be the best solutions. It is likely that a more complex signal processing algorithm will clean the signal more effectively and make the ultrasound measurements more reliable and less resource intensive.

The current setup is such that the ultrasound transducer measures a single cross section of the artery in order to obtain the wall thickness and diameter. This tacitly assumes that the artery is uniform and a single cross section is sufficient in describing the dimensions along the entire length of the artery. However, this is not the case, as an artery is not a tube of constant thickness nor diameter. Therefore, it would be a valuable addition if cross section dimensions could be taken along the length of the artery. This may be done with a single ultrasound transducer which can be moved along the long axis of the artery, or with multiple transducers. Still yet, there may be an alternative imaging technique that can be used to measure the cross sectional dimensions of an artery by taking a more comprehensive look at the artery.

While the aim of this study was to have a fully automated system requiring no user interaction after the initial start of the program, this system does require some minor user interaction/monitoring. Because the width of the zero subset is user defined (see Section 3.1.2.1 Method of Calculating the Artery Geometry from Ultrasound Signal), any significant change in the geometry of the artery may require the user to change this width in order to accurately locate all four peaks. This is especially pertinent to the initial adjustment period (first few hours of culture) when the artery is undergoing the greatest amount of active and passive geometry change. However, after a few hours of accurate ultrasound readings, the program becomes essentially fully automated. While this is not a major area of concern since the current system is a major improvement over the previous system with regard to user interaction and automation, it does represent an area that could be improved.

The utility of this method for controlling the local parameters in vivo is limited. Because this method requires accurate control of the global parameters and accurate calculation of the cross sectional geometry of the artery at any instant in time, it is not obvious how such a system could be adapted for in vivo studies. Although this method was never intended to be used in vivo, it would be extremely beneficial to this field of research if certain aspects of this study (control of the local environment, continuous control and monitoring) could be adapted into in vivo studies which feature experiments of much longer duration and more clinical relevance.

The method of analyzing the mechanical response curves described above in Section 4.2.3 Mechanical Testing is simplistic. For the case of axial stress-strain, this study assumed a bi-linear response with a somewhat arbitrarily chosen break point (in this case, E = 0.8). While this method was sufficient in providing a general approximation of the material properties, it is not ideal. A better bi-linear fit may be found if the break point is variable. This then becomes an optimization problem. Additionally, a polynomial or exponential regression may fit the data more accurately and allow us to more accurately describe the arterial response mathematically. For the case of circumferential stress-strain, this study looked at specific cases (either strain at 100 kPa circumferential stress, or stiffness over a relevant range of pressures). However, no quantitative comparison was made between circumferential response curves as a whole, which may provide further insight into the biological mechanisms described above.

# APPENDIX A: LabVIEW Code

This appendix contains screenshots of the LabVIEW code written for this research. In order to maximize computer performance as well as reduce the size of each file, sub-VI's were utilized. Sub-VI's are subroutines which execute only when called upon given a certain set of inputs. All sub-VI's displayed below will be boxed in with a dashed line. Those connectors to the left of the box are inputs, while those to the right are outputs.

Figure 59 - Ultrasound Waveform Generator (Sub-VI):

This sub-VI generates a single waveform of the ultrasound signal.

Figure 60 – Ultrasound Measurements (Sub-VI):

This sub-VI calls upon the following sub-VI's:

- Ultrasound Waveform Generator (Sub-VI)

In this program, 50 consecutive waveforms (from "Ultrasound Waveform Generator (Sub-VI)") are summed. The subsequent waveform is then raised to the eighth (waveform$^8$). A subset of this waveform is cropped from the signal. The four maximum y-values are then found and the corresponding time stamps associated with each y-value are recorded. Note that once a maximum is found, that location as well as the immediate surrounding location (whose width is determined by "Threshold Width") are replaced by zeroes so as to prevent the program from calculating the same maximum. Based on the four recorded time stamps, the geometry of the artery is calculated. This process is repeated 60 times. From the 60 calculated values, only those values within a certain threshold are allowed to pass out of the loop. Once outside the loop, the remaining geometric dimensions (thickness or outside diameter) are calculated.

Figure 61 - Axial A (Sub-VI) & Axial B (Sub-VI):

This sub-VI takes the current position of the artery and creates three unique positions: 1) current position, 2) current position + 0.3906 mm, and 3) current

position – 0.3906 mm. The program then cycles between the two +/- 0.3906 mm positions five times while reading the force output. The average force output is calculated at each position. Then these two forces are averaged. This force is compared to the required axial force (as determined by the governing equations) and the axial length is adjusted as necessary in increments of 0.1953 mm. Axial B (Sub-VI) is identical to Axial A (Sub-VI) except that it communicates with the hardware associated with Chamber B.

Figure 62 - Axial B – Maintain Stretch (Sub-VI):

This sub-VI stretches the artery to a desired length and measures the axial force (as detailed above in "Axial A (Sub-VI) & Axial B (Sub-VI)"). However, this sub-VI maintains the current length of the artery after reading force and is thus a monitoring program only.

Figure 63 - Chamber A (Sub-VI) & Chamber B (Sub-VI):

This sub-VI reads the voltage from the pressure transducer, pump, and pressure controller and translates these voltages using correlation equations. Simultaneously, the required values of pressure and flow rate are calculated (from governing equations). These required parameters are compared to the measured global parameters and adjusted for as appropriate. Adjustments are made by altering the voltage inputs into the pressure controller and pump. Chamber B (Sub-VI) is identical to Chamber A (Sub-VI) except that it communicates with the hardware associated with Chamber B.

Figure 64 - Chamber B – Maintain Global Parameters (Sub-VI):

This sub-VI measures the transluminal pressure, flow rate, and back pressure (as described above in "Chamber A (Sub-VI) & Chamber B (Sub-VI)." However, this program maintains the global parameters (pressure and flow rate) at their current levels and simply monitors all other parameters.

Figure 65 - Axial Force – Length Test VI:

This VI calls upon the following sub-VI's:

- Ultrasound Measurements (Sub-VI), which calls
    - Ultrasound Waveform Generator (Sub-VI)

This top-level VI incrementally increases the length of two arteries simultaneously. Through this process, the program is monitoring the geometry of both arteries. Each chamber will independently stop extending the artery once a stretch ratio of 1.8 is achieved. Once both arteries reach this length, the program stops.

Figure 66 - Pressure – Diameter Test VI:

This VI calls upon the following sub-VI's:

- Ultrasound Measurements (Sub-VI), which calls
    - Ultrasound Waveform Generator (Sub-VI)

This top-level VI incrementally increases the pressure in two chambers simultaneously while monitoring the geometry of both arteries. Each chamber independently shuts off once a pressure of 150 mmHg is achieved. Once both pressures reach 150 mmHg, the program shuts down.

Figure 67 - Global vs. Local Control VI:

This VI calls upon the following sub-VI's:

- Ultrasound Measurements (Sub-VI), which calls
    - Ultrasound Waveform Generator (Sub-VI)
- Axial A (Sub-VI)
- Axial B – Maintain Stretch (Sub-VI)
- Chamber A (Sub-VI)
- Chamber B – Maintain Parameters (Sub-VI)

This top-level VI monitors the geometry of two arteries. This program monitors adjusts the global parameters (pressure, flow rate, and axial position) such that the local parameters achieve some prescribed level in Chamber A. In chamber B, global parameters are found such that local parameters are satisfied initially.

However after finding these global parameters, they are held throughout the duration of the experiment without regard to the local parameters. The program ends upon user interruption.

Figure 68 - Local Control:

This VI calls upon the following sub-VI's:

- Ultrasound Measurements (Sub-VI), which calls
  - Ultrasound Waveform Generator (Sub-VI)
- Axial A (Sub-VI)
- Axial B (Sub-VI)
- Chamber A (Sub-VI)
- Chamber B (Sub-VI)

This top-level VI monitors the geometry of two arteries. For both chambers, continuous adjustments are made to the global parameters such that the prescribed local parameters are satisfied. The program ends on user interruption.

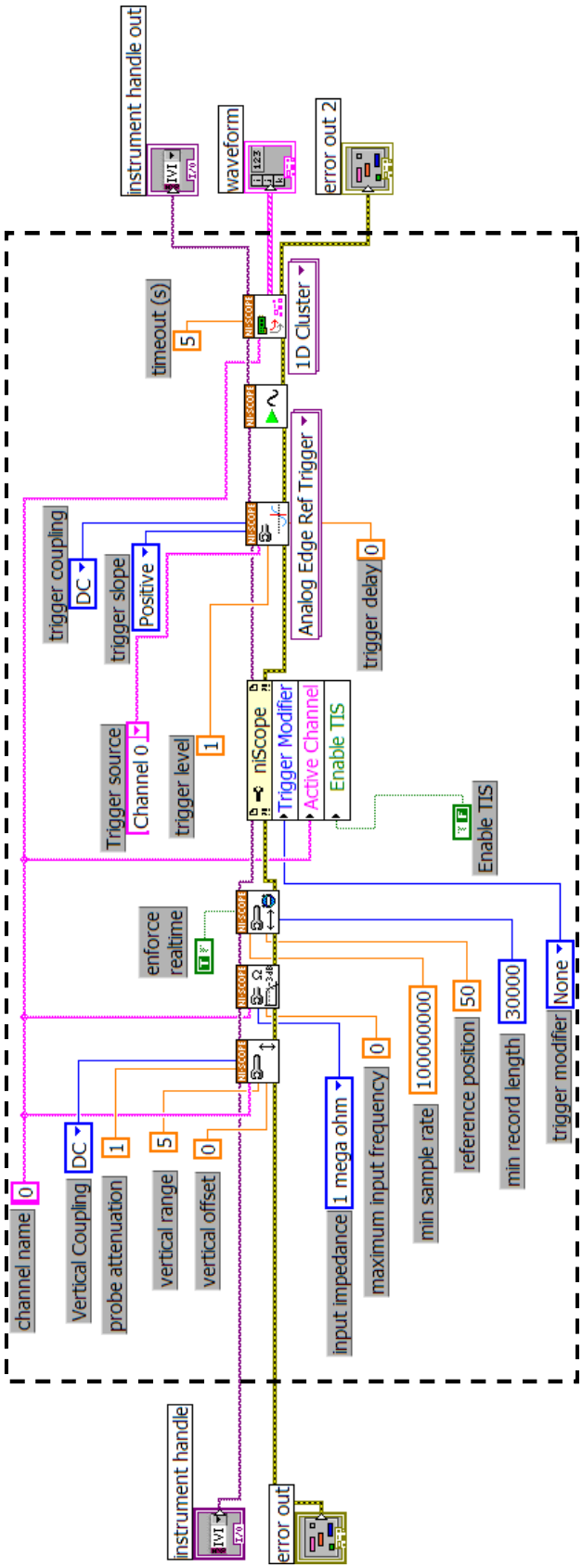


**Figure 59 - Ultrasound Waveform Generator (Sub-VI)**

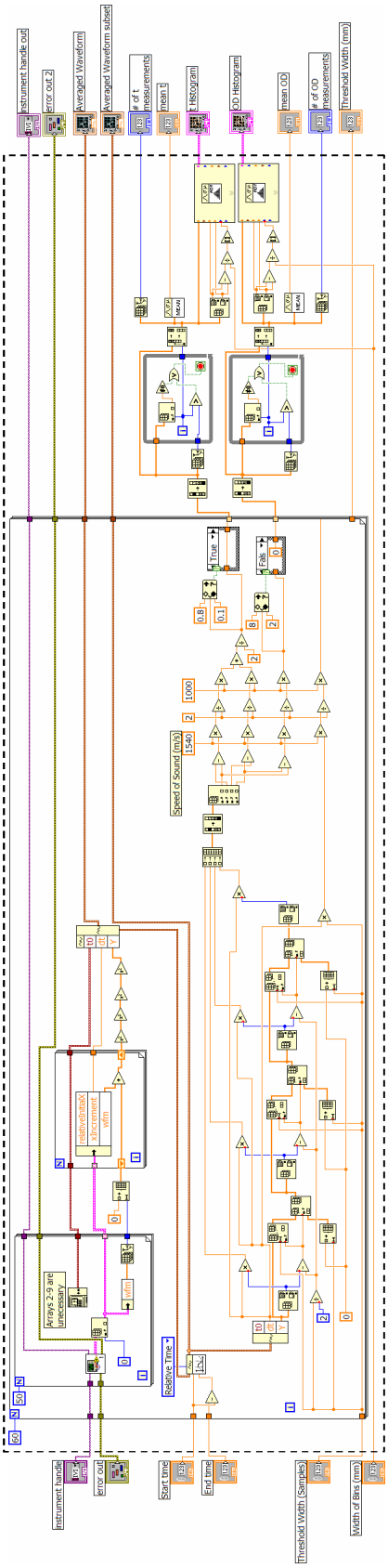


**Figure 60 – Ultrasound Measurements (Sub-VI)**

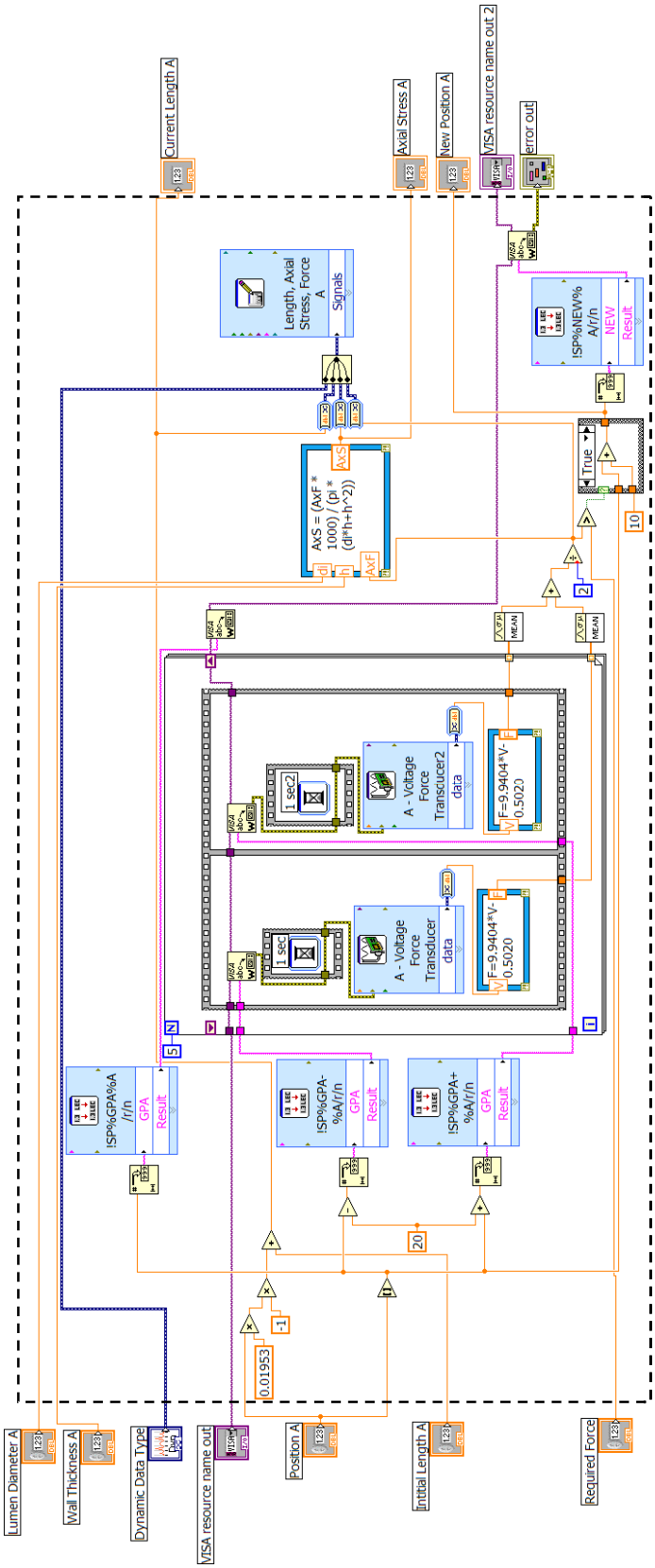


**Figure 61 - Axial A (Sub-VI) & Axial B (Sub-VI)**

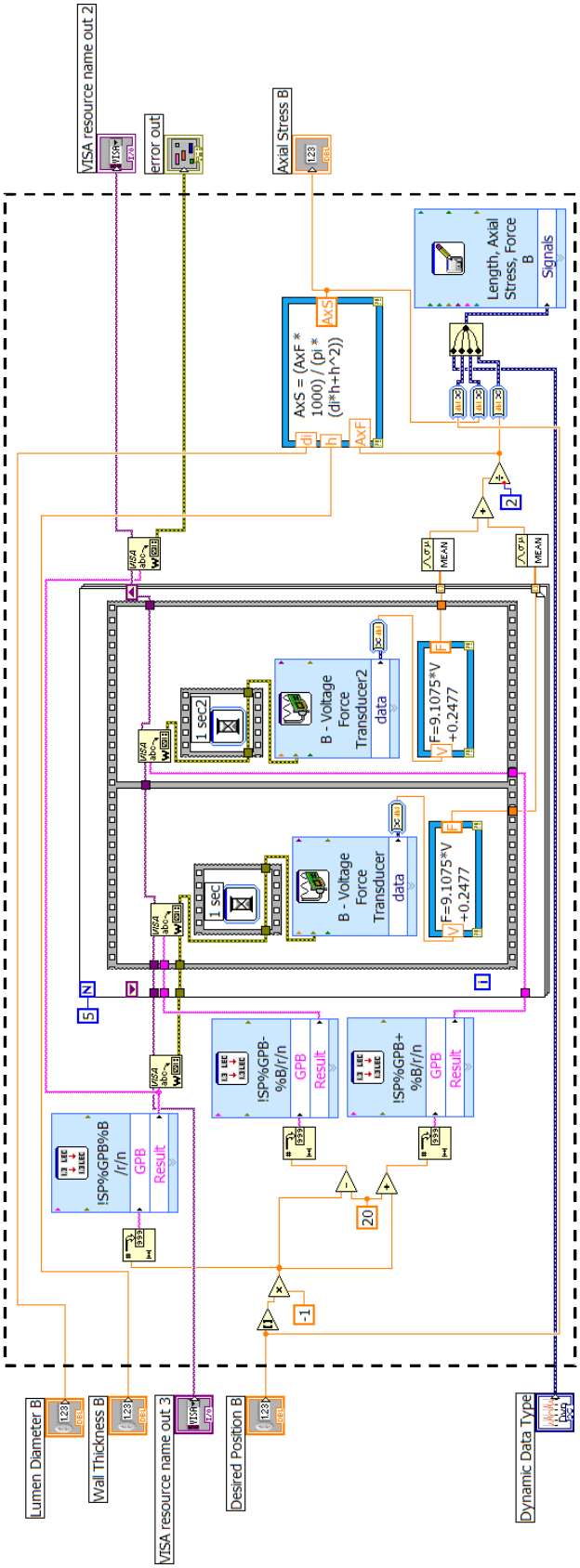


**Figure 62 - Axial B – Maintain Stretch (Sub-VI)**

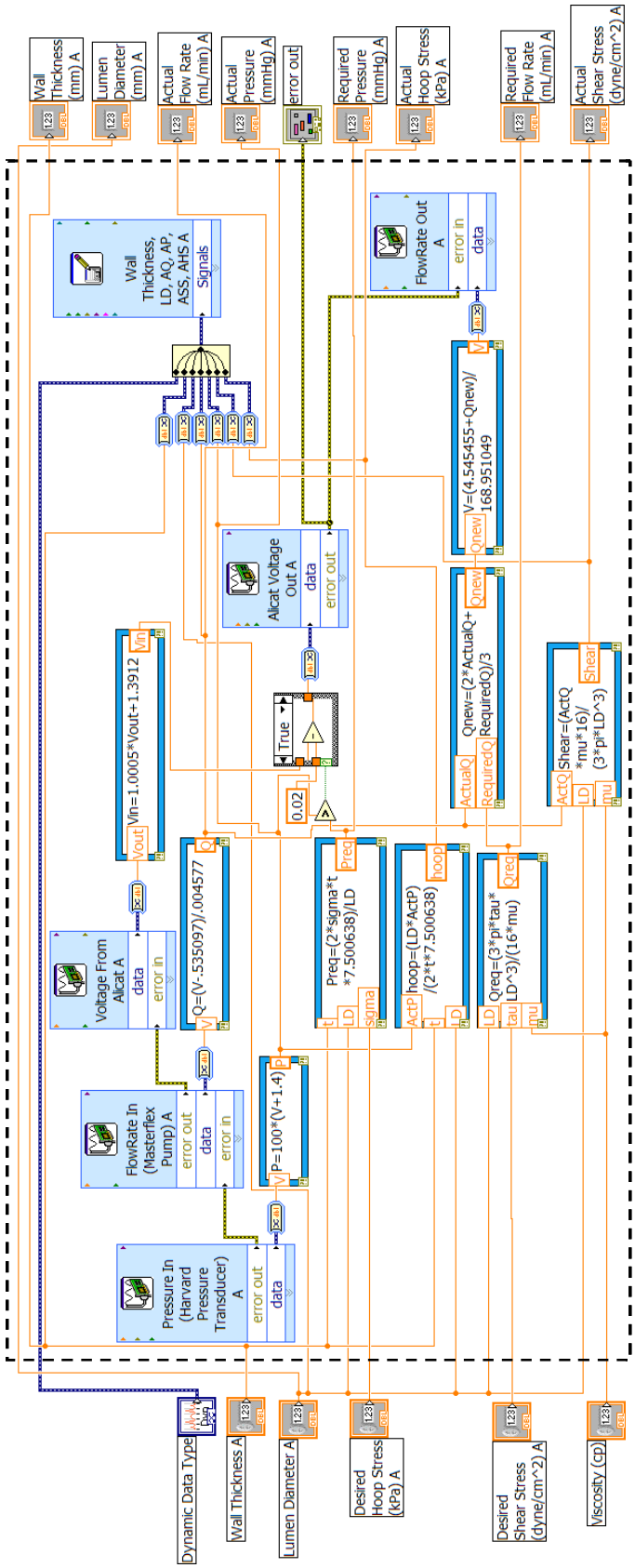


**Figure 63 - Chamber A (Sub-VI) & Chamber B (Sub-VI)**

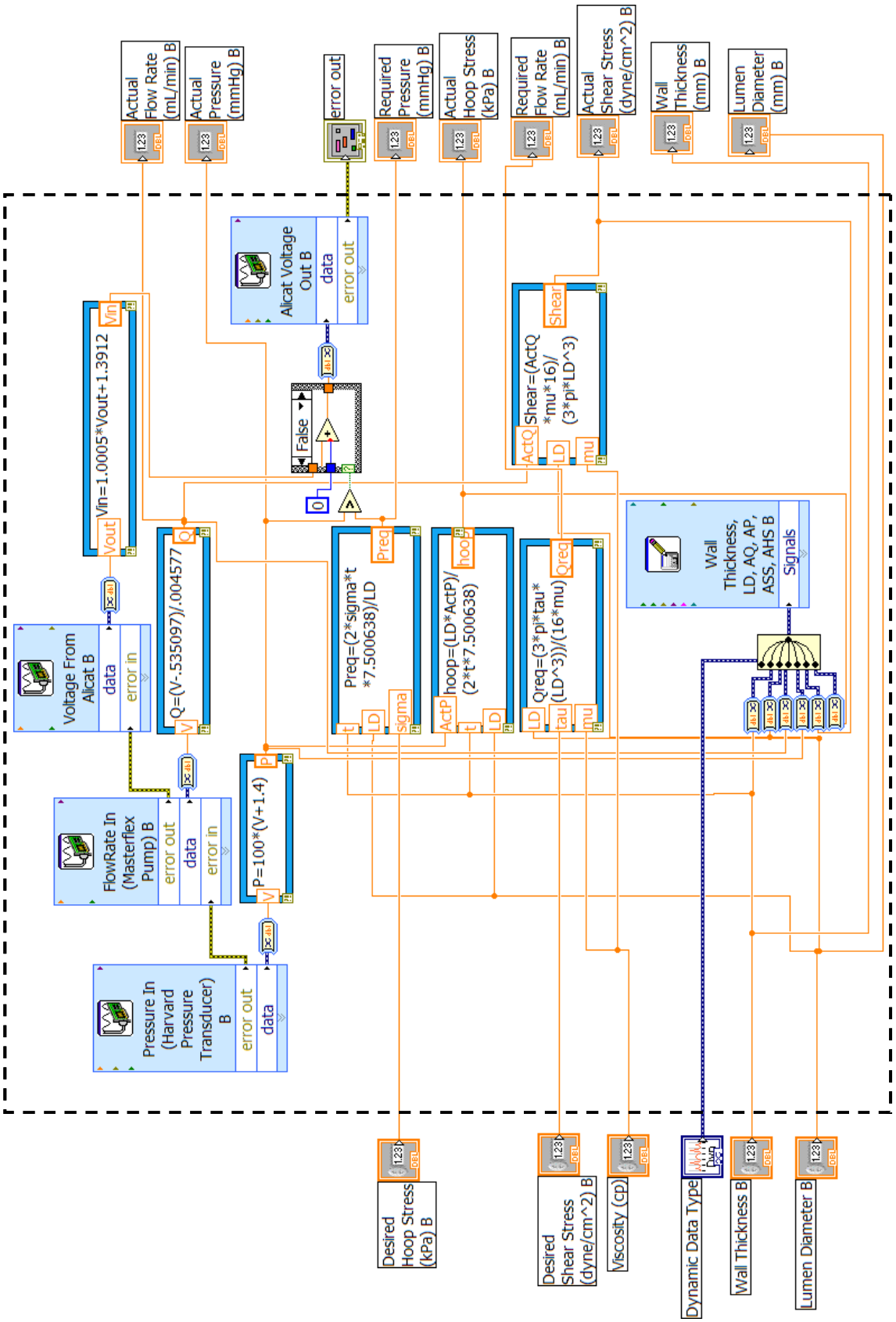


**Figure 64 - Chamber B – Maintain Global Parameters (Sub-VI)**

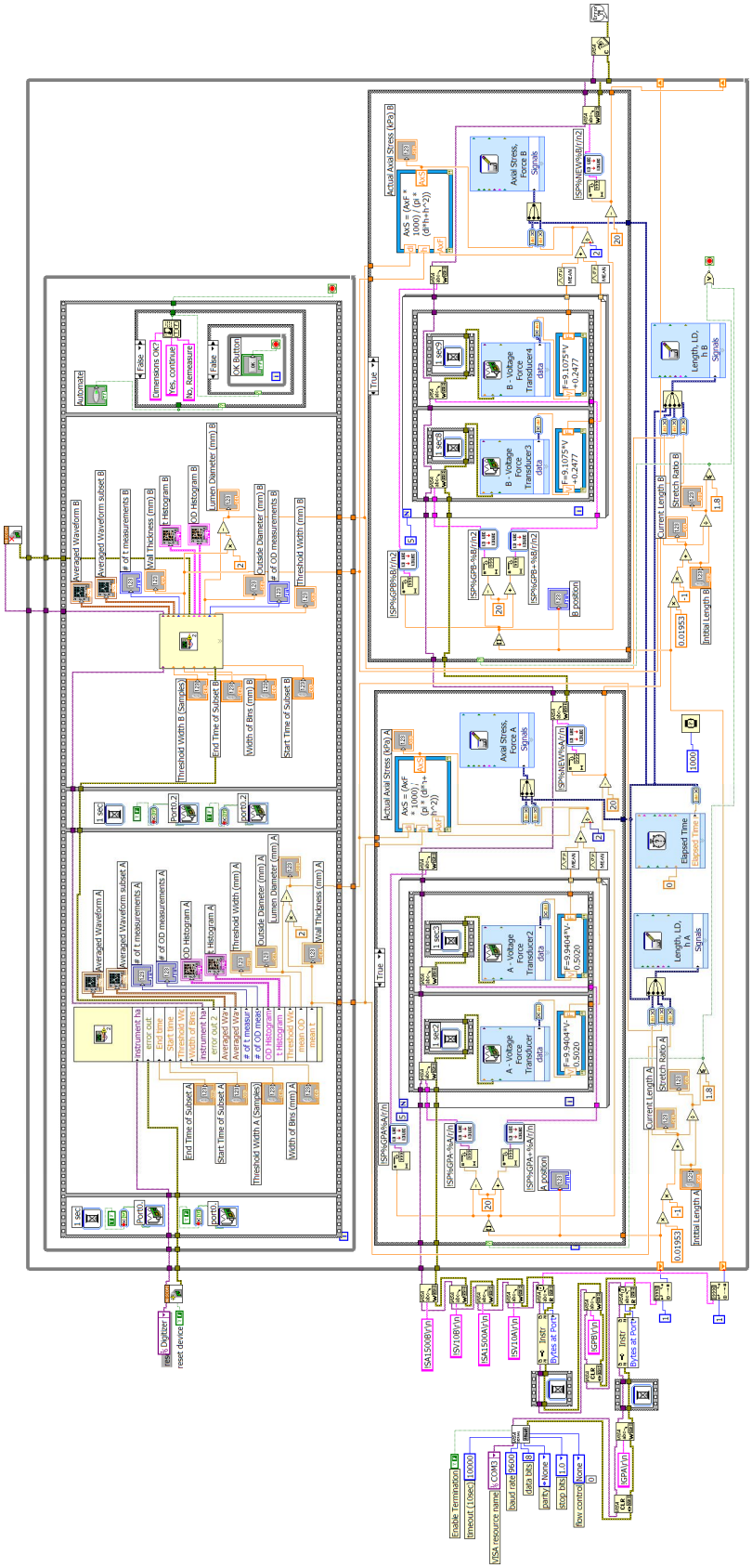

**Figure 65 - Axial Force – Length Test VI**

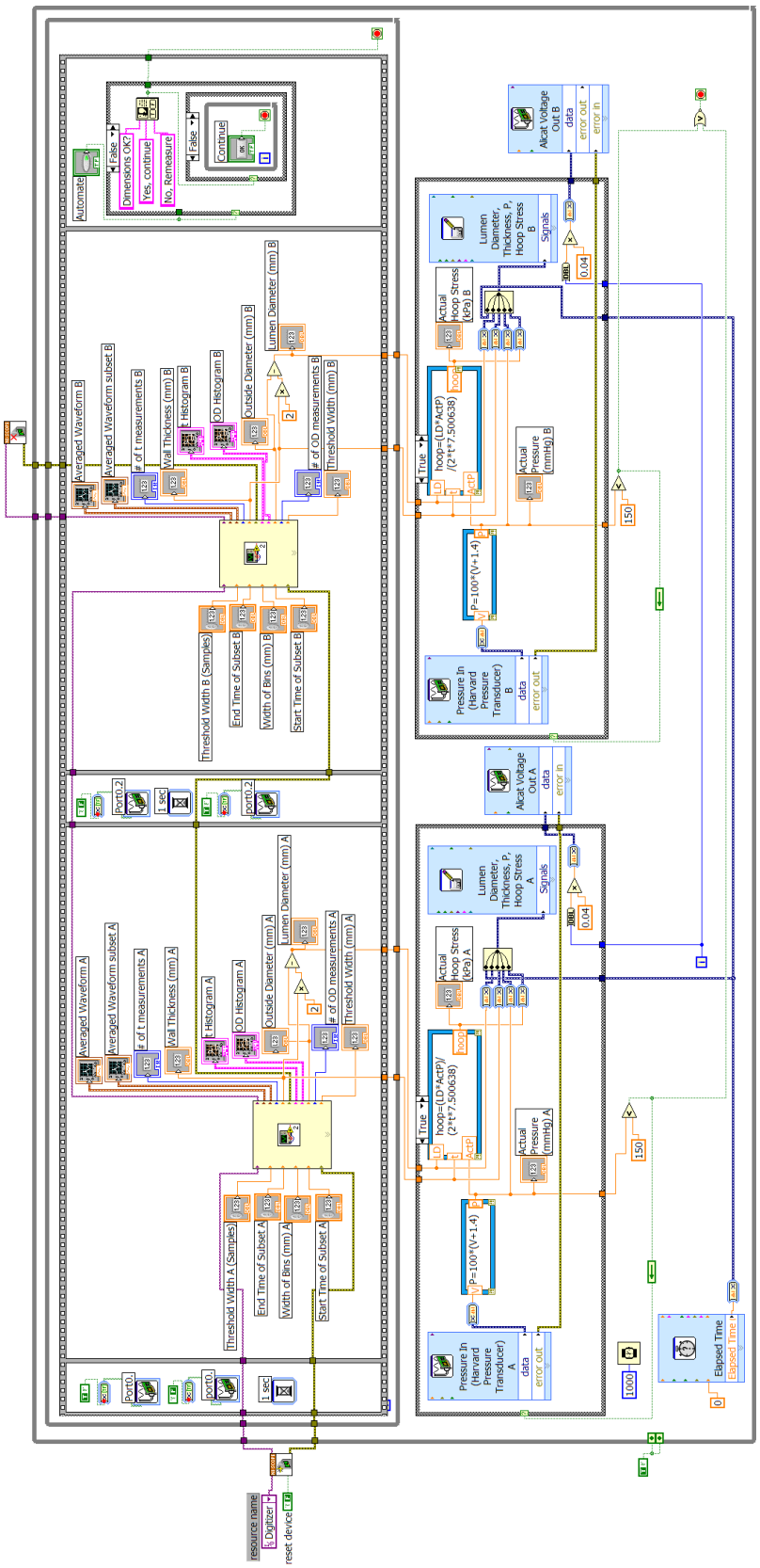


**Figure 66 - Pressure – Diameter Test VI**

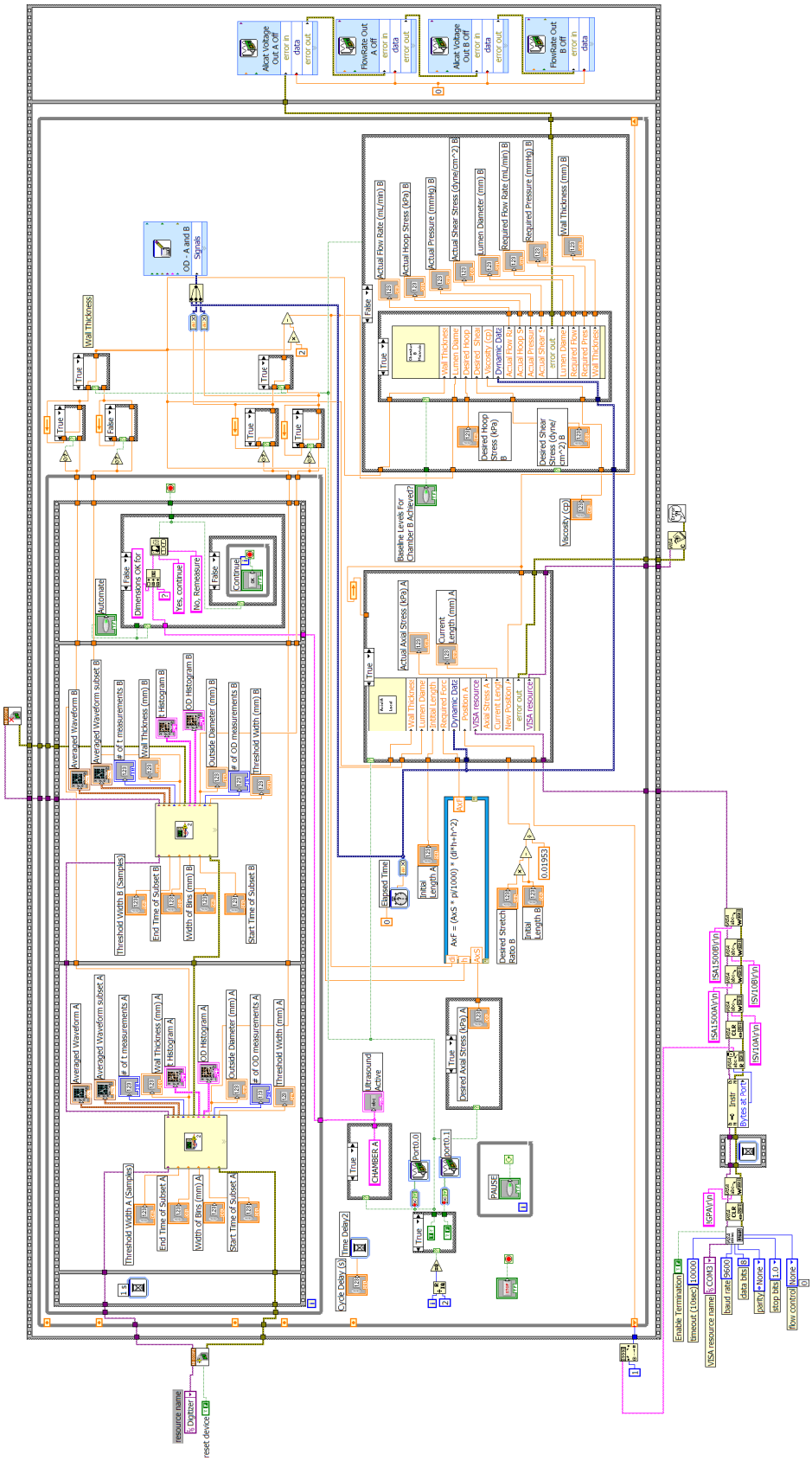

**Figure 67 - Global vs. Local Control VI**

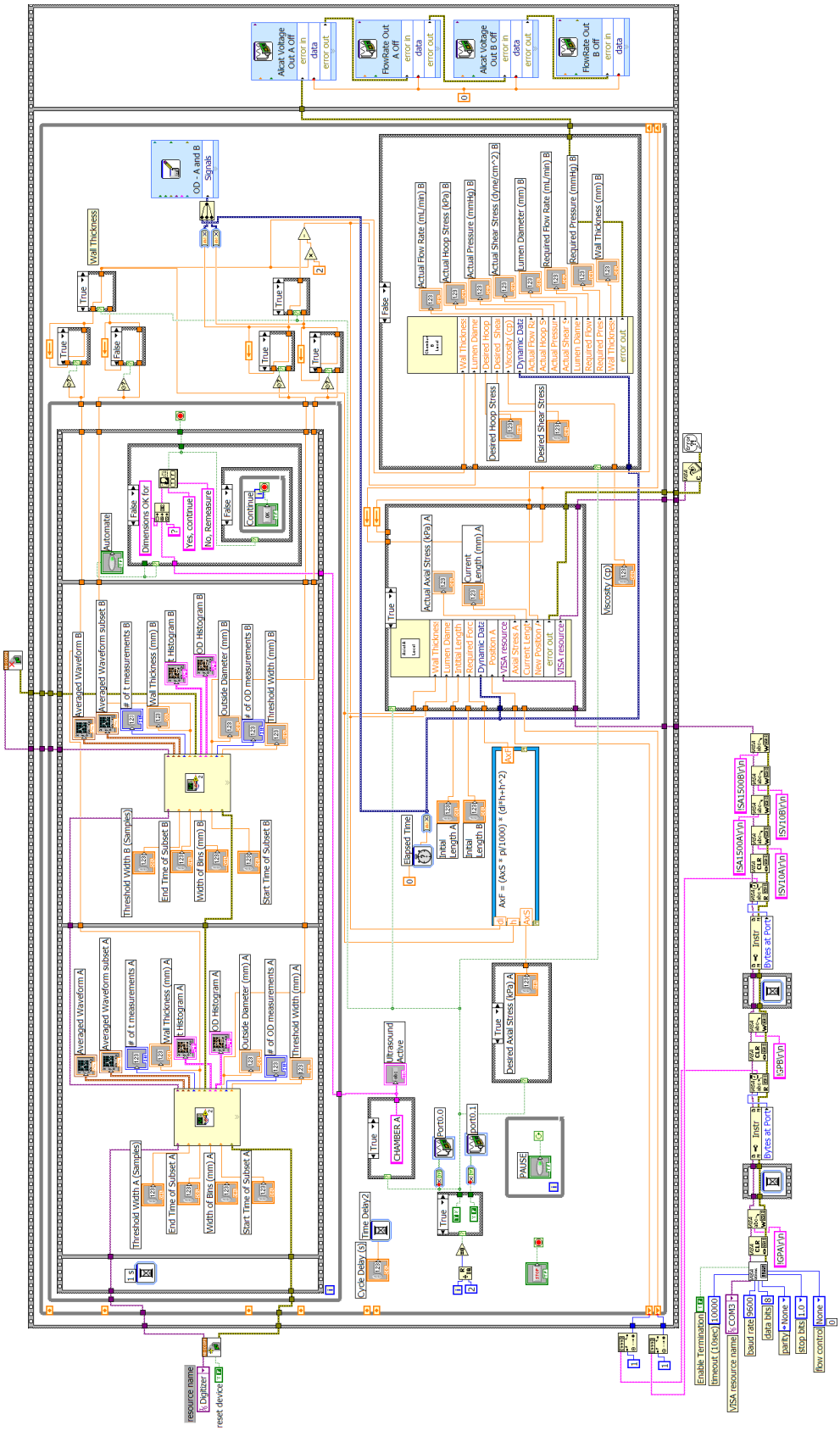

**Figure 68 - Local Control VI**

# REFERENCES


Bakker, E. N., E. T. van Der Meulen, J. A. Spaan and E. VanBavel (2000). Organoid culture of cannulated rat resistance arteries: effect of serum factors on vasoactivity and remodeling. Am J Physiol 278(4): H1233-40.

Brant, A. M., M. F. Teodori, R. L. Kormos and H. S. Borovetz (1987). Effect of variations in pressure and flow on the geometry of isolated canine carotid arteries. J Biomech 20(9): 831-8.

Chesler, N. C., D. N. Ku and Z. S. Galis (1999). Transmural pressure induces matrix-degrading activity in porcine arteries ex vivo. Am J Physiol 277(5 Pt 2): H2002-9.

Clerin, V., R. J. Gusic, J. O'Brien, P. M. Kirshbom, R. J. Myung, J. W. Gaynor and K. J. Gooch (2002). Mechanical Environment, Donor Age, and Presence of Endothelium Interact to Modulate Porcine Artery Viability Ex Vivo. Ann Biomed Eng 30: 1117-1127.

Clerin, V., J. W. Nichol, M. Petko, R. J. Myung, J. W. Gaynor and K. J. Gooch (2003). Tissue engineering of arteries by directed remodeling of intact arterial segments. Tissue Eng 9(3): 461-72.

Collins, S. A. and N. A. Swanson. (1993). Chronic tissue expansion. J Dermatol Surg Oncol 19(12): 1090-8.

Davis, N. P. (2002). Axial Stretch as a Means of Lengthening Arteries: An Investigation in Organ Culture. Georgia Institute of Technology, Ph. D. Thesis.

Davis, N. P., H. C. Han, B. Wayman and R. Vito (2005). Sustained axial loading lengthens arteries in organ culture. Ann Biomed Eng 33(7): 867-77.

De Mey, J. G., M. P. Uitendaal, H. C. Boonen, M. J. Vrijdag, M. J. Daemen and H. A. Struyker-Boudier (1989). Acute and long-term effects of tissue culture on contractile reactivity in renal arteries of the rat. Circ Res 65(4): 1125-35.

Fink B., J. Singer, S. Braunstein, G. Schwinger, G. Schmielau, and W. Ruther (1999). Behavior of blood vessels during lower-leg lengthening using the Ilizarov method. J Pediatr Orthop 19(6): 748-53.

Fu G., Y. Zeng, Z. Xia, and J. Lee (1997). Biorheological features of some soft tissues under a surgical tissue expansion procedure. Biorheology 34(4-5): 281-93.

Gleason, R. L., S. P. Gray, E. Wilson and J. D. Humphrey (2004). A multiaxial computer-controlled organ culture and biomechanical device for mouse carotid arteries. J Biomech Eng 126(6): 787-95.

Gleason, R. L., E. Wilson and J. D. Humphrey (2007). Biaxial biomechanical adaptations of mouse carotid arteries cultured at altered axial extension. J Biomech 40(4): 766-76.

Gotlieb, A. I. and P. Boden (1984). Porcine aortic organ culture: a model to study the cellular response to vascular injury. In Vitro 20(7): 535-42.

Gugenheim, J. J. Jr. (1998). The Ilizarov method. Orthopedic and soft tissue applications. Clin Plast Surg 25(4): 567-78.

Han, H. C. and D. N. Ku (2001). Contractile responses in arteries subjected to hypertensive pressure in seven-day organ culture. Ann Biomed Eng 29(6): 467-75.

Han, H. C., D. N. Ku and R. P. Vito (2003). Arterial wall adaptation under elevated longitudinal stretch in organ culture. Ann Biomed Eng 31: 403-411.

Hong C., G. B. Stark, and J. W. Futrell (1987). Elongation of axial blood vessels with a tissue expander. Clin Plast Surg 14(3): 465-7.

Huang K., Y. Zeng, H. Xia, and C. Liu (1998). Alterations in the biorheological features of some soft tissues after limb lengthening. Biorheology 35(4-5): 355-63.

Ippolito E., G. Peretti, M. Bellocci, P. Farsetti, C. Tudisco, R. Caterini, and C. De Martino (1994). Histology and ultrastructure of arteries, veins, and peripheral nerves during limb lengthening. Clin Orthop Relat Res (308): 54-62.

Jackson, Z. S., A. I. Gotlieb and B. L. Langille (2002). Wall tissue remodeling regulates longitudinal tension in arteries. Circ Res 90(8): 918-25.

Kamiya, A. and T. Togawa (1980). Adaptive regulation of wall shear stress to flow change in the canine carotid artery. Am J Physiol 239(1): H14-21.

Koo, E. W. and A. I. Gotlieb (1991). Neointimal formation in the porcine aortic organ culture. I. Cellular dynamics over 1 month. Lab Invest 64(6): 743-53.

Labadie, R. F., J. F. Antaki, J. L. Williams, S. Katyal, J. Ligush, S. C. Watkins, S. M. Pham and H. S. Borovetz (1996). Pulsatile perfusion system for ex vivo investigation of biochemical pathways in intact vascular tissue. Am J Physiol 270(2 Pt 2): H760-8.

Lavini F., L. Renzi-Brivio, and G. de Bastiani (1990). Psychologic, vascular, and physiologic aspects of lower limb lengthening in achondroplastics. Clin Orthop (250): 138-42.

Liu, S. Q. and Y. C. Fung (1989). Relationship between hypertension, hypertrophy, and opening angle of zero-stress state of arteries following aortic constriction. J Biomech Eng 111(4): 325-35.

Lockwood G. R., L. K. Ryan, J. W. Hunt, and F. S. Foster (1991). Measurement of the ultrasonic properties of vascular tissues and blood from 35-65 MHz. Ultrasound Med Biol 17(7): 653-66.

Masuda, H., H. Bassiouny, S. Glagov and C. K. Zarins (1989). Artery wall restructuring in response to increased flow. Surg Forum 40: 285-286.

Matsumoto, T. and K. Hayashi (1994). Mechanical and dimensional adaptation of rat aorta to hypertension. J Biomech Eng 116(3): 278-83.

Matsumoto, T., E. Okumura, Y. Miura and M. Sato (1999). Mechanical and dimensional adaptation of rabbit carotid artery cultured in vitro. Med Biol Eng Comput 37(2): 252-6.

Moneta G. L., C. Rumwell, and J. M. Porter (2000). Carotid artery duplex scanning. In C. M. Loftus & T. F. Kresowik (Eds.), Carotid Artery Surgery (pp. 1-14). Thieme.

Nichol, J. W., M. Petko, R. J. Myung, J. W. Gaynor and K. J. Gooch (2005). Hemodynamic conditions alter axial and circumferential remodeling of arteries engineered ex vivo. Ann Biomed Eng 33(6): 721-32.

Peterkofsky, B. and D. J. Prockop (1962). A method for the simultaneous measurement of the radioactivity of proline-C14 and hydroxyproline-C14 in biological materials. Anal Biochem 4: 400-6.

Ruiz-Razura A., J. L. Williams Jr., C. L. Reilly, B. E. Cohen, V. B. Schini, P. M. Vanhoutte, and S. Thomsen (1994). Acute intraoperative arterial elongation: histologic, morphologic, and vascular reactivity studies. J Reconstr Microsurg 10(6): 367-73.

Schwartz, L. B., C. M. Purut, M. F. Massey, J. C. Pence, P. K. Smith and R. L. McCann (1996). Effects of pulsatile perfusion on human saphenous vein vasoreactivity: a preliminary report. Cardiovasc Surg 4(2): 143-9.

Stark G. B., C. Hong, and J. W. Futrell (1987). Rapid elongation of arteries and veins in rats with a tissue expander. Plast Reconstr Surg 80(4): 570-81.

Surowiec, S. M., B. S. Conklin, J. S. Li, P. H. Lin, V. J. Weiss, A. B. Lumsden and C. Chen (2000). A new perfusion culture system used to study human vein. J Surg Res 88(1): 34-41.

Vaishnav, R. N., J. Vossoughi, D. J. Patel, L. N. Cothran, B. R. Coleman and E. L. Ison-Franklin (1990). Effect of hypertension on elasticity and geometry of aortic tissue from dogs. J Biomech Eng 112(1): 70-4.

Voisard, R., J. von Eicken, R. Baur, J. E. Gschwend, U. Wenderoth, K. Kleinschmidt, V. Hombach and M. Hoher (1999). A human arterial organ culture model of postangioplasty restenosis: results up to 56 days after ballooning. Atherosclerosis 144(1): 123-34.

Vorp, D. A., D. A. Severyn, D. L. Steed and M. W. Webster (1996). A device for the application of cyclic twist and extension on perfused vascular segments. Am J Physiol 270(2 Pt 2): H787-95.

Wayman, B. H. (2007). Arterial response to local mechanical variables in organ culture: The effects of circumferential and shear stress. Georgia Institute of Technology, Ph. D. Thesis.

Wayman, B. H., W.R. Taylor, A. Rachev, and R. P. Vito (2008). Arteries respond to independent control of circumferential and shear stress in organ culture. Ann Biomed Eng 36(5): 673-84.

Zarins, C. K., M. A. Zatina, D. P. Giddens, D. N. Ku and S. Glagov (1987). Shear stress regulation of artery lumen diameter in experimental atherogenesis. J Vasc Surg 5(3): 413-20.

Zulliger, M. A., G. Montorzi and N. Stergiopulos (2002). Biomechanical adaptation of porcine carotid vascular smooth muscle to hypo and hypertension in vitro. J Biomech 35(6): 757-65.